AD-A083 347 WEIDLINGER ASSOCIATES NEW YORK F/G 20/4
PRELIMINARY STUDY OF A TEST PROCEDURE FOR OBTAINING STEP WAVE L--ETC(U)
APR 79 J P WRIGHT, M L BARON, F L DIMAGGIO DNA001-79-C-0078
UNCLASSIFIED DNA-4933T NL

1 OF 2
AD
A083 347

1 OF 2

AD A083 347

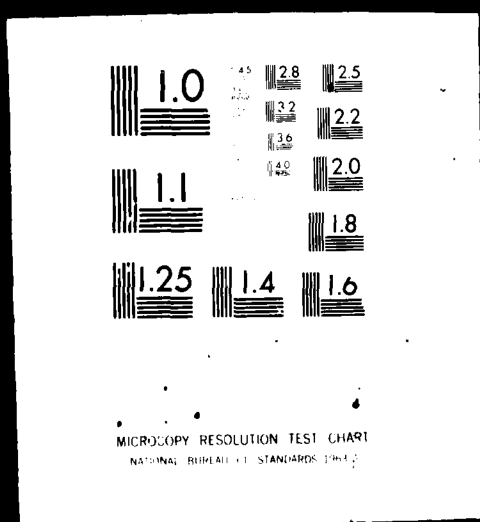

Special forms of the third equation are needed for $r=0$, $\theta=0$ and $\theta=\pi$.

(12) LEVEL III

AD-E300 724

ADA083347

DNA 4933T

PRELIMINARY STUDY OF A TEST PROCEDURE FOR OBTAINING STEP WAVE LOADINGS ON STRUCTURES AT DEEP SUBMERGENCE

Weidlinger Associates
110 East 59th Street
New York, New York 10022

30 April 1979

Topical Report for Period 1 December 1978—30 April 1979

CONTRACT No. DNA 001-79-C-0078

APPROVED FOR PUBLIC RELEASE;
DISTRIBUTION UNLIMITED.

THIS WORK SPONSORED BY THE DEFENSE NUCLEAR AGENCY
UNDER RDT&E RMSS CODE B344079464 Y99QAXSF50119 H2590D.

Prepared for
Director
DEFENSE NUCLEAR AGENCY
Washington, D. C. 20305

Destroy this report when it is no longer needed. Do not return to sender.

PLEASE NOTIFY THE DEFENSE NUCLEAR AGENCY, ATTN: STTI, WASHINGTON, D.C. 20305, IF YOUR ADDRESS IS INCORRECT, IF YOU WISH TO BE DELETED FROM THE DISTRIBUTION LIST, OR IF THE ADDRESSEE IS NO LONGER EMPLOYED BY YOUR ORGANIZATION.

UNCLASSIFIED

SECURITY CLASSIFICATION OF THIS PAGE (When Data Entered)

REPORT DOCUMENTATION PAGE		READ INSTRUCTIONS BEFORE COMPLETING FORM
1. REPORT NUMBER DNA 4933T	2. GOVT ACCESSION NO. AD-A083 347	3. RECIPIENT'S CATALOG NUMBER
4. TITLE (and Subtitle) PRELIMINARY STUDY OF A TEST PROCEDURE FOR OBTAINING STEP WAVE LOADINGS ON STRUCTURES AT DEEP SUBMERGENCE		5. TYPE OF REPORT & PERIOD COVERED Topical Report for Period 1 Dec 78—30 Apr 79 6. PERFORMING ORG. REPORT NUMBER
7. AUTHOR(s) J. P. Wright F. L. DiMaggio M. L. Baron		8. CONTRACT OR GRANT NUMBER(s) DNA 001-79-C-0078 new
9. PERFORMING ORGANIZATION NAME AND ADDRESS Weidlinger Associates 110 East 59th Street New York, New York 10022		10. PROGRAM ELEMENT, PROJECT, TASK AREA & WORK UNIT NUMBERS Subtask Y99QAXSF501-19
11. CONTROLLING OFFICE NAME AND ADDRESS Director Defense Nuclear Agency Washington, D.C. 20305		12. REPORT DATE 30 April 1979 13. NUMBER OF PAGES 108
14. MONITORING AGENCY NAME & ADDRESS(if different from Controlling Office)		15. SECURITY CLASS (of this report) UNCLASSIFIED 15a. DECLASSIFICATION DOWNGRADING SCHEDULE

16. DISTRIBUTION STATEMENT (of this Report)

Approved for public release; distribution unlimited.

17. DISTRIBUTION STATEMENT (of the abstract entered in Block 20, if different from Report)

18. SUPPLEMENTARY NOTES

This work sponsored by the Defense Nuclear Agency under RDT&E RMSS Code B344079464 Y99QAXSF50119 H2590D.

19. KEY WORDS (Continue on reverse side if necessary and identify by block number)

Step Wave Loading
External Pressure
Internal Pressure
Structural Model

20. ABSTRACT (Continue on reverse side if necessary and identify by block number)

This investigation is concerned with the development of a possible technique for obtaining step wave loading on deeply submerged structures. In this technique, a fluid-filled cylinder would be used as the test device and the cylinder itself submerged. A structural model would be placed inside the cylinder and the internal fluid brought to the required test pressure. A charge designed to produce a step wave would be placed in the water outside

DD FORM 1473 1 JAN 73 EDITION OF 1 NOV 65 IS OBSOLETE

UNCLASSIFIED

SECURITY CLASSIFICATION OF THIS PAGE (When Data Entered)

20. ABSTRACT (Continued)

the test device. The shock wave from the charge would thus produce a loading in the pressurized cylinder and hence on the test mode.

One of the first questions that arises is what is the form of the pressure wave that is produced within the cylinder. This report presents a preliminary study of this problem by considering the response of a submerged fluid-filled ring subjected to a transverse step wave. The external fluid is represented by using the plane wave approximation. The ring and internal fluid equations are replaced by finite difference approximations using central differences in space and time. Details of the numerical method, and the results of six calculations are given. In these six calculations, water is used as the internal and external fluids, and the ring, which has the properties of either steel or aluminum, has two different radii and two or three different thicknesses.

The primary reason for these calculations is to determine whether the ring is "transparent." That is, does the internal pressure time history look nearly the same as the external pressure. The results show that the ring is transparent if it is thin enough but, as the thickness increases, strong ring vibrations become important. Nonetheless, it appears that there are realistic ring parameters (moduli, radius, thickness) which make the test procedure feasible. Consequently, it is recommended that a combined experimental-theoretical program be seriously considered.

TABLE OF CONTENTS

INTRODUCTION

This investigation is concerned with the development of a possible technique for obtaining step wave loadings on deeply submerged structures. This type of loading has been successfully obtained at shallow depths, through the use of specially designed charges. For such shallow experiments, the venting of the bubble produced by the explosion has resulted in the alleviation of any bubble pulse effects from the charge, thus resulting in a reasonable pressure wave simulation. For deep submergence applications however, the exploding of a charge produces a bubble where pulsations would produce an additional loading on the model. It is both costly and questionable whether any artificial bubble entrapment mechanisms would work at these depths. Since this additional bubble pulse loading is undesireable for the present purposes, the consideration of some other means of avoiding the bubble became appropriate.

For several years the possibility of utilizing a pressurized cylinder as a test device has been under consideration. The test device cylinder would itself be submerged. Inside the cylinder, a model would be placed and the water brought to the required at-depth pressure for the test. A charge designed to produce a step wave would be placed in the water outside the test device. The shock wave from this charge would thus envelop the test device cylinder, and produce a loading in the pressurized tank and thus on the test model.

One of the first questions that arises is that of the form of the pressure wave that is produced within the test device. We would of course require a plateau-like pressure signal which would be maintained for a minimum of three transit times of the shock wave across the model. The problem to be investigated thus becomes a question of the transparency of the test device cylinder with respect to the pressure wave from the outside explosion which envelopes it, and thus produces a pressure wave in the internal fluid. Of prime importance is whether or not the wave in the internal fluid can be made to maintain the plateau-like pressure signal for three or more envelopment times of the shock wave across the test model.

This report presents a preliminary study of this problem. It considers the response of a submerged fluid-filled ring subjected to a transverse step wave. The results of particular interest are the pressure signals produced at points in the fluid in the interior of the ring. Details of the numerical methods and the results are given in the following sections.

NUMERICAL METHOD

A finite difference method is used to study the problem of a submerged fluid-filled ring, subjected to a transverse step wave. The basic equations are written in polar coordinates with sign conventions as shown in Fig. 1.

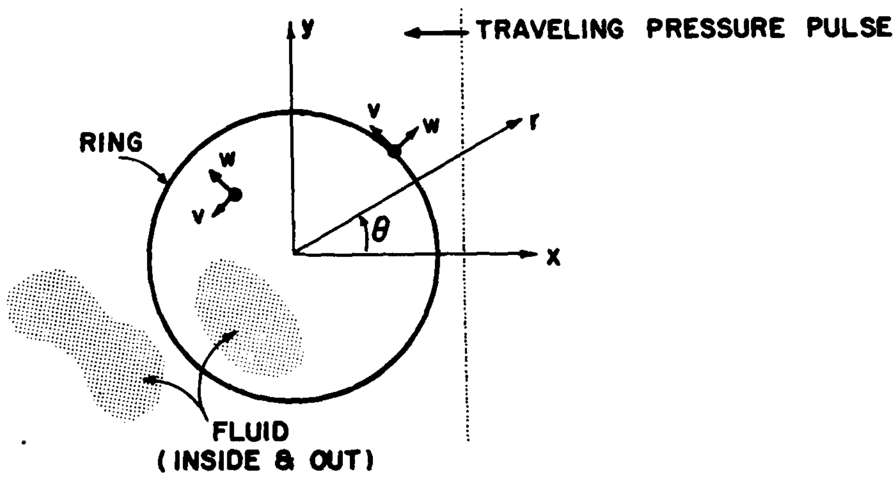

FIG. 1 FLUID-FILLED RING SUBJECTED TO TRANSVERSE STEP PULSE

The external fluid is represented by using the plane wave approximation. The shell and internal fluid equations are replaced by finite difference approximations using central differences in space and time; thus the time integration method is explicit and numerical stability conditions must be considered. Symmetry in space is taken into account so that only points in $0 \leq \theta \leq \pi$ are included in the calculation.

Ring Equations

The equations of motion for the ring are based on those in Stresses in Shells by Wilhelm Flügge (Springer-Verlag, 1960, pp. 208-215), specialized to the case of a ring.

$$\bar{\rho}h\ \dot{v} = \frac{1}{a}\frac{\partial N}{\partial\theta} - \frac{1}{a^2}\frac{\partial M}{\partial\theta}$$

$$\bar{\rho}h\ \dot{w} = -\frac{1}{a^2}\frac{\partial^2 M}{\partial\theta^2} - \frac{1}{a}N - (p_{TE} - p_{TI})$$

Here v and w represent the tangential and radial velocities of the shell, M and N the moment and stress resultant, a the shell radius, $\bar{\rho}$ and h the shell density and thickness, and p_{TE} and p_{TI} are the total external and internal pressures. The moment and stress resultant are given by

$$M = K\ \kappa$$

$$N = D\varepsilon + \frac{1}{a}K\ \kappa$$

with

$$D = \frac{Eh}{(1-\nu^2)}$$

and

$$K = \frac{Dh^2}{12}$$

where ν is Poisson's ratio, E is Young's modulus, ε is the hoop strain at the center-line, given in incremental form by

$$\dot{\varepsilon} = \frac{1}{a}\left(\frac{\partial v}{\partial\theta} + w\right)$$

and κ is the curvature, given in incremental form by

$$\dot{\kappa} = \frac{1}{a^2}\left(\frac{\partial^2 w}{\partial\theta^2} + w\right)$$

The finite difference grid for the ring is shown in Fig. 2, with all points equally spaced in the θ-direction (spacing $\Delta\theta$). The quantities w, M, N, ε and κ are calculated at $\theta_i = i\Delta\theta$ for $i = (0, 1, \ldots, n)$ with the last point $\theta_n = \pi$. The tangential shell velocity, v, is calculated at midpoints, $\theta_{i+1/2} = (i + 1/2)\Delta\theta$ for $i = (0, 1, \ldots, n-1)$.

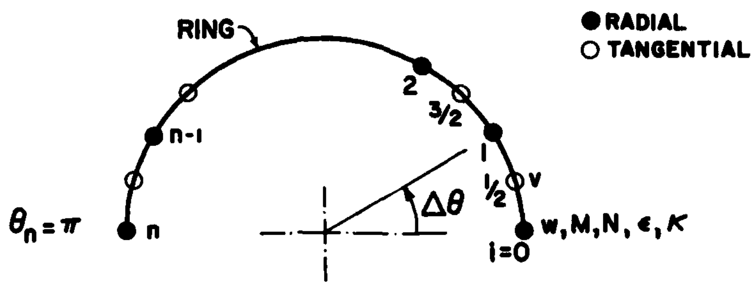

FIG. 2 FINITE DIFFERENCE GRID FOR RING

Let $v_{i+1/2}$ denote $v(\theta_{i+1/2}, t)$. Let w_i denote $w(\theta_i, t)$; similarly for M_i, N_i, ε_i, κ_i . The finite difference form of the equations of motion is given by

$$\bar{\rho}h\ \dot{v}_{i+1/2} = \frac{1}{a\Delta\theta}(N_{i+1} - N_i) - \frac{1}{a^2\Delta\theta}(M_{i+1} - M_i)$$

$$\bar{\rho}h\ \dot{w}_i = -\frac{1}{a^2\Delta\theta^2}(M_{i+1} - 2M_i + M_{i-1}) - \frac{1}{a}N_i - (p_{TE} - p_{TI})_i$$

The first equation applies for $i = (0, 1, \ldots, n-1)$; the second applies only for $i = (1, 2, \ldots, n-1)$. From symmetry, the appropriate form of the second equation, for $\theta_0 = 0$, is given by

$$\bar{\rho}h\ \dot{w}_0 = -\frac{1}{a^2\Delta\theta^2}(2M_1 - 2M_0) - \frac{1}{a}N_0 - (p_{TE} - p_{TI})_0$$

and for $\theta_n = \pi$,

$$\bar{\rho} h \dot{w}_n = - \frac{1}{a^2 \Delta\theta^2} (2M_{n-1} - 2M_n)$$

$$- \frac{1}{a} N_n - (p_{TE} - p_{TI})_n$$

The strain rates for $i = (1, 2, \ldots, n-1)$ are given by

$$\dot{\varepsilon}_i = \frac{1}{a\Delta\theta} (v_{i+1/2} - v_{i-1/2}) + \frac{1}{a} w_i$$

and the curvature rates by

$$\dot{\kappa}_i = \frac{1}{a^2 \Delta\theta^2} (w_{i+1} - 2w_i + w_{i-1}) + \frac{1}{a^2} w_i$$

By symmetry, for $\theta_0 = 0$,

$$\dot{\varepsilon}_0 = \frac{1}{a\Delta\theta} (2\, v_{1/2}) + \frac{1}{a} w_0$$

$$\dot{\kappa}_0 = \frac{1}{a^2 \Delta\theta^2} (2w_1 - 2w_0) + \frac{1}{a^2} w_0$$

and for $\theta_n = \pi$

$$\dot{\varepsilon}_n = \frac{1}{a\Delta\theta} (-2v_{n-1/2}) + \frac{1}{a} w_n$$

$$\dot{\kappa}_n = \frac{1}{a^2 \Delta\theta^2} (2w_{n-1} - 2w_n) + \frac{1}{a^2} w_n$$

Internal Fluid Equations

The equations of motion in the fluid are those of an inviscid acoustic fluid.

$$\rho \dot{v} = - \frac{1}{r} \frac{\partial p}{\partial \theta}$$

$$\rho \dot{w} = - \frac{\partial p}{\partial r}$$

Here v and w are the tangential and radial velocites of the fluid particles, p is the fluid pressure and ρ is the fluid density. The fluid pressure is determined by

$$\dot{p} = -\rho c^2 \frac{1}{r} \left[\frac{\partial (rw)}{\partial r} + \frac{\partial v}{\partial \theta}\right]$$

where c is the fluid wave speed.

The finite difference grid for the fluid (see Fig. 3) is obtained by drawing an even number, 2ℓ, of constant radius lines which are equally spaced in the r-direction. A pressure is associated with the point at r=0. The innermost line and every other line is associated with radial velocities. The remaining lines are associated with pressures and tangential velocities.

The distance $\Delta r = (\frac{2a}{2\ell+1})$ is convenient for writing the finite difference equations. Radial velocity lines are defined at $r_{j+1/2} = (j+1/2)\ \Delta r$ for $j = (0, 1, \ldots, \ell)$, pressure lines at $r_j = j\Delta r$ for $j = (0, 1, \ldots, \ell)$ and tangential velocity lines at $r_j = j\Delta r$ for $j = (1, 2, \ldots, \ell)$. Each line (j or j+1/2) is divided into a set of equally spaced points in the θ-direction. Radial velocities and pressures are defined at $\theta=0$ and $\theta=\pi$; tangential velocities are defined at midpoints between the pressure points. The number of pressure points on each line is calculated to maintain arc separation roughly equal to radial separation; that is, $r_j \Delta\theta_j \cong \Delta r$.

Hence, the number of pressure points on a j-line is variable and chosen to be $3j+1$ for $j=(0,1,\ldots,\ell)$. The same number of points is chosen for the next inner (radial velocity) line.

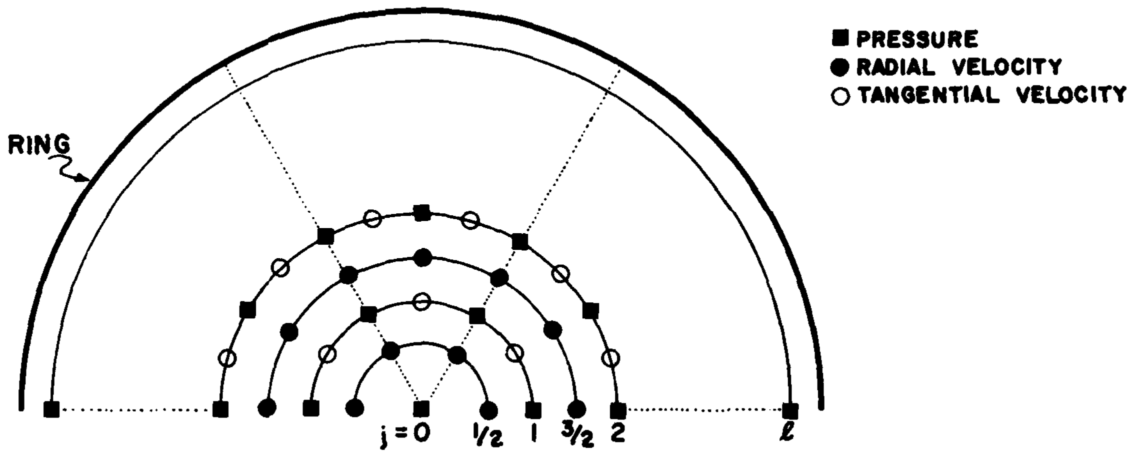

FIG.3 FINITE DIFFERENCE GRID FOR INTERNAL FLUID

Let $p_{j,i}$ denote $p(r_j, \theta_i, t)$, let $v_{j,i+1/2}$ denote $v(r_j,\theta_{i+1/2}, t)$ and let $w_{j+1/2,i}$ denote $w(r_{j+1/2}, \theta_i, t)$. The finite difference equations for the fluid are given by

$$\rho\dot{v}_{j,i+1/2} = -\frac{1}{r_j\Delta\theta_j}(p_{j,i+1} - p_{j,i})$$

$$\rho\dot{w}_{j+1/2,i} = -\frac{1}{\Delta r}(\bar{p}_{j+1,i} - \bar{p}_{j,i})$$

$$\dot{p}_{j,i} = -\rho c^2\left[\frac{(r_{j+1/2}\,\bar{w}_{j+1/2,i} - r_{j-1/2}\,\bar{w}_{j-1/2,i})}{r_j\Delta r} + \frac{(v_{j,i+1/2} - v_{j,i-1/2})}{r_j\Delta\theta_j}\right]$$

The over-bar symbol ($\bar{\ }$) in the second and third equations indicates that linear interpolation in θ is used since radial velocities and pressures are not always defined at the same θ values.

Special forms of the third equation are needed for r=0, θ=0 and θ=π .

For r=0, the average value of the divergence $\langle\nabla . w\rangle_0$ is used

$$\langle\nabla . w\rangle_0 = \frac{w_{1/2,0} + 2w_{1/2,1} + 2w_{1/2,2} + w_{1/2,3}}{3\Delta r}$$

so that $\dot{p}_{o,o} = -\rho c^2 \langle\nabla . w\rangle_0$. By symmetry, for θ=0

$$\dot{p}_{j,0} = -\rho c^2 \left[\frac{(r_{j+1/2}\,\bar{w}_{j+1/2,0} - r_{j-1/2}\,\bar{w}_{j-1/2,0})}{r_j \Delta r} + \frac{2v_{j,1/2}}{r_j \Delta\theta_j} \right]$$

and for θ=π

$$\dot{p}_{j,3j} = -\rho c^2 \left[\frac{(r_{j+1/2}\,\bar{w}_{j+1/2,3j} - r_{j-1/2}\,\bar{w}_{j-1/2,3j})}{r_j \Delta r} - \frac{2v_{j,3j-1/2}}{r_j \Delta\theta_j} \right]$$

Fluid-Shell Coupling

The internal fluid pressure p_{TI} is determined by using the pressures on the $j=\ell$ line nearest the ring. Since the θ spacing for the ring is not necessarily the same as that for the $j=\ell$ pressures, linear interpolation in θ is used to calculate p_{TI} .

The effect of the external fluid is represented by the plane wave approximation which, for the transverse step wave traveling in the negative x-direction, is given by

$$p_{TE} = P_0(1 + \cos\theta)\ H(t + (x-a)/c) + \rho c w$$

Here p_{TE} is the total exterior pressure in the fluid, P_0 is the pressure jump, $H(t)$ is the unit step function, ρ and c are the fluid density and wave speed and w is the radial velocity of the shell. In the numerical calculations, the unit step function is replaced by a waveform with a finite rise-time. This modification reduces the high frequency components in the computed results.

Time Integration

The time integration method for the ring and internal fluid is explicit (based on central differences) and uses a constant time step, Δt, which is determined by numerical stability considerations. Appropriate initial values of velocities and stress-type quantities (M, N and p) are assumed to be known and the following iterative procedure is used. Accelerations (radial and tangential) are calculated from spatial differences of stress-type quantities. Let A_k denote such an acceleration at time $t_k = k\Delta t$. Velocities at time $t_{k+1/2} = (k + 1/2)\Delta t$, denoted by $V_{k+1/2}$, are calculated by

$$V_{k+1/2} = V_{k-1/2} + \Delta t \; A_k$$

Strain rates (or curvature rates, or fluid divergence rates) at time $t_{k+1/2}$, denoted by $\dot{E}_{k+1/2}$, are calculated from spatial differences of the new velocities. Stress-type quantities at time t_{k+1}, denoted by S_{k+1}, are calculated by

$$S_{k+1} = S_k + \Delta t \; D \; \dot{E}_{k+1/2}$$

where D symbolizes the appropriate constitutive relation (pressure-volume, moment-curvature, etc.). These two calculations are performed for all points in the fluid and on the ring.

This method does not use a pseudo-viscosity which is often used in finite difference calculations to remove spurious, high-frequency numerical oscillations. Consequently, high frequency components in the external pressure waveform have been reduced by using a finite rise-time of $10\, a/c(2\ell+1)$ in the unit step function. That is, $10\, \Delta t_3$ is used where Δt_3 is defined in the next section.

Numerical Stability

The shell equations are hyperbolic with respect to the tangential displacement and the wave speed of this motion is controlled by $\bar{c} = \sqrt{E/\bar{\rho}(1-\nu^2)}$. The effective separation is $a\Delta\theta$. Hence the numerical stability condition for this effect is taken as

$$\Delta t_1 \leq \frac{a\Delta\theta}{\bar{c}}$$

(The shell equations are parabolic with respect to the radial displacement but for $h < 2a\Delta\theta$, approximately, the condition from the tangential motion is more critical.) The plane wave approximation contains a viscous damping term which can affect numerical stability for certain ranges of parameters. The condition corresponding to this effect is represented by

$$\Delta t_2 \leq \frac{\bar{\rho}h}{\rho c}$$

The fluid behavior is hyperbolic in both the radial and tangential directions. Numerical stability for this effect is represented by

$$\Delta t_3 \leq \frac{\Delta \ell}{c}$$

where $\Delta\ell$ is the minimum distance between points in the fluid. This corresponds to the distance between the radial velocities which surround the origin ($r=0$), and thus $\Delta\ell = a/(2\ell+1)$

The time step used in the calculation is determined by

$$\Delta t = s \min(\Delta t_1, \Delta t_2, \Delta t_3)$$

where $s = 1/2$ has been used as a safety factor.

DISCUSSION OF RESULTS

The results of six calculations are contained in Appendices A, B, C, D, E and F. These calculations correspond to the following six different cases for the ring.

Ring	Material	a=radius (inches)	h=thickness (inches)
A	Steel	200	2
B	Steel	100	2
C	"	"	0.5
D	Aluminum	100	3.5
E	"	"	1
F	"	"	0.3

All lengths are in inches, pressures are in ksi (kilo-pounds per square inch), and time in milliseconds. Properties of the fluid (inside and out) and the ring are taken as shown in the following tables.

Fluid	ρ = density (ksi-msec^2/in^4)	c = wave speed (in/msec)
Water	0.093	59

Material	$\bar{\rho}/\rho$	E = Young's Modulus (ksi)	ν = Poisson's Ratio
Steel	7.8	28,000	0.28
Aluminum	2.7	10,000	0.33

Time t=0 corresponds to first arrival of the external pressure wave at the right side (θ=0) of the ring· the external fluid pressure jump is P_o = 1 ksi. The time scale in case A is 16 msec long but is only 8 msec long in the other five cases (due to change in radius a).

Twelve time histories are shown in each appendix as indicated in Fig. 4.

Curve Label:	Meaning
P-CENTER:	pressure at $r = 0$
P-RIGHT:	pressure at $r = a/2$, $\theta = 0$
P-TOP:	pressure at $r = a/2$, $\theta = 90$ deg.
P-LEFT:	pressure at $r = a/2$, $\theta = 180$ deg.
SRV-RIGHT:	shell radial velocity at $\theta = 0$
SM-RIGHT:	shell moment at $\theta = 0$
SN-RIGHT:	shell stress resultant at $\theta = 0$
SRV-TOP:	shell radial velocity at $\theta = 90$ deg.
STV-TOP:	shell tangential velocity at $\theta = 90$
SM-TOP:	shell moment at $\theta = 90$
SN-TOP:	shell stress resultant at $\theta = 90$
SRV-LEFT:	shell radial velocity at $\theta = 180$ deg.

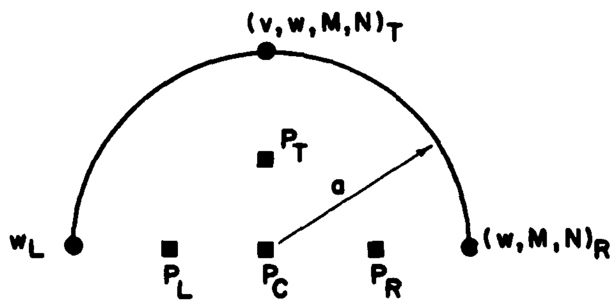

FIG. 4 KEY TO TIME HISTORIES IN APPENDICES

All calculations were performed with 31 points on the ring and 651 points in the fluid (ℓ=20) with 61 pressure points adjacent to the ring. A typical calculation of about 500 time steps required about 60 seconds of computer time on the CDC 6600.

Numerical Oscillations

As noted previously, the finite difference equations do not contain any pseudo-viscosity terms. Consequently, the calculated time histories may contain spurious high-frequency numerical oscillations. Most of these oscillations can be removed by making sure that the applied pressure time history is smooth compared to the cut-off frequency of the numerical scheme. This has been done by introducing a finite rise-time of 10 Δt_3 into the external pressure, as noted on pages 10 and 11. However, some time histories show a "beat" phenomenon which appears first in SM-RIGHT (e.g. see case C, $t \cong 3$ msec). This beat phenomenon may be the result of numerical oscillations interacting with physical oscillations of ring-fluid system or it may be symptomatic of a real physical effect. Since the plane wave approximation (PWA) is generally good only for early times ($ct \lesssim 2a$), this later time phenomenon may not be important. On the other hand, the PWA is reasonable in this problem, at long times (though possibly not at intermediate times) since the fluid-filled ring is near neutral buoyancy. Further study will be required to understand the beat phenomenon.

Transparency of the Ring

The primary reason for these calculations is to determine whether (or to what extent) the ring is "transparent". That is, does the internal pressure time history look nearly the same as the external pressure - at least for about 3.5 msec. For a sufficiently thin ring this is clearly the case. For example in case F ($h/a = 0.003$) the pressure at all four interior points is nearly constant and equal to $P_0 = 1$ (within about 10 per cent). In case E ($h/a = 0.01$) the deviation is more noticeable and in case D ($h/a = 0.035$) the deviation at the center is about 40 per cent after about 2.5 msec. P-LEFT in case D shows that a small tension wave is the first signal felt at that point: this is caused by the early radial motion of the ring at θ = 180 deg (see SRV-LEFT). In case D, ring vibrations (primarily the ovaling mode) are so large that the pressure signal at center is significantly altered. The best response in case D is at P-RIGHT ($r = a/2$, $\theta=0$) where the initial pressure is near p = 1 at about t = 1 and drops to about p = .8 at about t = 3.5 msec. After that time, the strong ring vibrations are apparent and the pressure drops quickly to p = .4.

Comparing the 2 in. thick steel (Case B) with the 3.5 in. thick aluminum (both of radius 100 in.), the aluminum is slightly more transparent than the steel, as expected.

Finally, the larger radius (200 in.) 2 in. thick steel ring shows that, although P-LEFT has a significant deviation from $P_0 = 1$, P-CENTER drops about 35 per cent after 3.5 msec, and P-RIGHT drops less than 20 per cent after 3.5 msec. In fact, the results in case A (steel, a=200, h=2) look surprisingly like those in case D (alum., a=100, h=3.5) except for the longer time scales in case A (and the related differences in SM-RIGHT, SM-TOP and SN-TOP) caused by the larger radius.

SUMMARY AND CONCLUSIONS

This preliminary study has thus far indicated that pressure signals of acceptable form and duration would probably be produced in the suggested device. It appears to us that additional numerical studies and possible small-scale experimentation should be initiated.

Insofar as the numerical studies are concerned, we would consider the following possibilities:

(1) Study the beat phenomenon to identify its source and to determine whether it is in fact real.

(2) Consider a modal type re-calculation. This may make it considerably easier to study the beat phenomena.

(3) Consider other materials for the test vehicle, eg. rubber or plastics.

(4) Initiate, in coordination with UERD, a study on charge shaping. The object of this work would be to attempt to produce a pressure signal in the outside fluid which would result in a more plateau-like pressure signal in the interior fluid. Calculations would be made with the prepared new loadings to study this phenomena.

At the same time that the numerical studies are in progress, we strongly recommend that UERD initiate an experimental study of this problem. Experimental verification of the calculated transparency of the shell is required. This can be done in the UERD test basin, using relatively small scale models of different materials and dimensions.

To summarize, preliminary calculations indicate that the idea is feasible and should be seriously studied. The possibility of using existing structures for the test chamber, eg. the AB-1 model, appears attractive and should also be pursued. We also recommend that the additional numerical studies be implemented and that a meeting to discuss the implications of the proposed test device be scheduled at an appropriate time.

APPENDIX A (Case A)

RING: Steel

Radius = 200 inches
Thickness = 2 inches

Curve Label:	Meaning
P-CENTER:	pressure at r = 0
P-RIGHT:	pressure at r = a/2, θ = 0
P-TOP:	pressure at r = a/2, θ = 90 deg.
P-LEFT:	pressure at r = a/2, θ = 180 deg.
SRV-RIGHT:	shell radial velocity at θ = 0
SM-RIGHT:	shell moment at θ = 0
SN-RIGHT:	shell stress resultant at θ = 0
SRV-TOP:	shell radial velocity at θ = 90 deg.
STV-TOP:	shell tangential velocity at θ = 90
SM-TOP:	shell moment at θ = 90
SN-TOP:	shell stress resultant at θ = 90
SRV-LEFT:	shell radial velocity at θ = 180 deg.

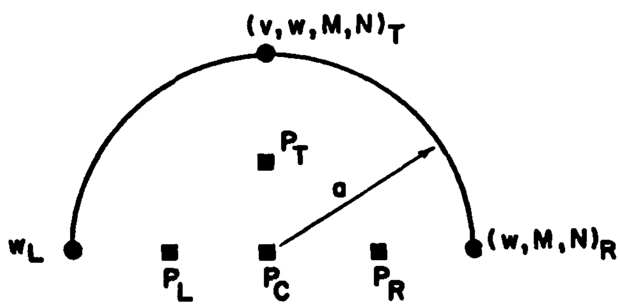

KEY TO TIME HISTORIES IN APPENDICES

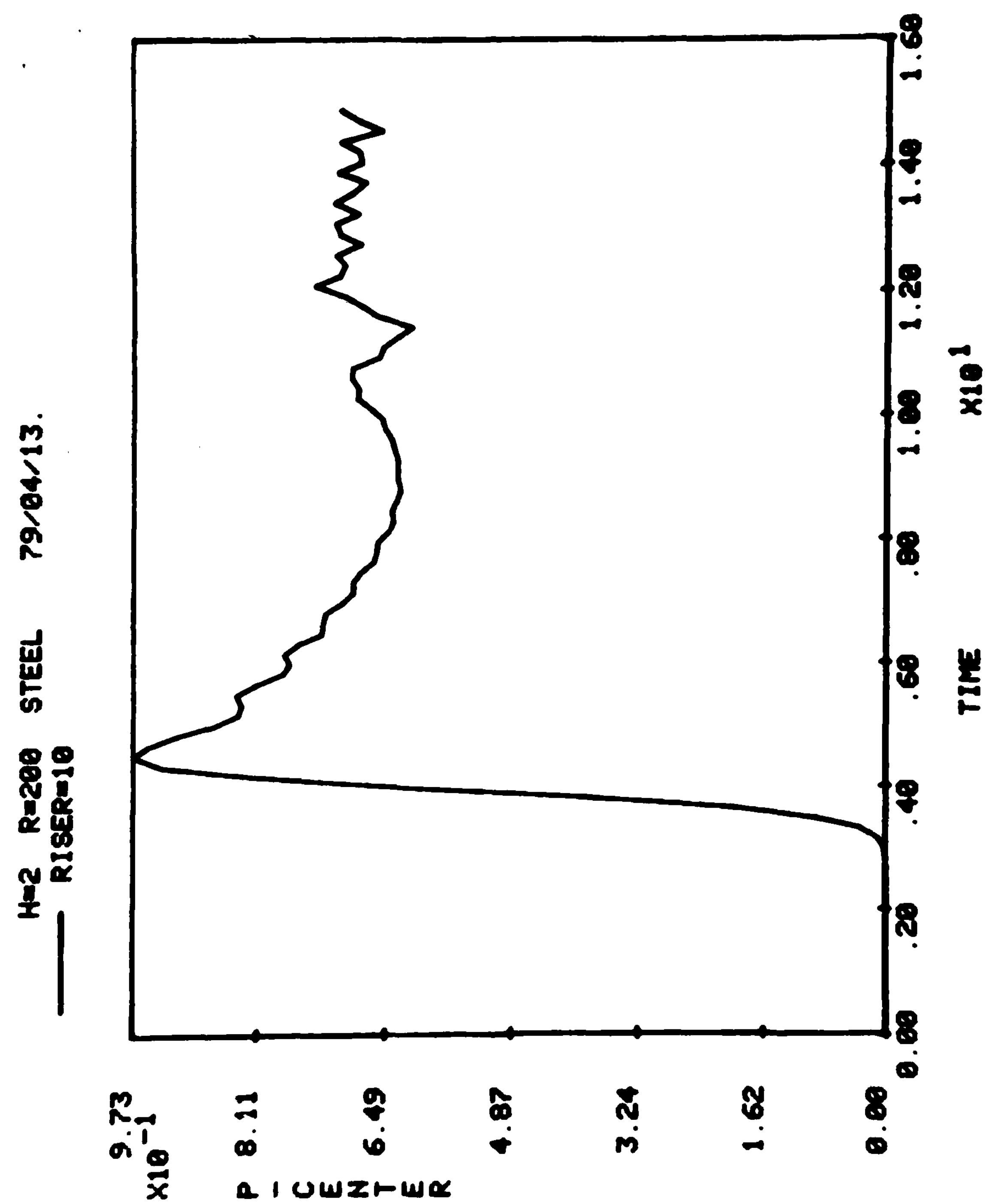

H=2 R=200 STEEL 79/04/13.
RISER=10
P CENTER
X10-1
9.73
8.11
6.49
4.87
3.24
1.62
0.00
0.00
.20
.40
.60
.80
1.00
1.20
1.40
1.60
TIME
X10 1

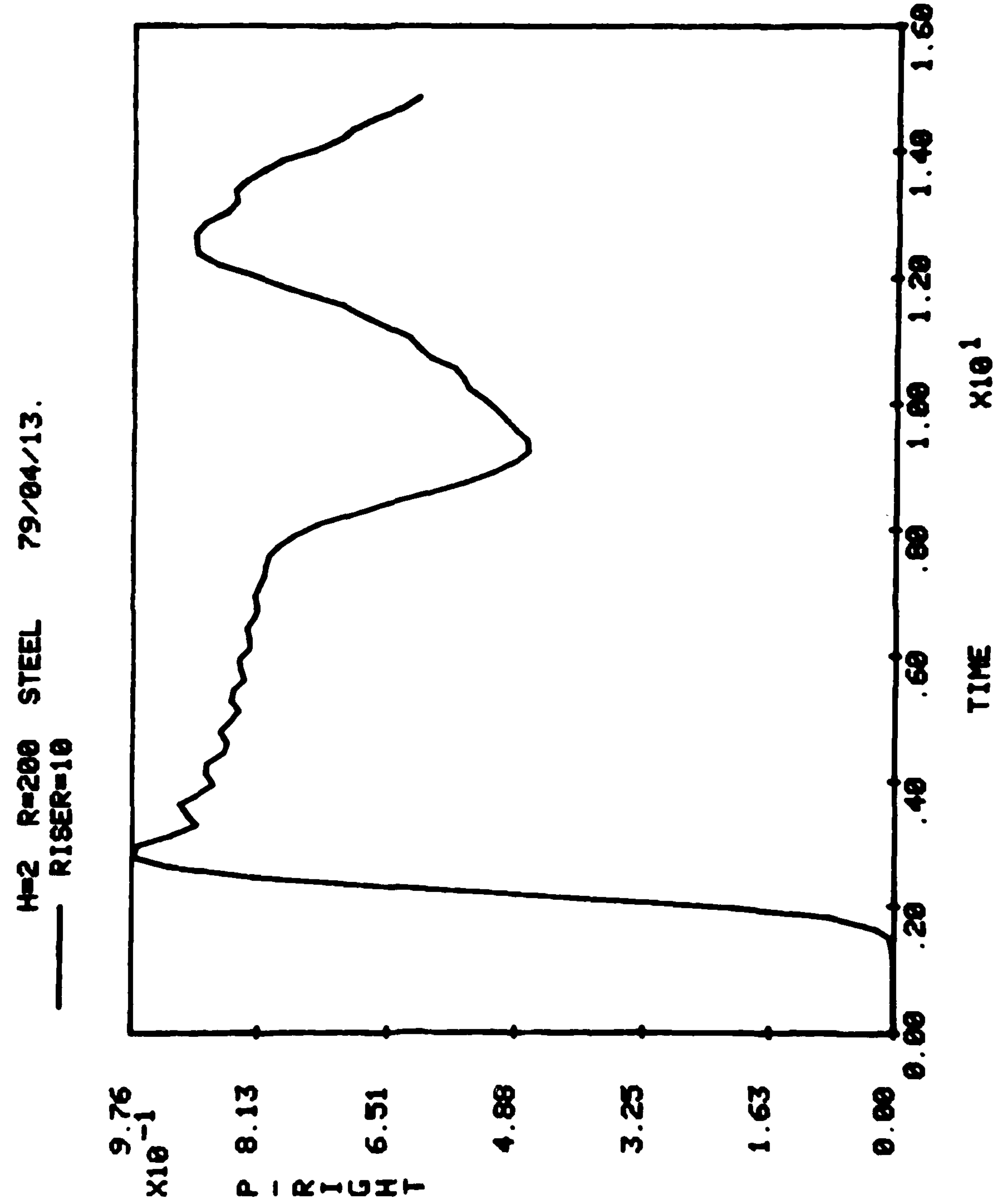
H=2 R=200 STEEL 79/04/13.
RISER=10
P RIGHT
X10-1
9.76
8.13
6.51
4.88
3.25
1.63
0.00
0.00
.20
.40
.60
.80
1.00
1.20
1.40
1.60
TIME
X10 1

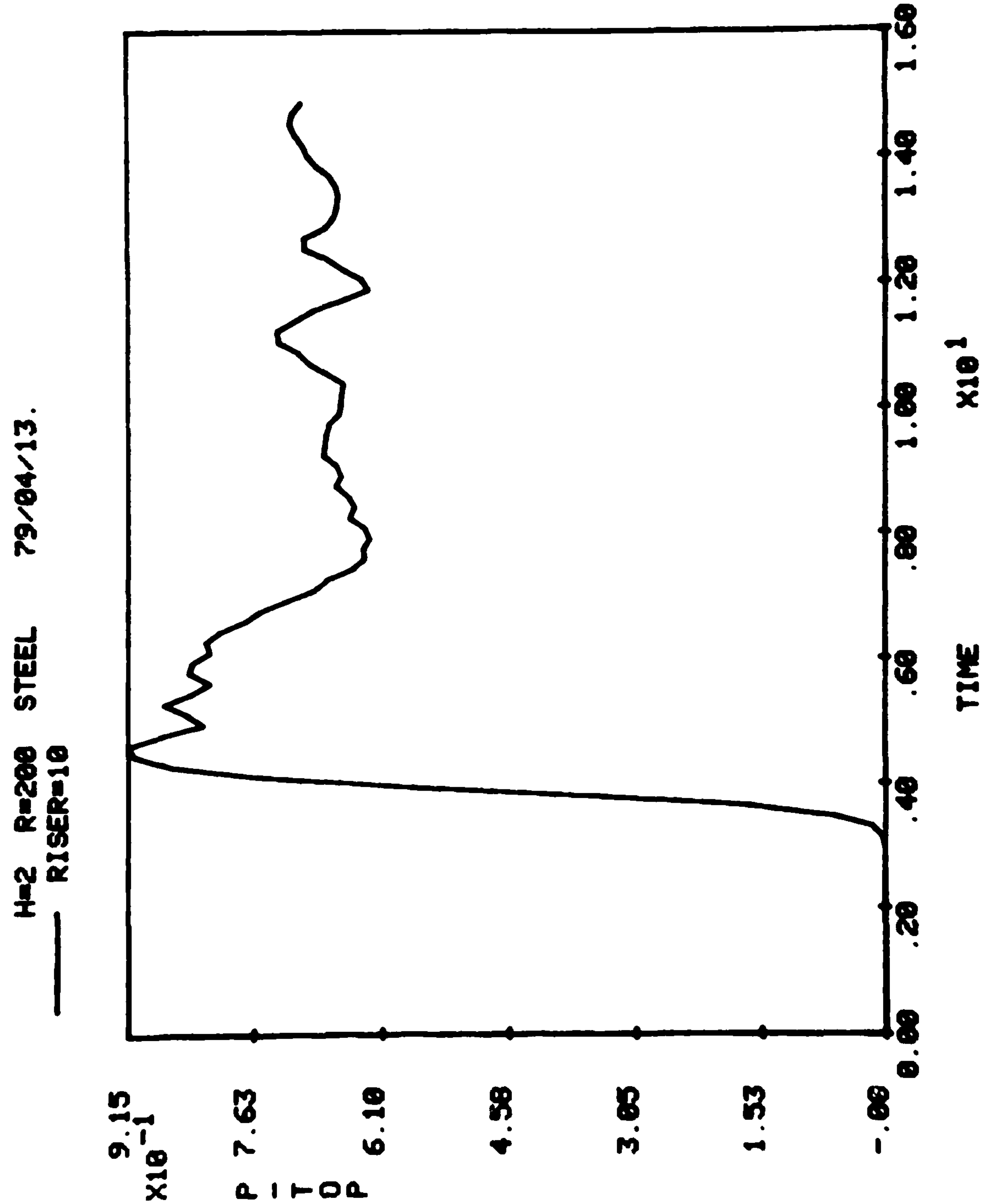

H=2 R=200 STEEL 79/04/13.
RISER=10
9.15
X10^-1
P TOP
7.63
6.10
4.58
3.05
1.53
-.00
0.00
.20
.40
.60
.80
1.00
1.20
1.40
1.60
TIME
X10^1

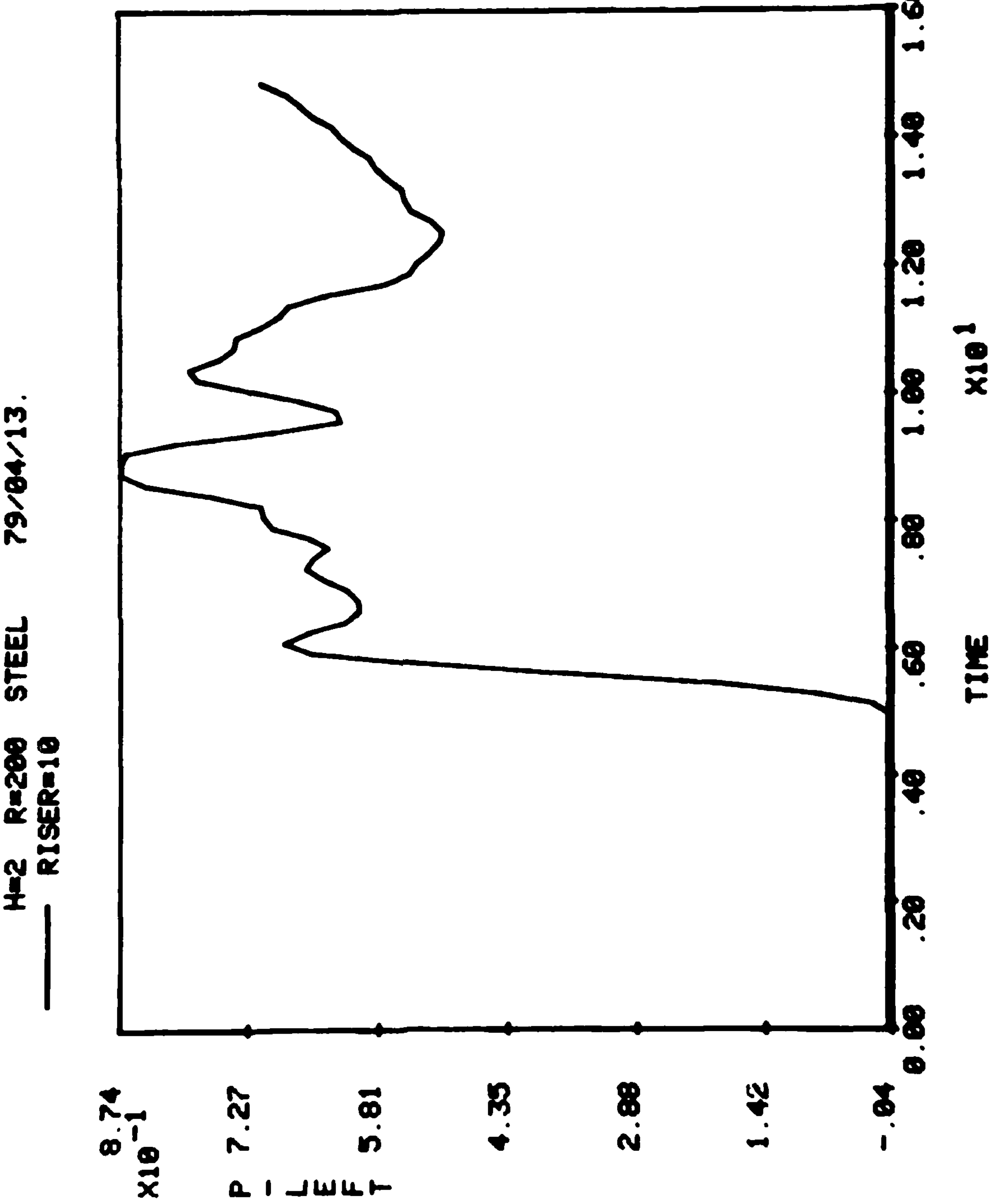
H=2 R=200 STEEL 79/04/13.
RISER=10
P-LEFT
X10^-1
8.74
7.27
5.81
4.35
2.88
1.42
-.04
0.00
.20
.40
.60
.80
1.00
1.20
1.40
1.60
TIME
X10^1

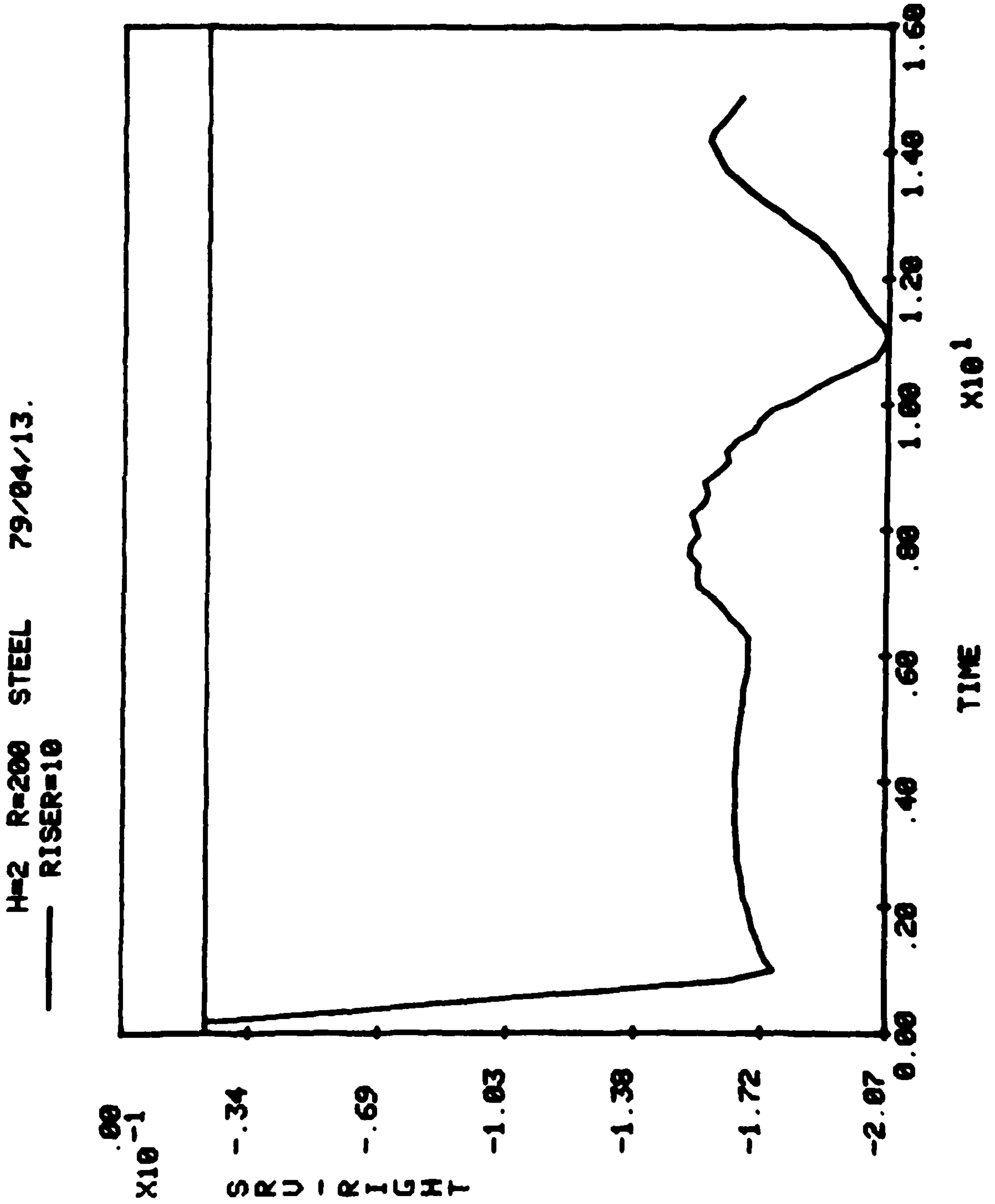
H=2 R=200 STEEL 79/04/13.
RISER=10
.00
X10^-1
-.34
-.69
-1.03
-1.38
-1.72
-2.07
SRU-RIGHT
0.00
.20
.40
.60
.80
1.00
1.20
1.40
1.60
TIME
X10^1

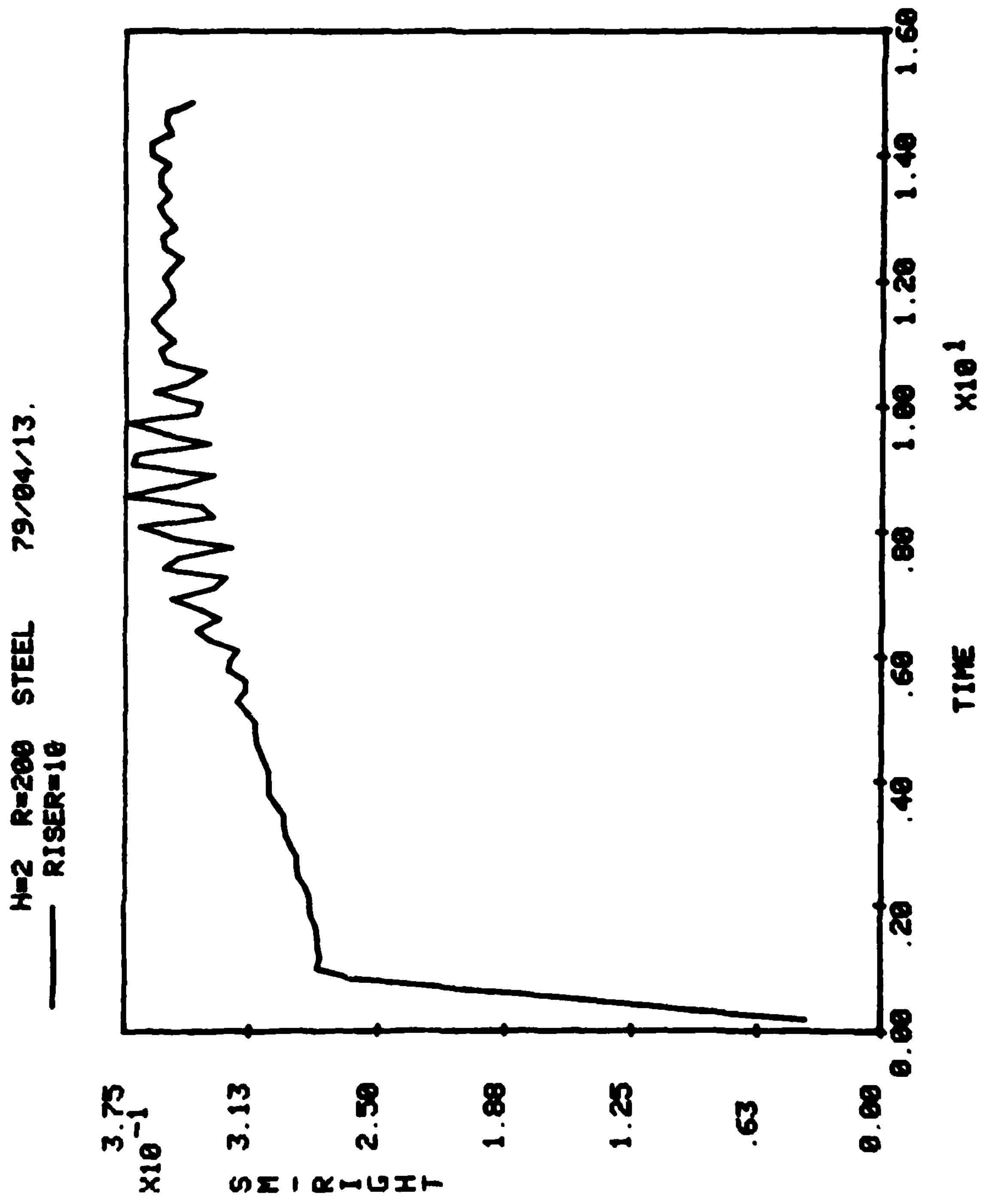

H=2 R=200 STEEL 79/04/13.
RISER=10
3.75
3.13
2.50
1.88
1.25
.63
0.00
X10^-1
SH-RIGHT
0.00
.20
.40
.60
.80
1.00
1.20
1.40
1.60
TIME
X10^1

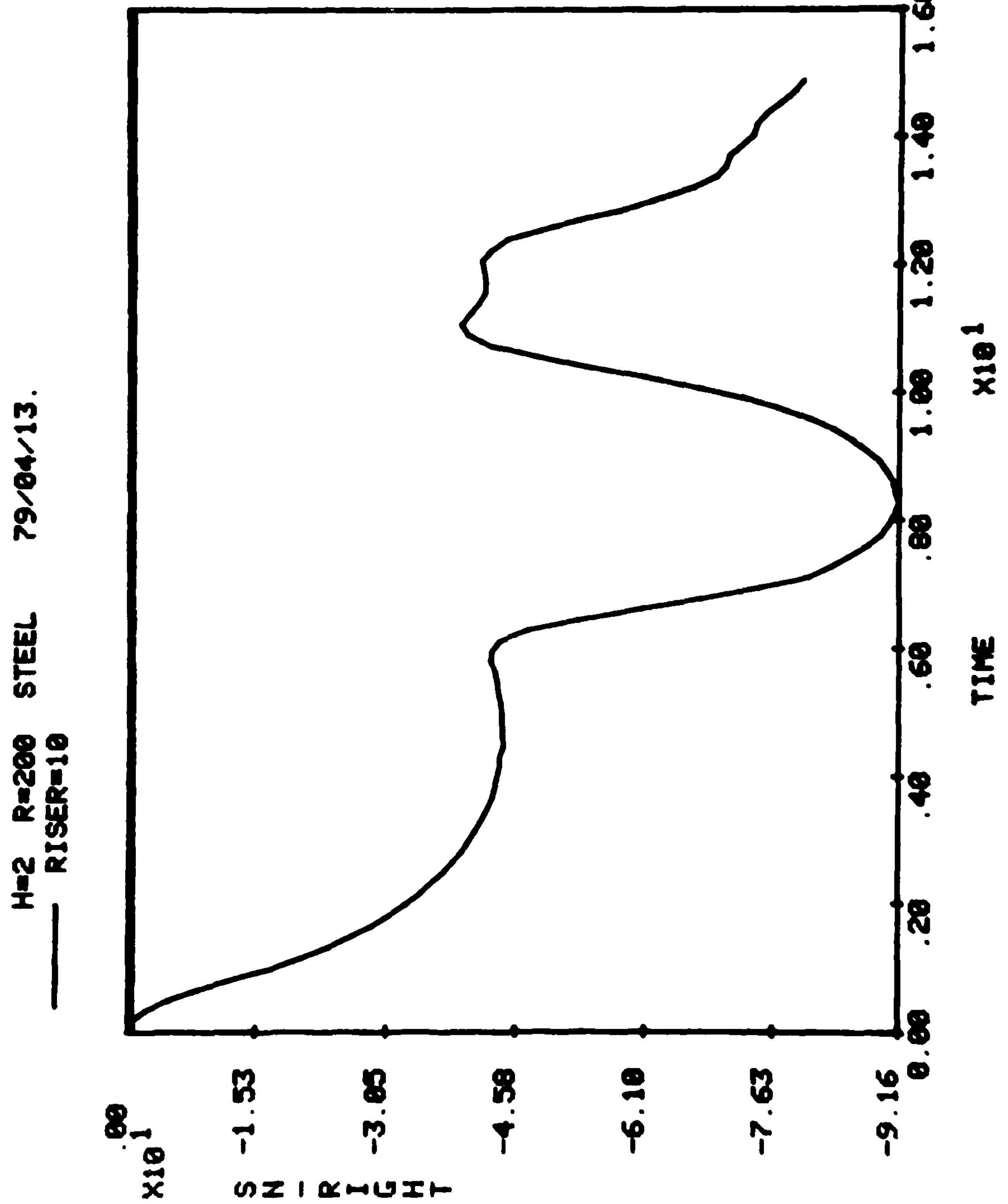
H=2 R=200 STEEL 79/04/13.
RISER=10
SNIRIGHT
X10 1
.00
-1.53
-3.05
-4.58
-6.10
-7.63
-9.16
0.00
.20
.40
.60
.80
1.00
1.20
1.40
1.60
TIME
X10 1

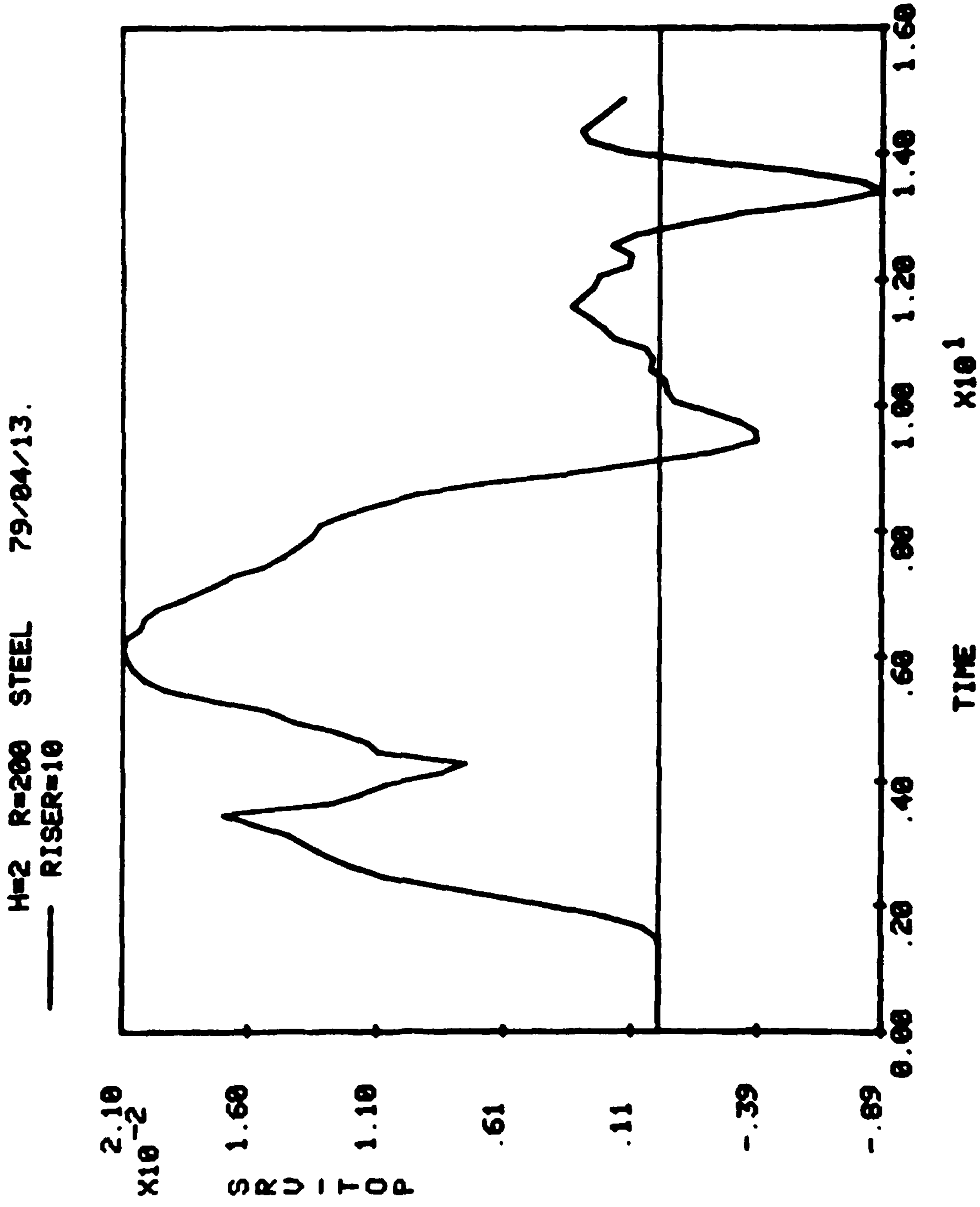
H=2 R=200 STEEL 79/04/13.
RISER=10
2.10
X10^-2
1.60
1.10
.61
.11
-.39
-.89
0.00
.20
.40
.60
.80
1.00
1.20
1.40
1.60
TIME
X10^1

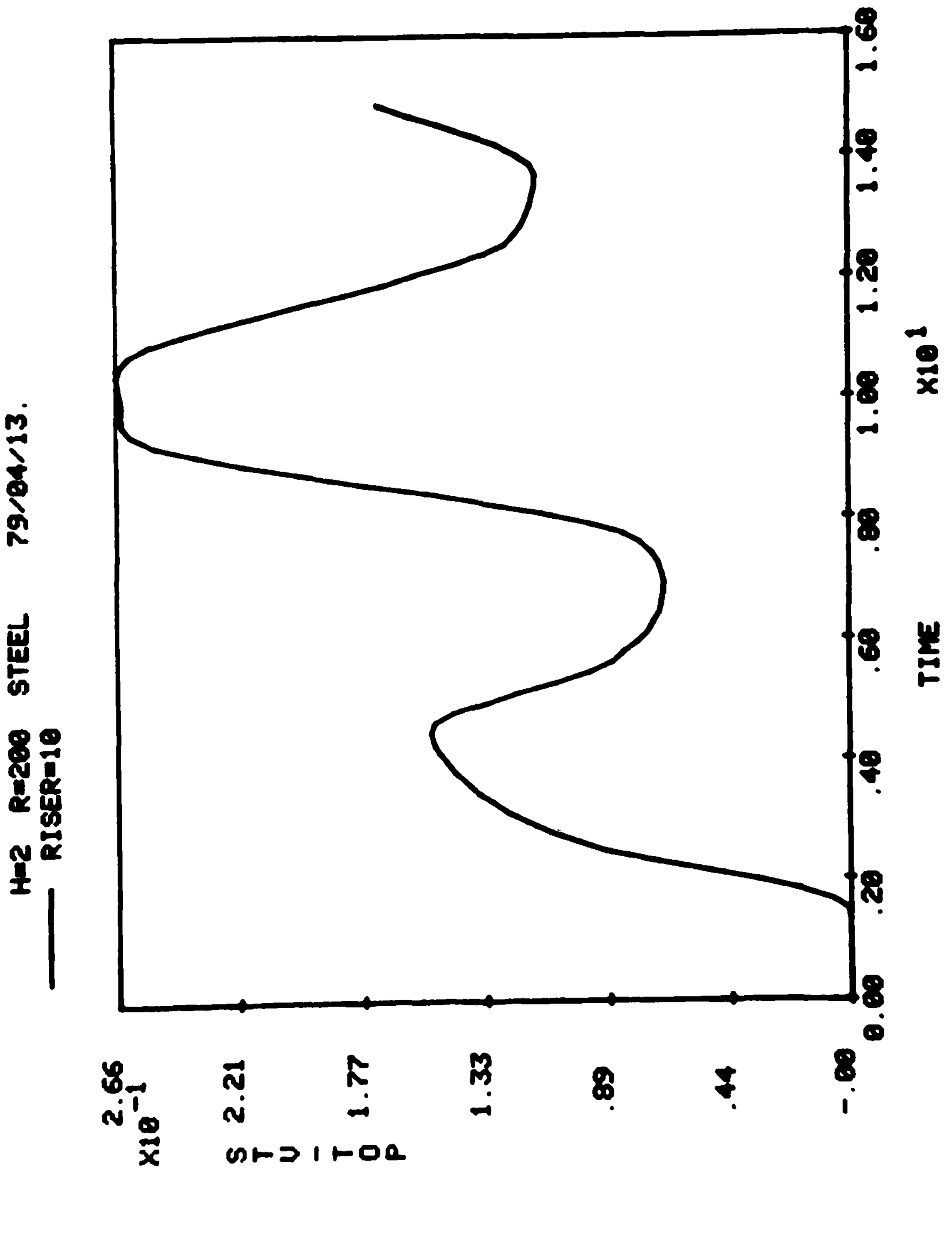

H=2 R=200 STEEL 79/04/13.
RISER=10
2.66
2.21
1.77
1.33
.89
.44
-.00
X10^-1
0.00
.20
.40
.60
.80
1.00
1.20
1.40
1.60
TIME
X10^1

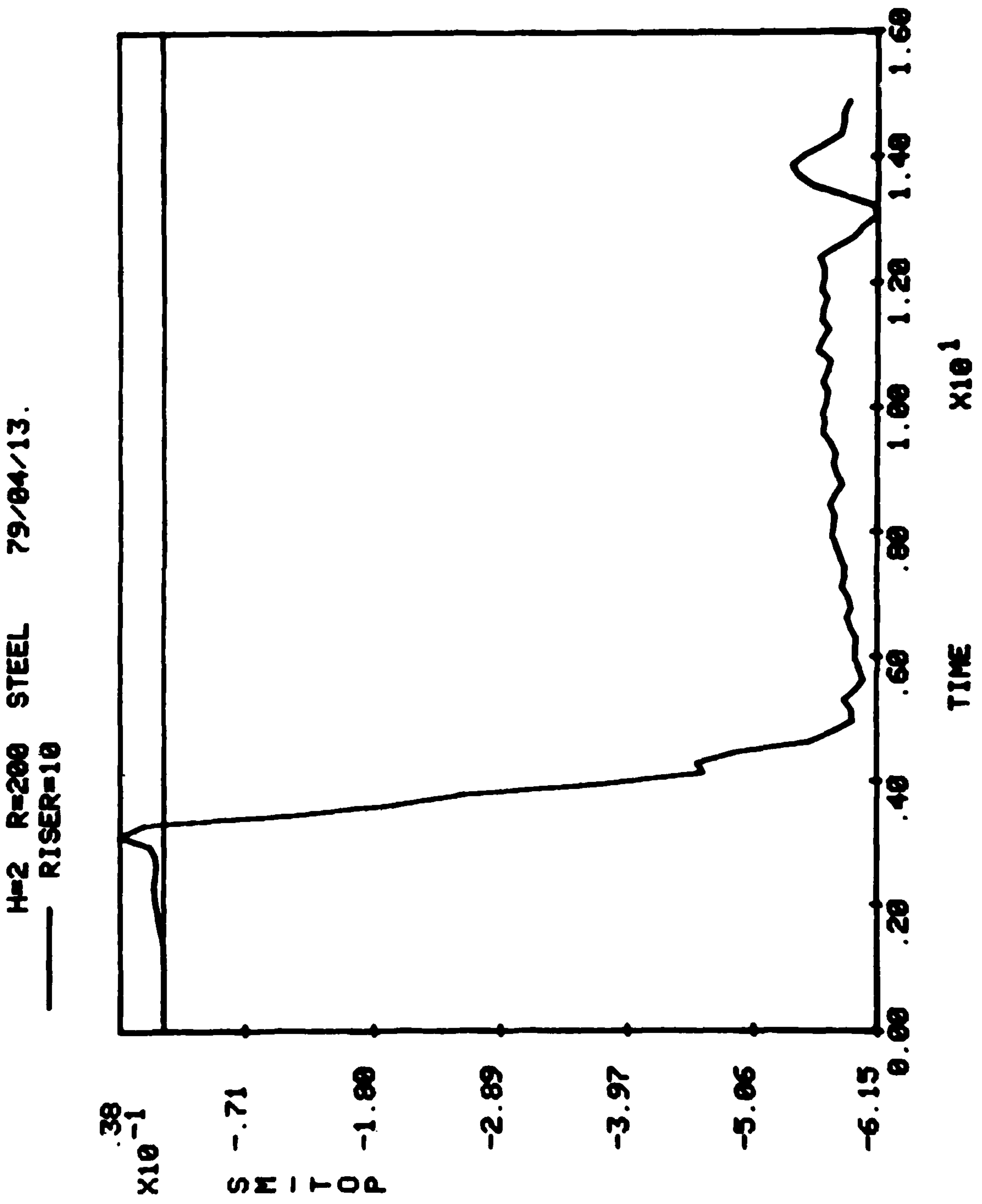
H=2 R=200 STEEL 79/04/13.
RISER=10
.38
X10^-1
-.71
-1.80
-2.89
-3.97
-5.06
-6.15
S
H
-
T
O
P
0.00
.20
.40
.60
.80
1.00
1.20
1.40
1.60
TIME
X10^1

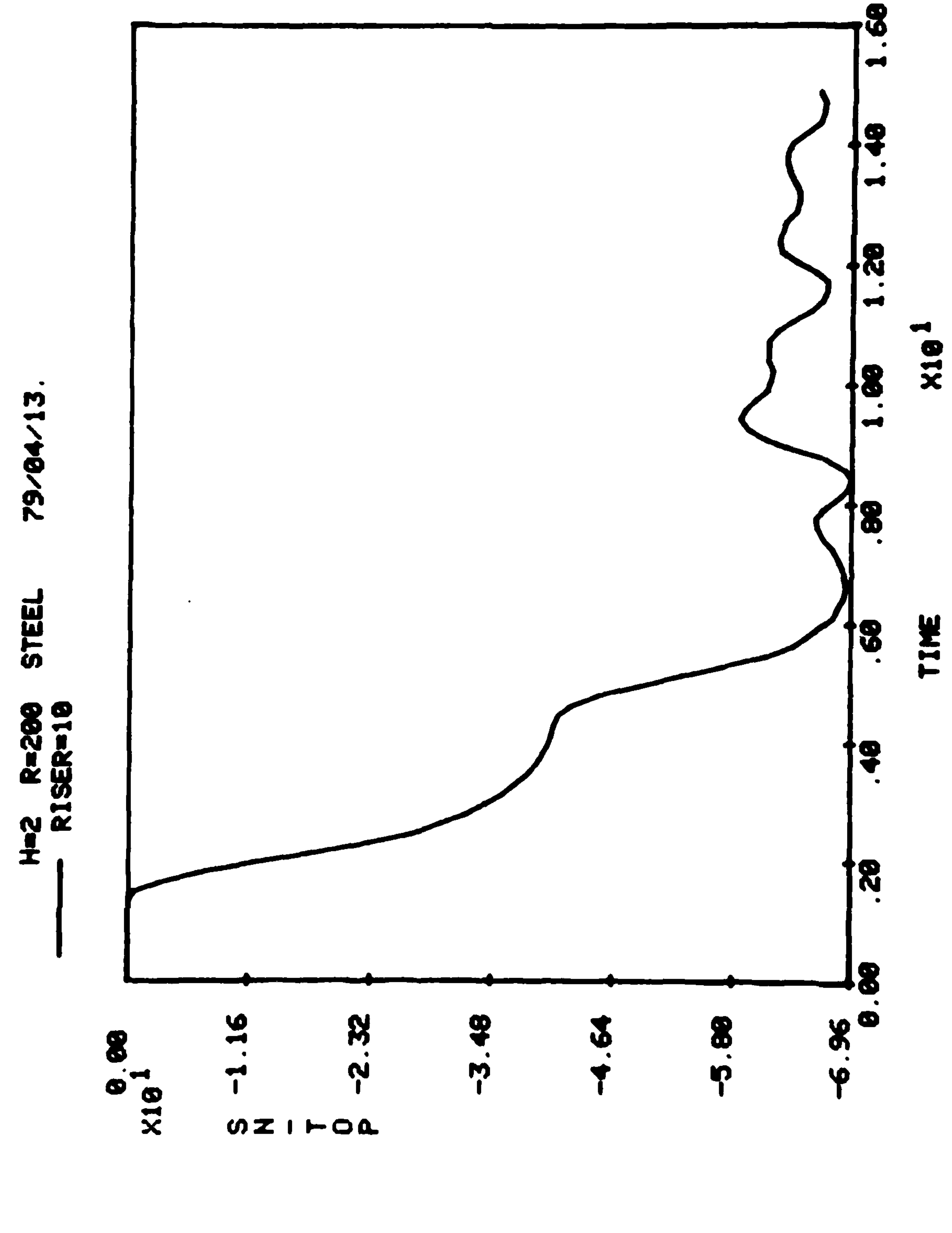
H=2 R=200 STEEL 79/04/13.
RISER=10
POINTS
X10^1
0.00
-1.16
-2.32
-3.48
-4.64
-5.80
-6.96
0.00
.20
.40
.60
.80
1.00
1.20
1.40
1.60
TIME
X10^1

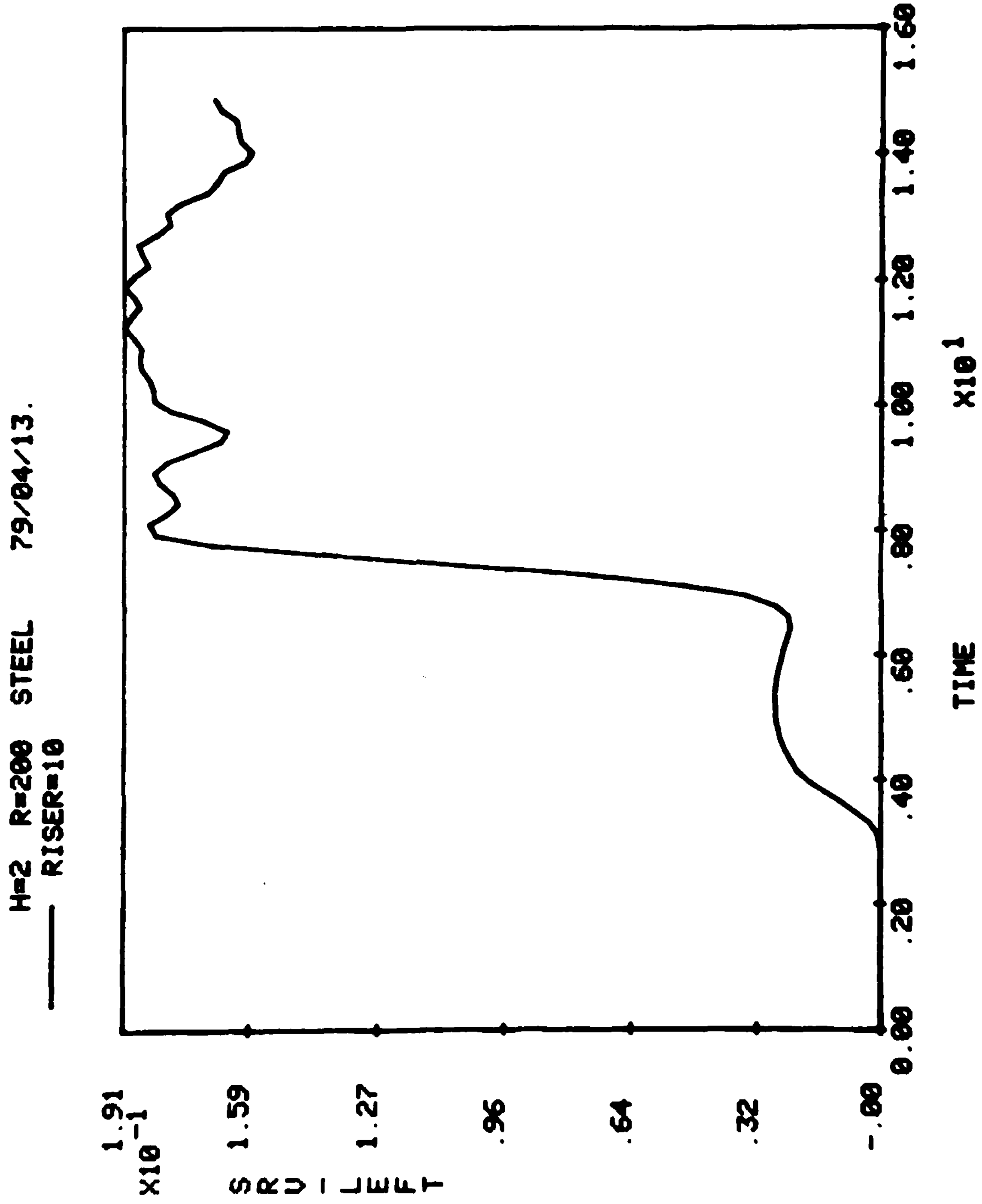

H=2 R=200 STEEL 79/04/13.
RISER=10
1.91
X10^-1
1.59
1.27
.96
.64
.32
-.00
SRVLEFT
0.00
.20
.40
.60
.80
1.00
1.20
1.40
1.60
X10^1
TIME

APPENDIX B (Case B)

RING: Steel

Radius = 100 inches
Thickness = 2 inches

Curve Label:	Meaning
P-CENTER:	pressure at $r = 0$
P-RIGHT:	pressure at $r = a/2$, $\theta = 0$
P-TOP:	pressure at $r = a/2$, $\theta = 90$ deg.
P-LEFT:	pressure at $r = a/2$, $\theta = 180$ deg.
SRV-RIGHT:	shell radial velocity at $\theta = 0$
SM-RIGHT:	shell moment at $\theta = 0$
SN-RIGHT:	shell stress resultant at $\theta = 0$
SRV-TOP:	shell radial velocity at $\theta = 90$ deg.
STV-TOP:	shell tangential velocity at $\theta = 90$
SM-TOP:	shell moment at $\theta = 90$
SN-TOP:	shell stress resultant at $\theta = 90$
SRV-LEFT:	shell radial velocity at $\theta = 180$ deg.

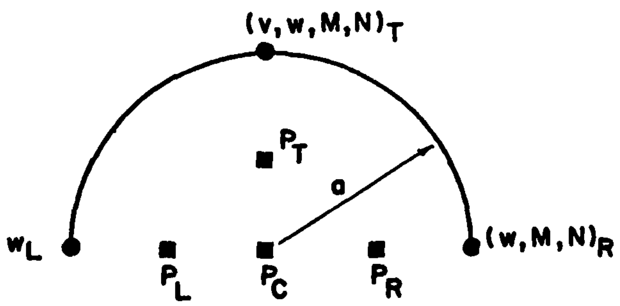

KEY TO TIME HISTORIES IN APPENDICES

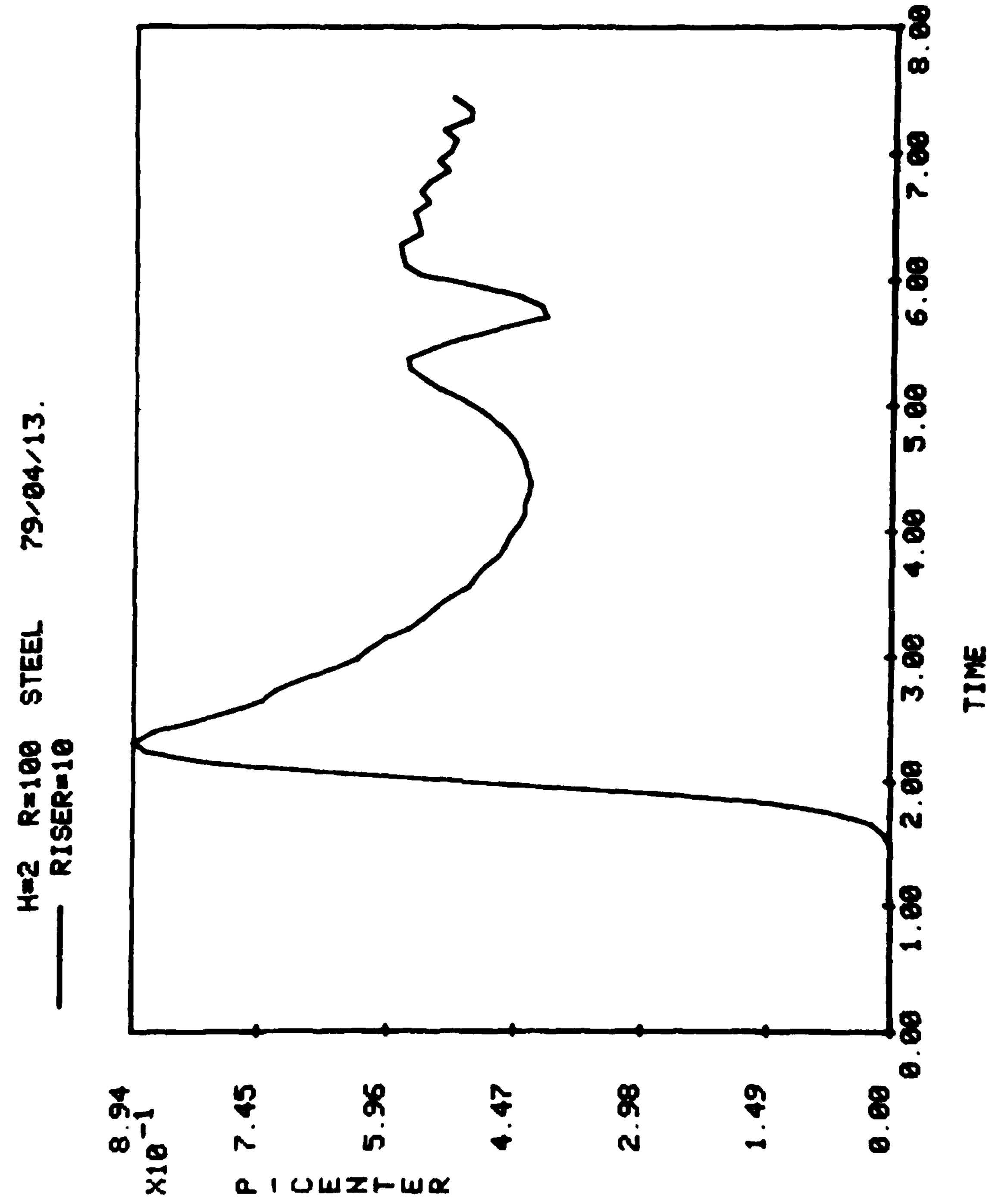
H=2 R=100 STEEL 79/04/13.
RISER=10
8.94
X10^-1
7.45
5.96
4.47
2.98
1.49
0.00
P CENTER
0.00
1.00
2.00
3.00
4.00
5.00
6.00
7.00
8.00
TIME

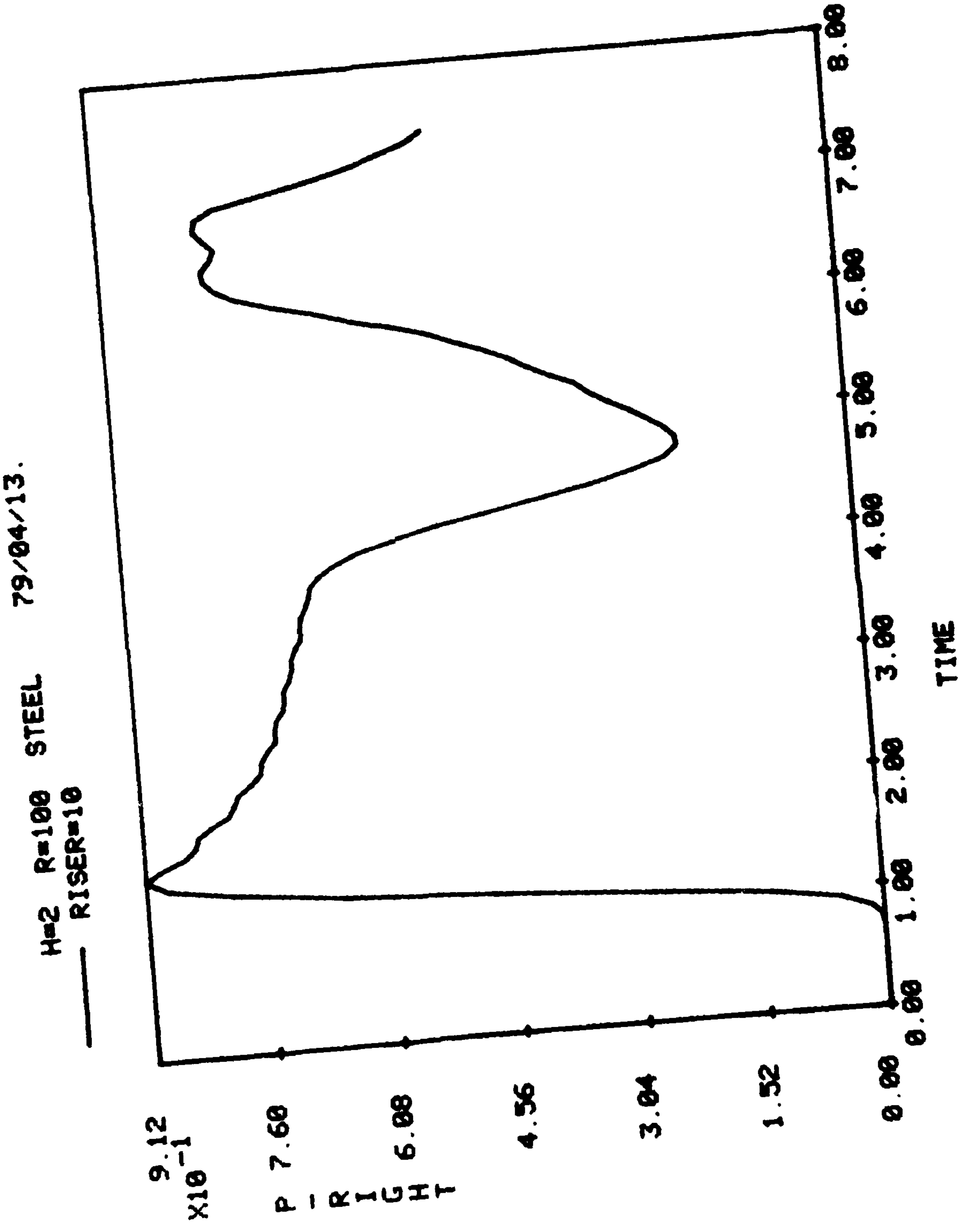

H=2 R=100 STEEL 79/04/13.
RISER=10
9.12
X10^-1
7.60
6.08
4.56
3.04
1.52
0.00
P RIGHT
0.00
1.00
2.00
3.00
4.00
5.00
6.00
7.00
8.00
TIME

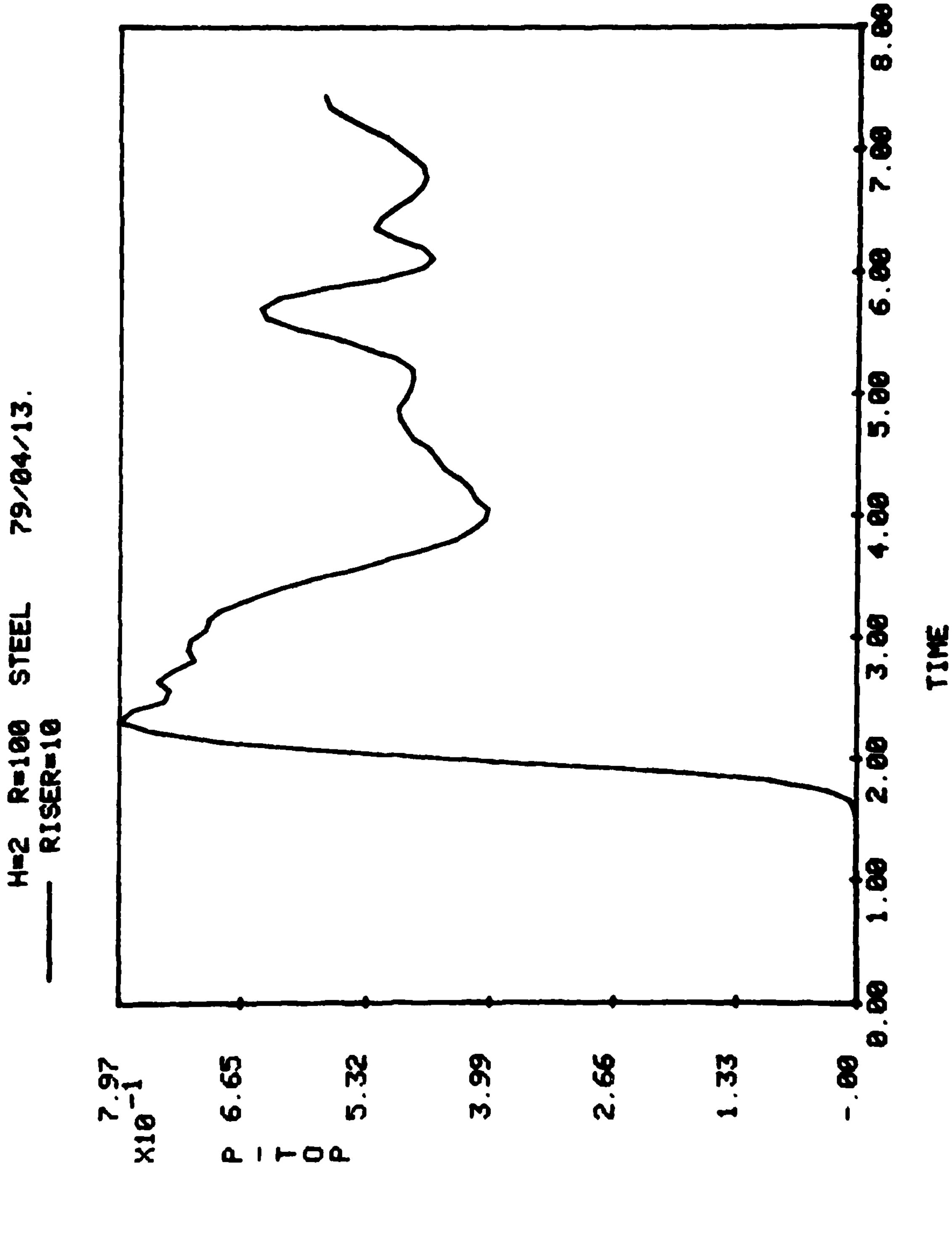

H=2 R=100 STEEL 79/04/13.
RISER=10
P-TOP
7.97
X10^{-1}
6.65
5.32
3.99
2.66
1.33
-.00
0.00
1.00
2.00
3.00
4.00
5.00
6.00
7.00
8.00
TIME

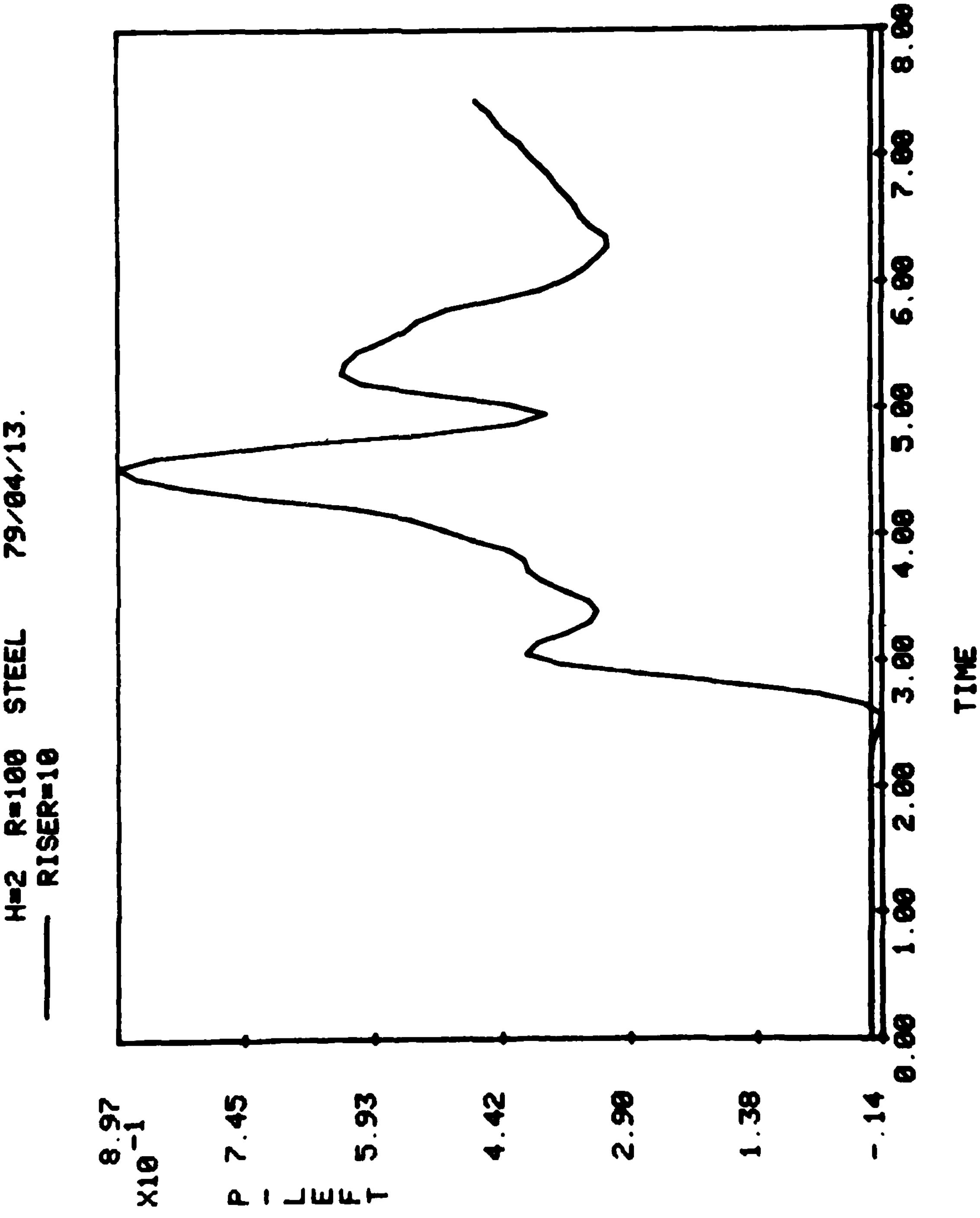
H=2 R=100 STEEL 79/04/13.
RISER=10
P-LEFT
X10^-1
8.97
7.45
5.93
4.42
2.90
1.38
-.14
0.00
1.00
2.00
3.00
4.00
5.00
6.00
7.00
8.00
TIME

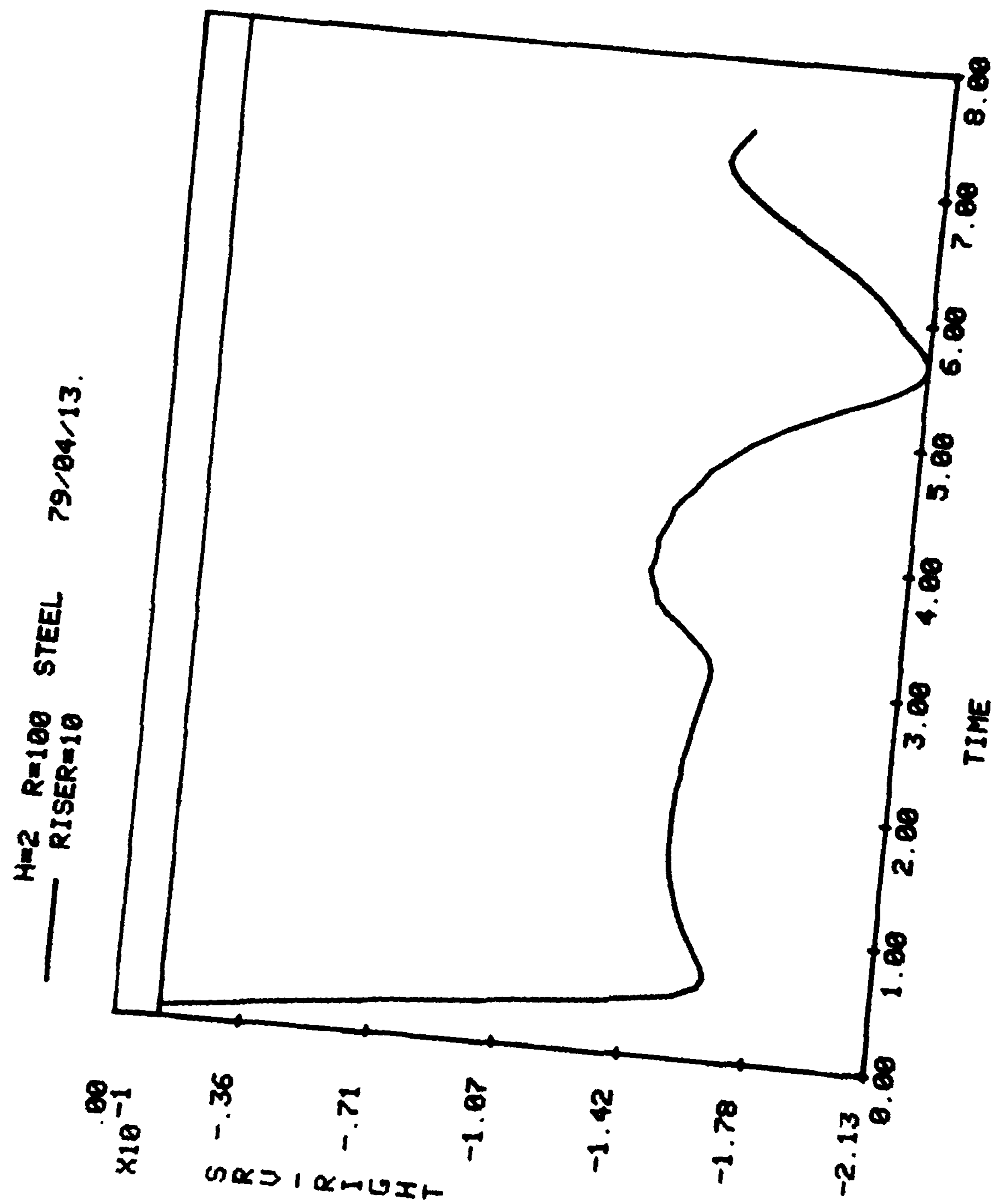
H=2 R=100 STEEL 79/04/13.
RISER=10
X10^-1
SRU-RIGHT
.00
-.36
-.71
-1.07
-1.42
-1.78
-2.13
0.00
1.00
2.00
3.00
4.00
5.00
6.00
7.00
8.00
TIME

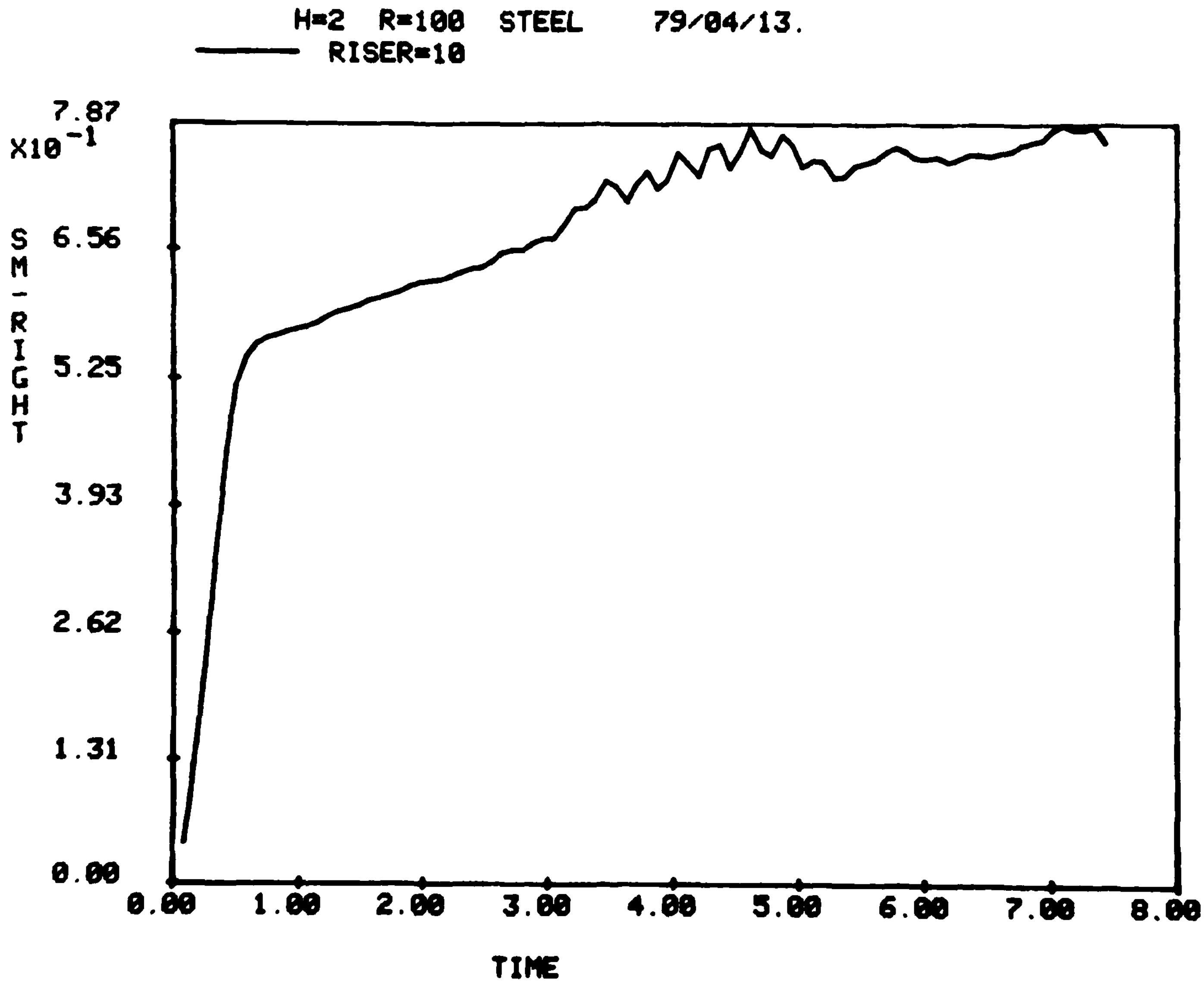
H=2 R=100 STEEL 79/04/13.
RISER=10
7.87
X10^-1
6.56
5.25
3.93
2.62
1.31
0.00
SM-RIGHT
0.00
1.00
2.00
3.00
4.00
5.00
6.00
7.00
8.00
TIME

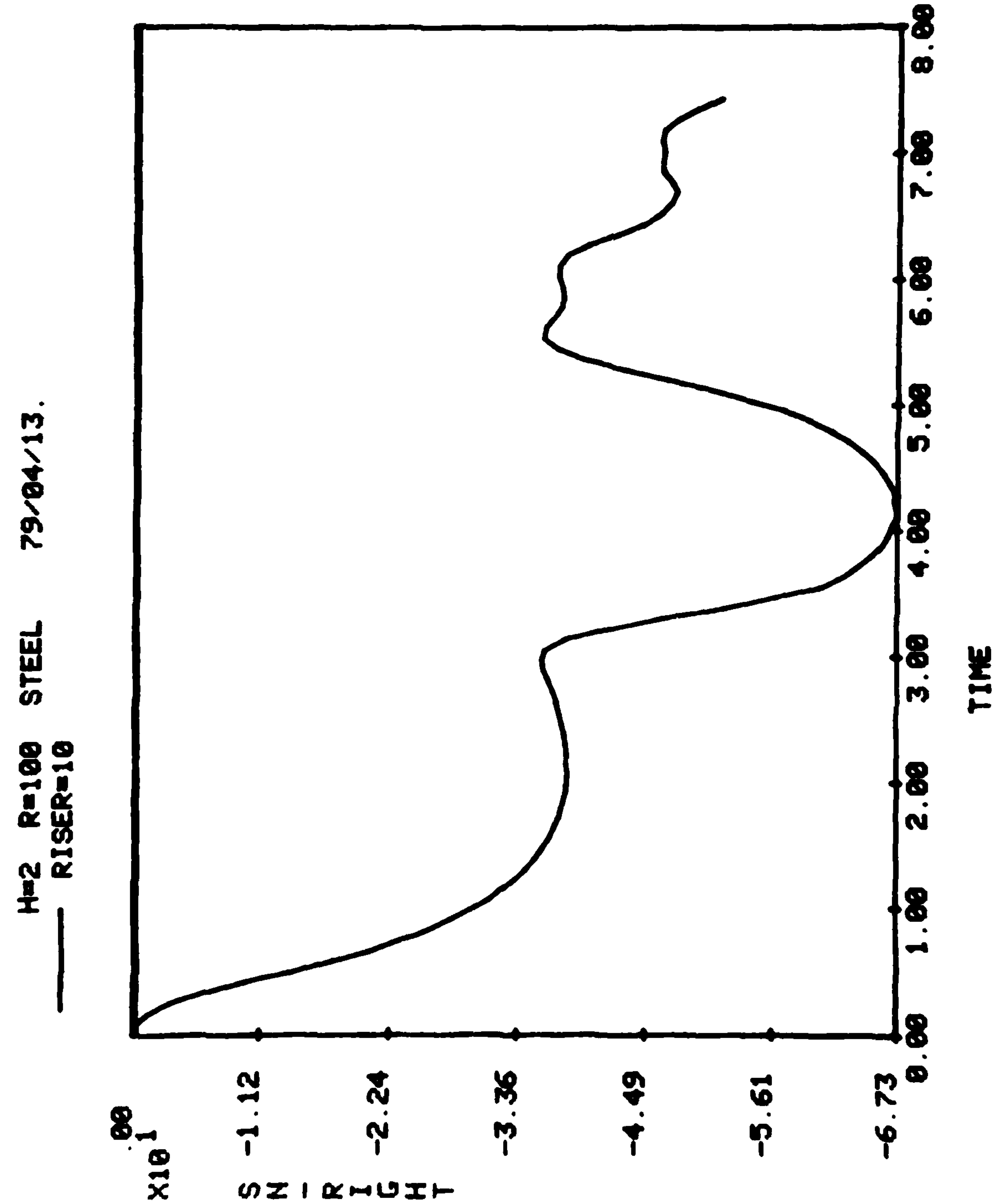

H=2 R=100 STEEL 79/04/13.
RISER=10
X10^1
.00
-1.12
-2.24
-3.36
-4.49
-5.61
-6.73
0.00
1.00
2.00
3.00
4.00
5.00
6.00
7.00
8.00
TIME

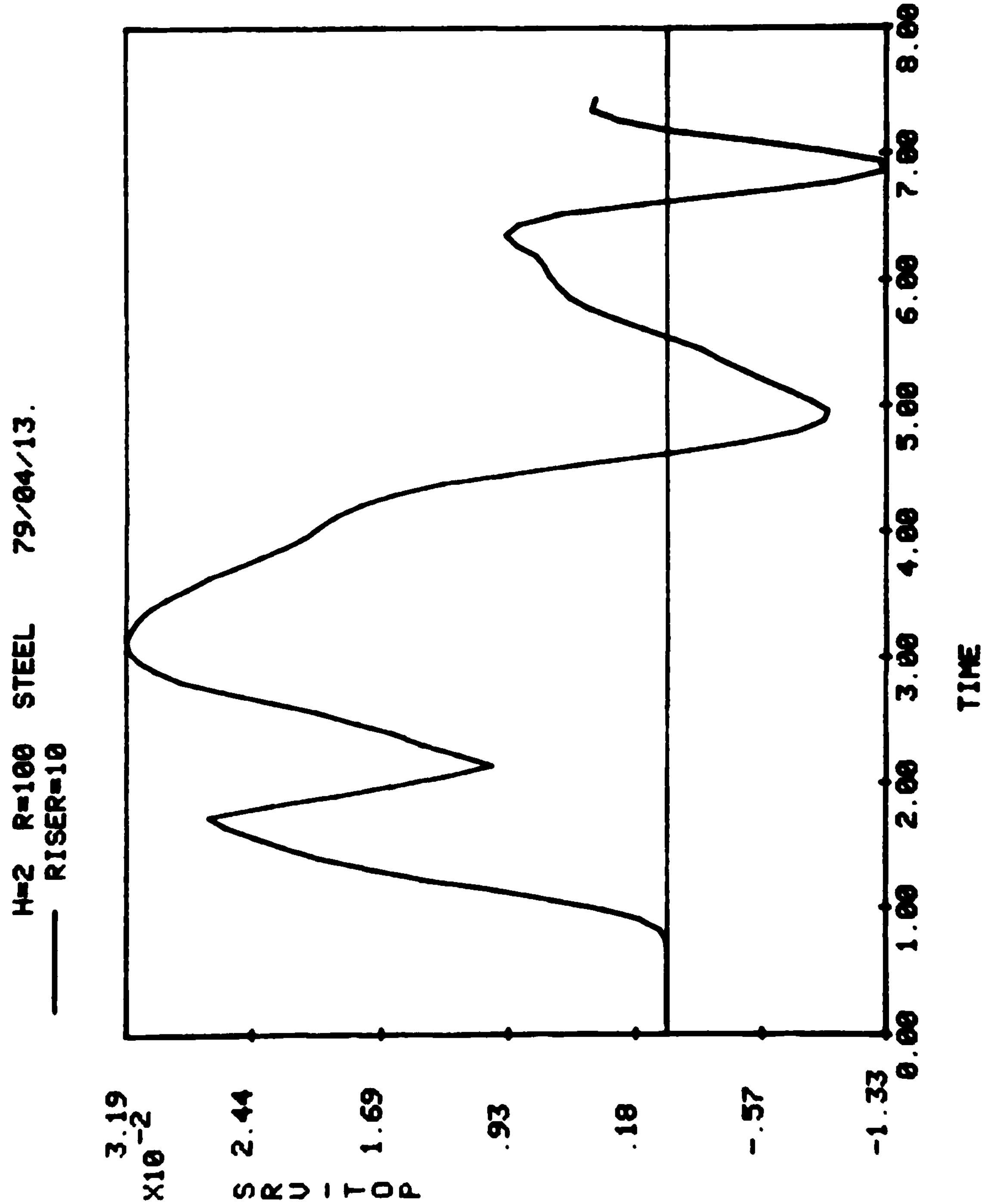
H=2 R=100 STEEL 79/04/13.
RISER=10
3.19
X10^-2
2.44
1.69
.93
.18
-.57
-1.33
0.00
1.00
2.00
3.00
4.00
5.00
6.00
7.00
8.00
TIME

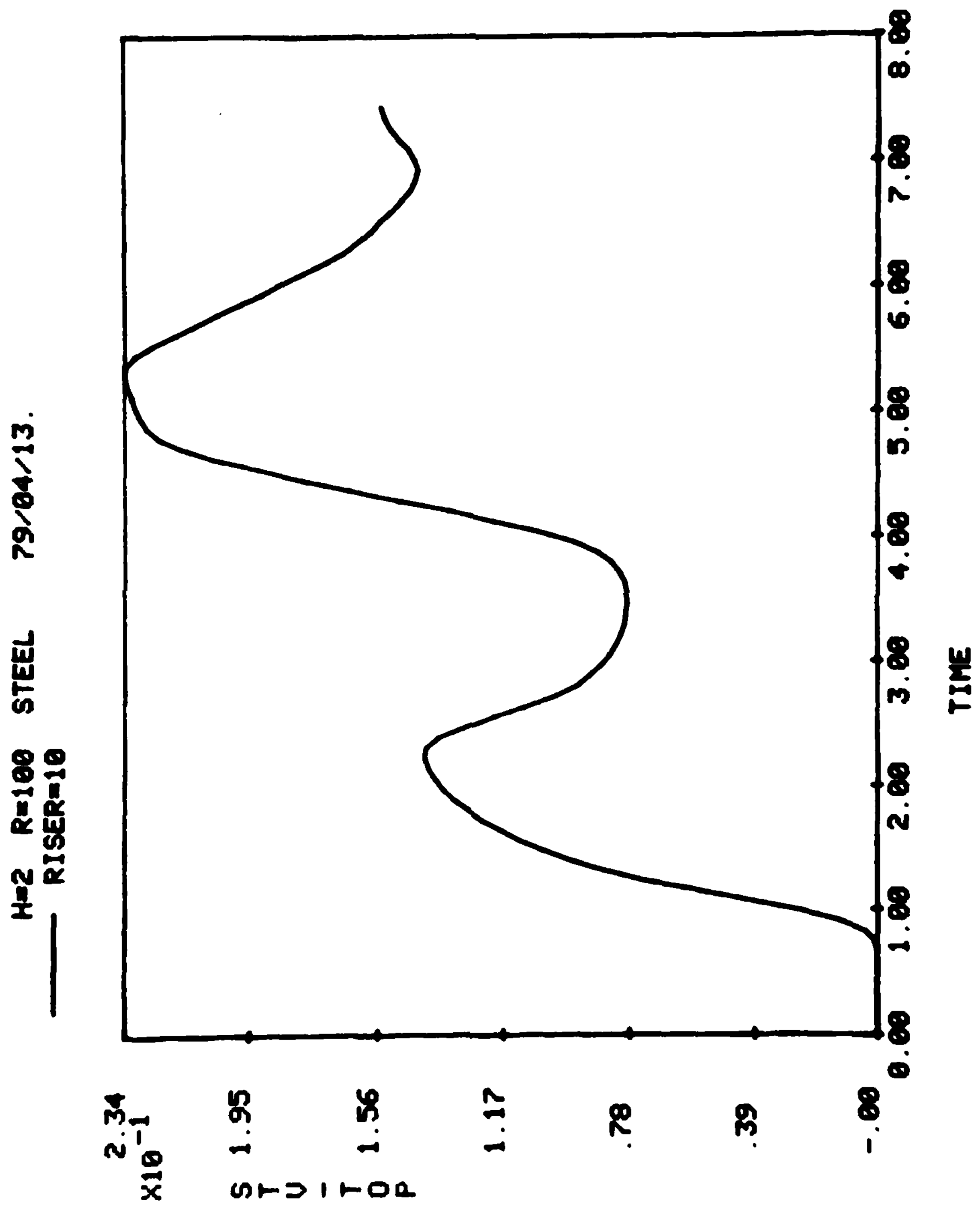
H=2 R=100 STEEL 79/04/13.
RISER=10
2.34
X10^-1
1.95
1.56
1.17
.78
.39
-.00
STUTTOP
0.00
1.00
2.00
3.00
4.00
5.00
6.00
7.00
8.00
TIME

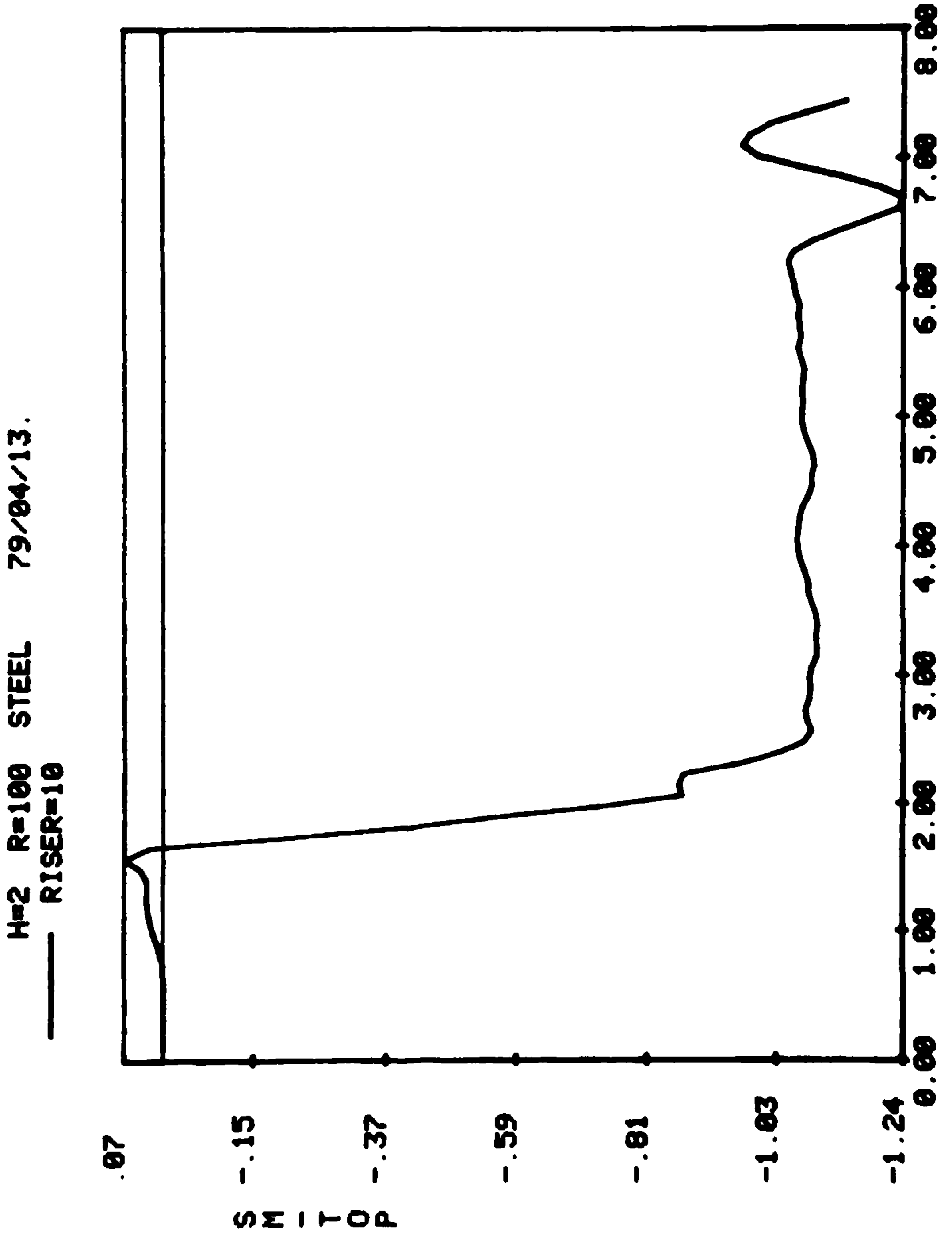
H=2 R=100 STEEL 79/04/13.
RISER=10
.07
-.15
-.37
-.59
-.81
-1.03
-1.24
0.00
1.00
2.00
3.00
4.00
5.00
6.00
7.00
8.00
TIME

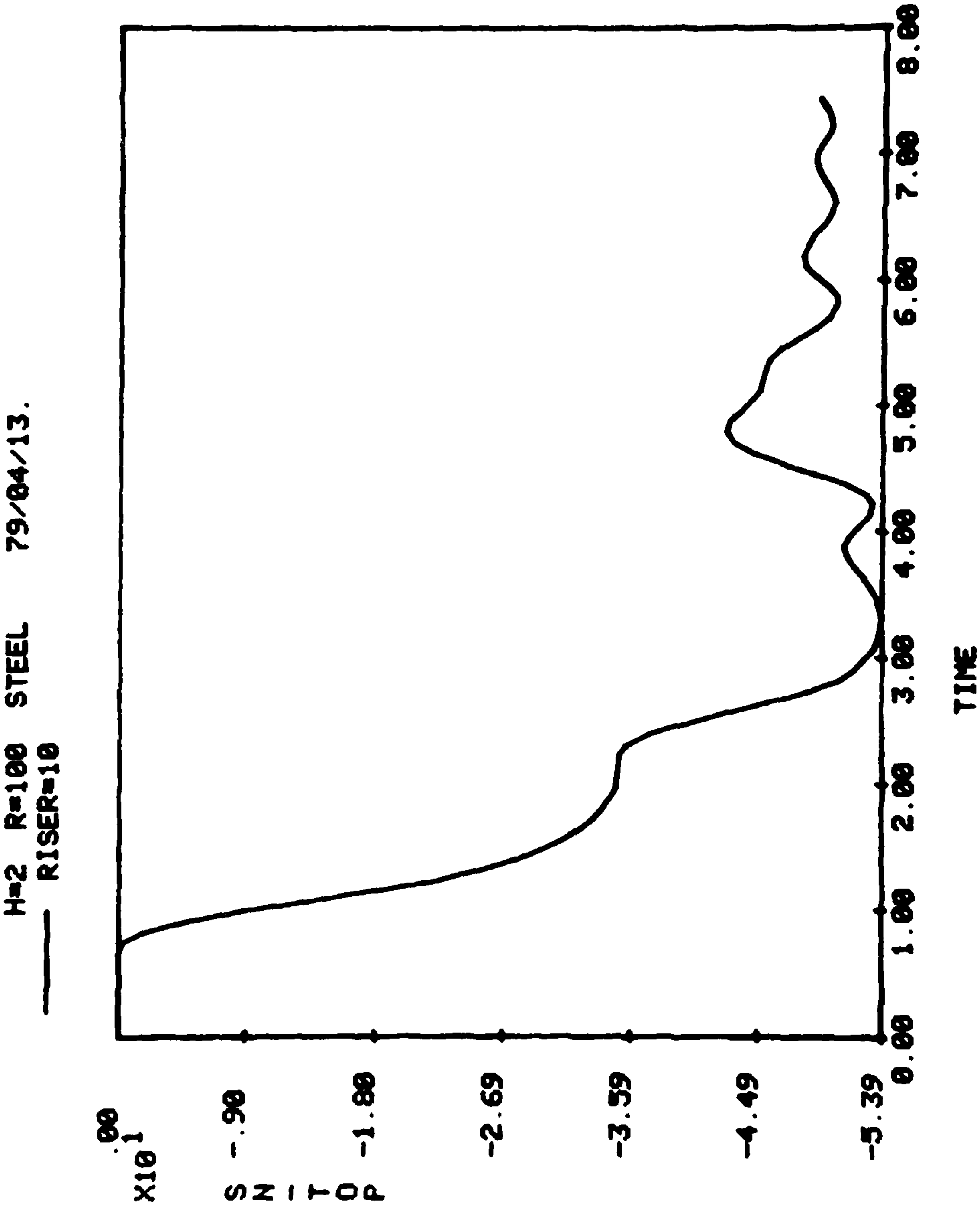

H=2 R=100 STEEL 79/04/13.
RISER=10
X10^1
POINTS
.00
-.90
-1.80
-2.69
-3.59
-4.49
-5.39
0.00
1.00
2.00
3.00
4.00
5.00
6.00
7.00
8.00
TIME

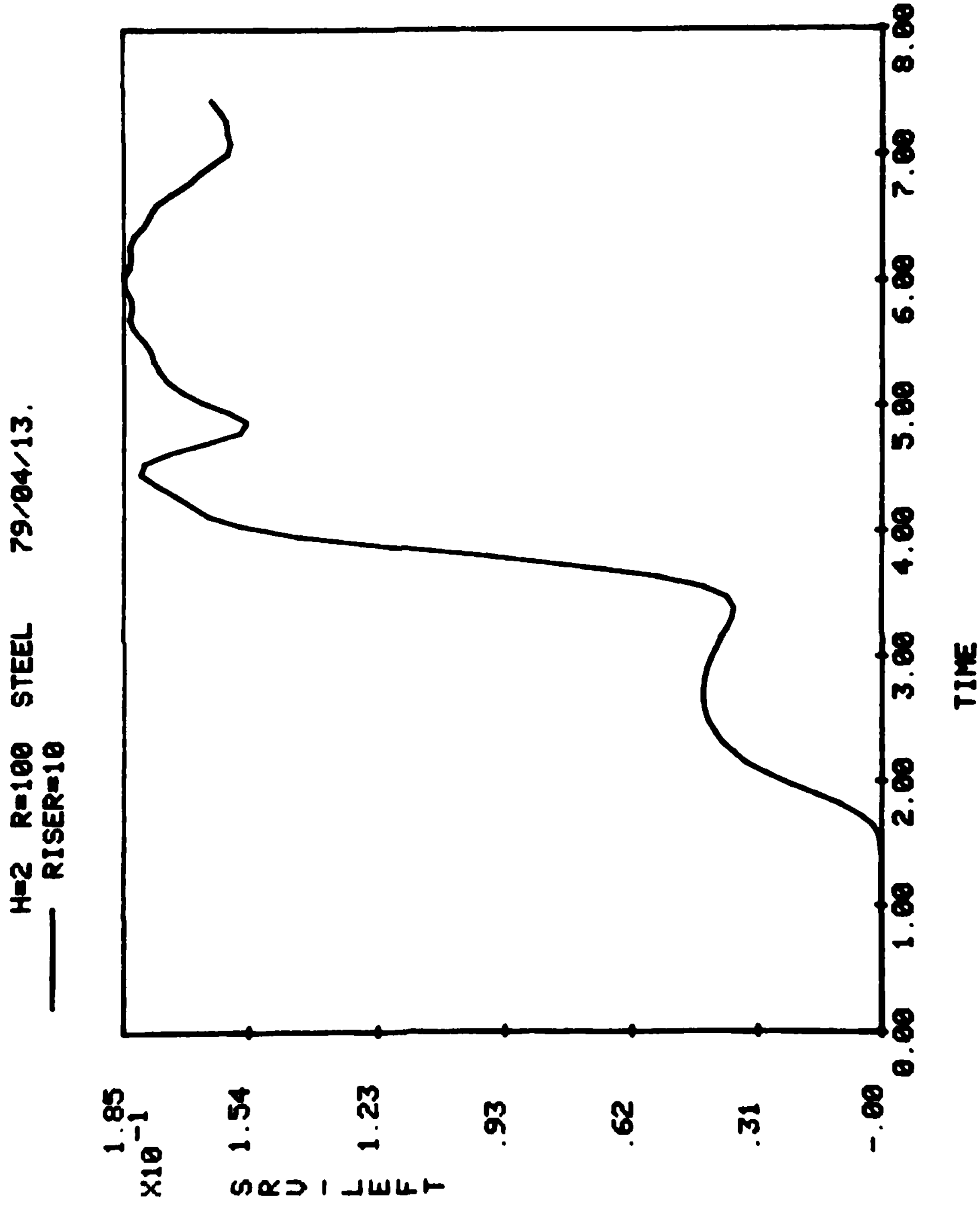
H=2 R=100 STEEL 79/04/13.
RISER=10
1.85
X10^-1
1.54
1.23
.93
.62
.31
-.00
SRU-LEFT
0.00
1.00
2.00
3.00
4.00
5.00
6.00
7.00
8.00
TIME

APPENDIX C (Case C)

RING: Steel

Radius = 100 inches
Thickness = 0.5 inches

Curve Label:	Meaning
P-CENTER:	pressure at r = 0
P-RIGHT:	pressure at r = a/2, θ = 0
P-TOP:	pressure at r = a/2, θ = 90 deg.
P-LEFT:	pressure at r = a/2, θ = 180 deg.
SRV-RIGHT:	shell radial velocity at θ = 0
SM-RIGHT:	shell moment at θ = 0
SN-RIGHT:	shell stress resultant at θ = 0
SRV-TOP:	shell radial velocity at θ = 90 deg.
STV-TOP:	shell tangential velocity at θ = 90
SM-TOP:	shell moment at θ = 90
SN-TOP:	shell stress resultant at θ = 90
SRV-LEFT:	shell radial velocity at θ = 180 deg.

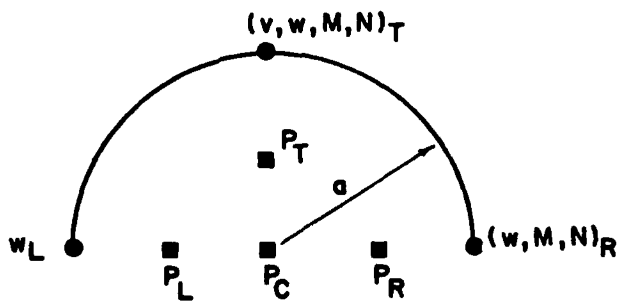

KEY TO TIME HISTORIES IN APPENDICES

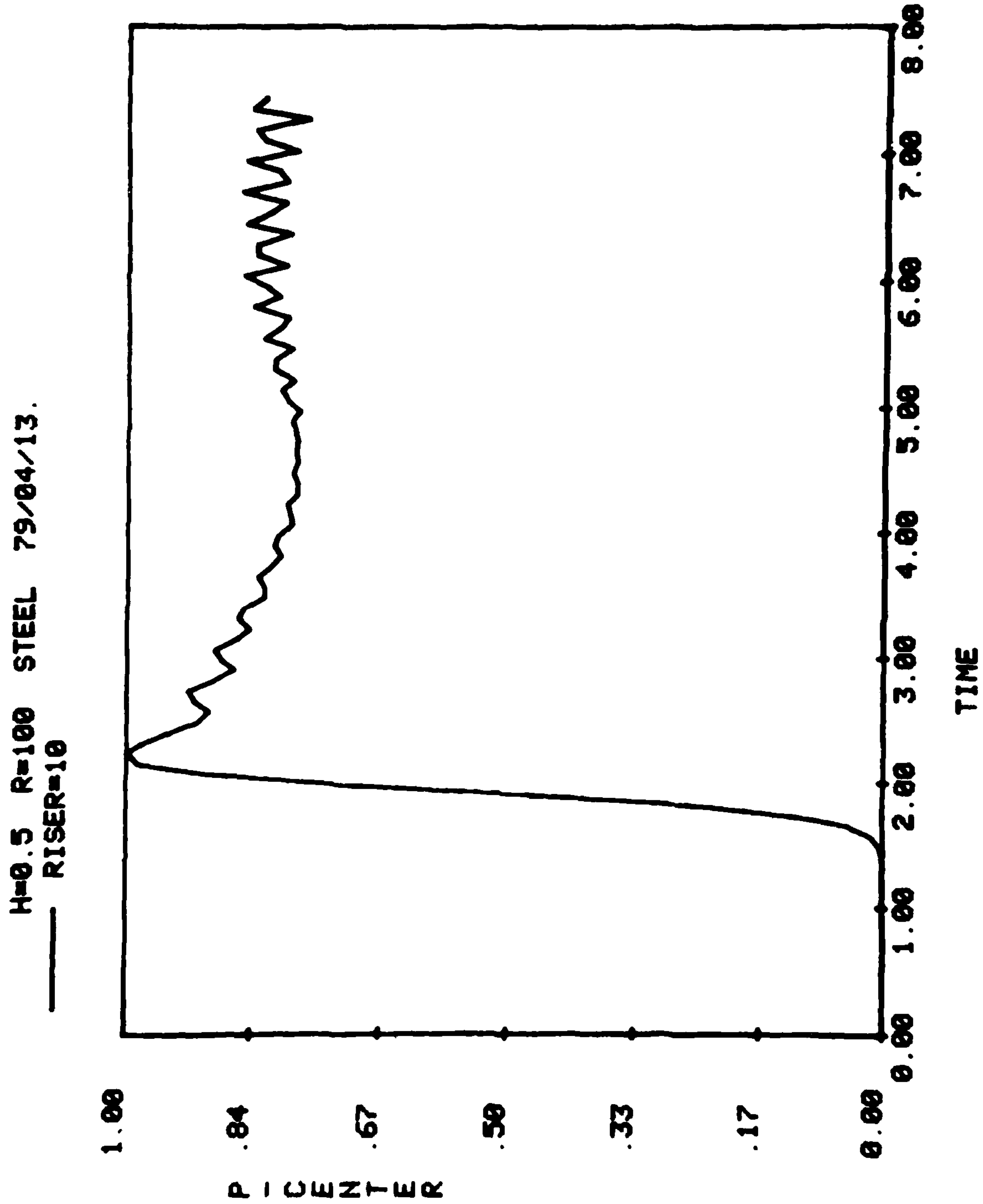

H=0.5 R=100 STEEL 79/04/13.
RISER=10
P-CENTER
TIME
1.00
.84
.67
.50
.33
.17
0.00
0.00
1.00
2.00
3.00
4.00
5.00
6.00
7.00
8.00

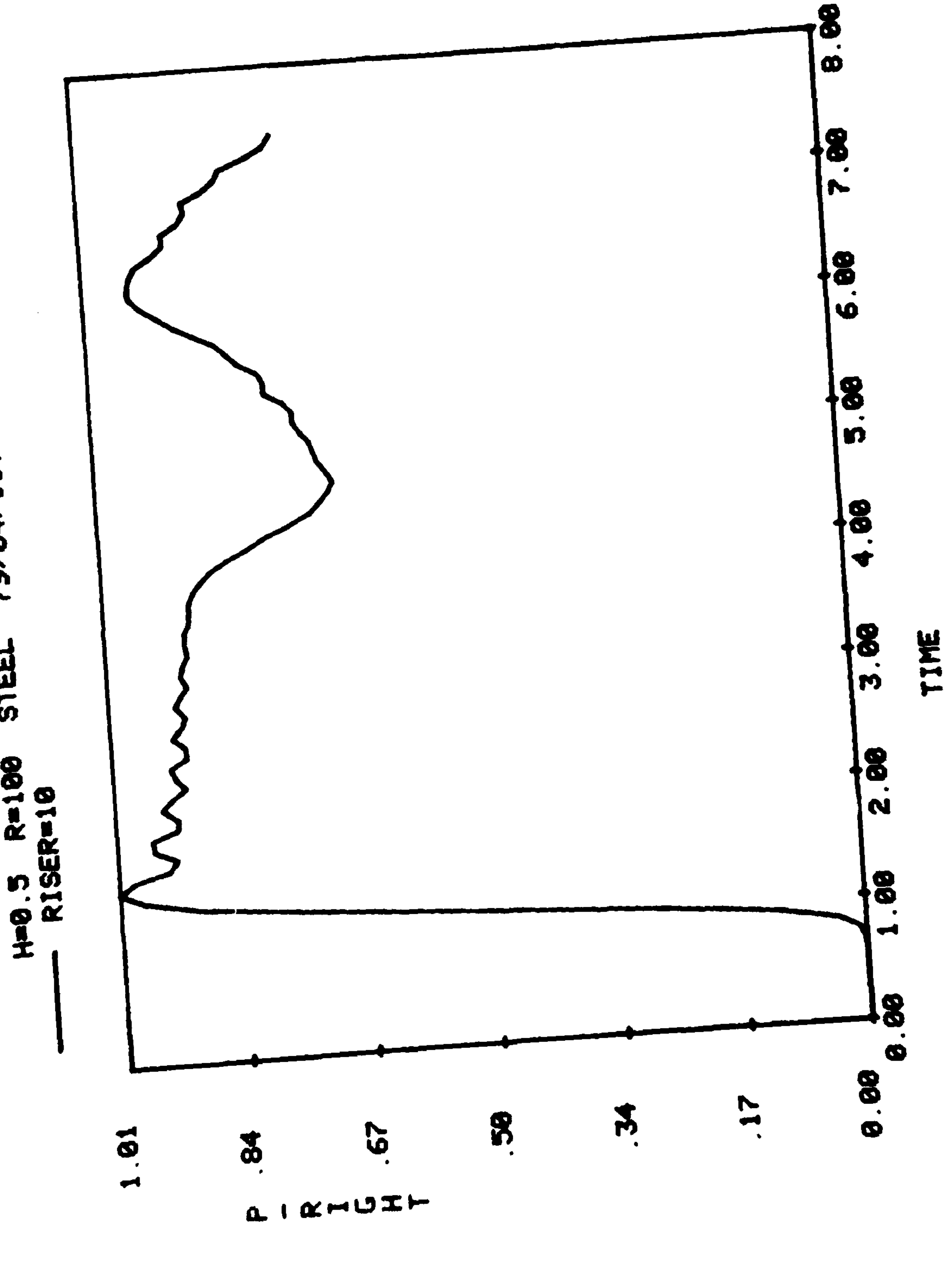

H=0.5 R=100 STEEL 79/04/13.
RISER=10
P-RIGHT
1.01
.84
.67
.50
.34
.17
0.00
0.00
1.00
2.00
3.00
4.00
5.00
6.00
7.00
8.00
TIME

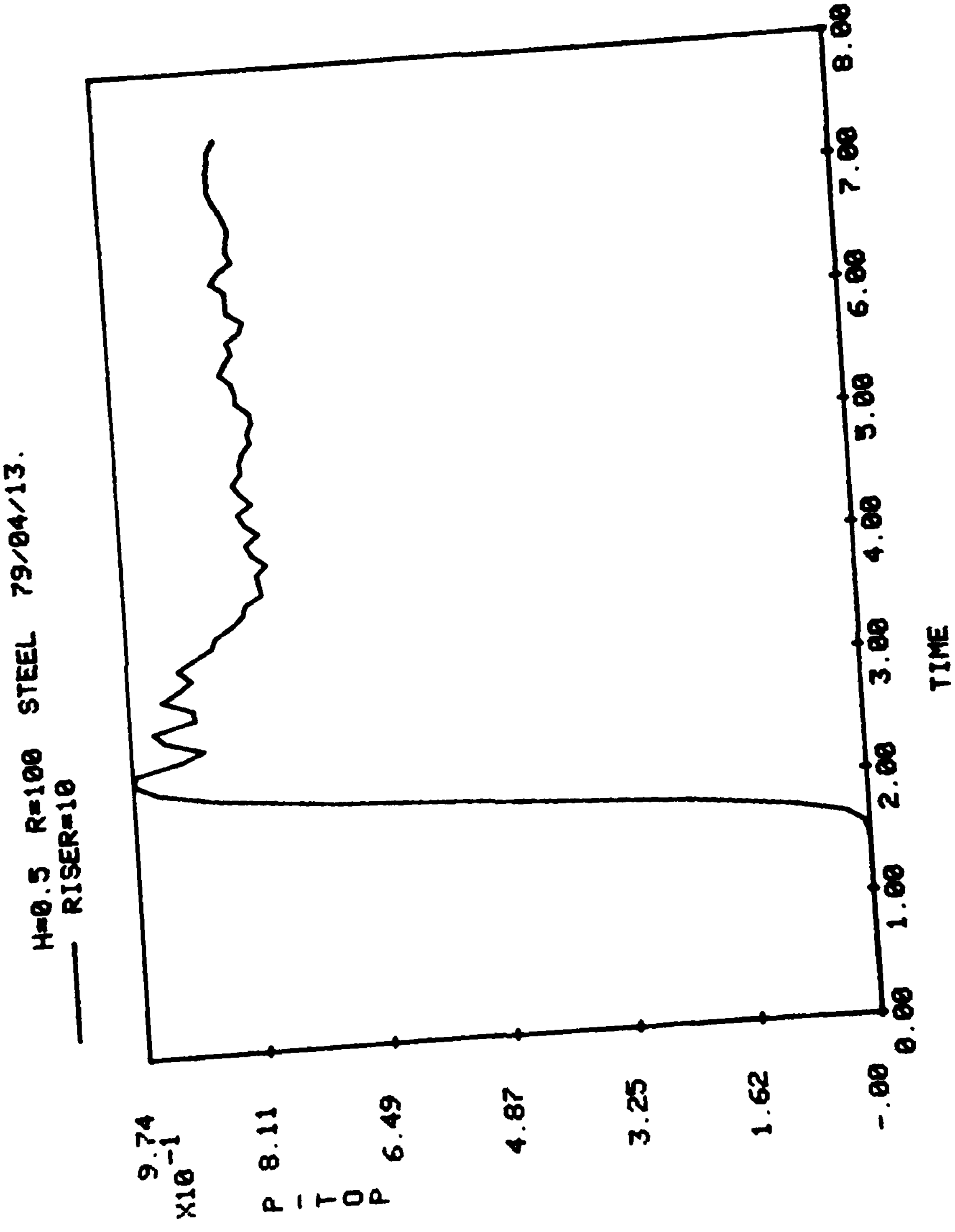

H=0.5 R=100 STEEL 79/04/13.
RISER=10
9.74
X10^-1
P-TOP
8.11
6.49
4.87
3.25
1.62
-.00
0.00
1.00
2.00
3.00
4.00
5.00
6.00
7.00
8.00
TIME

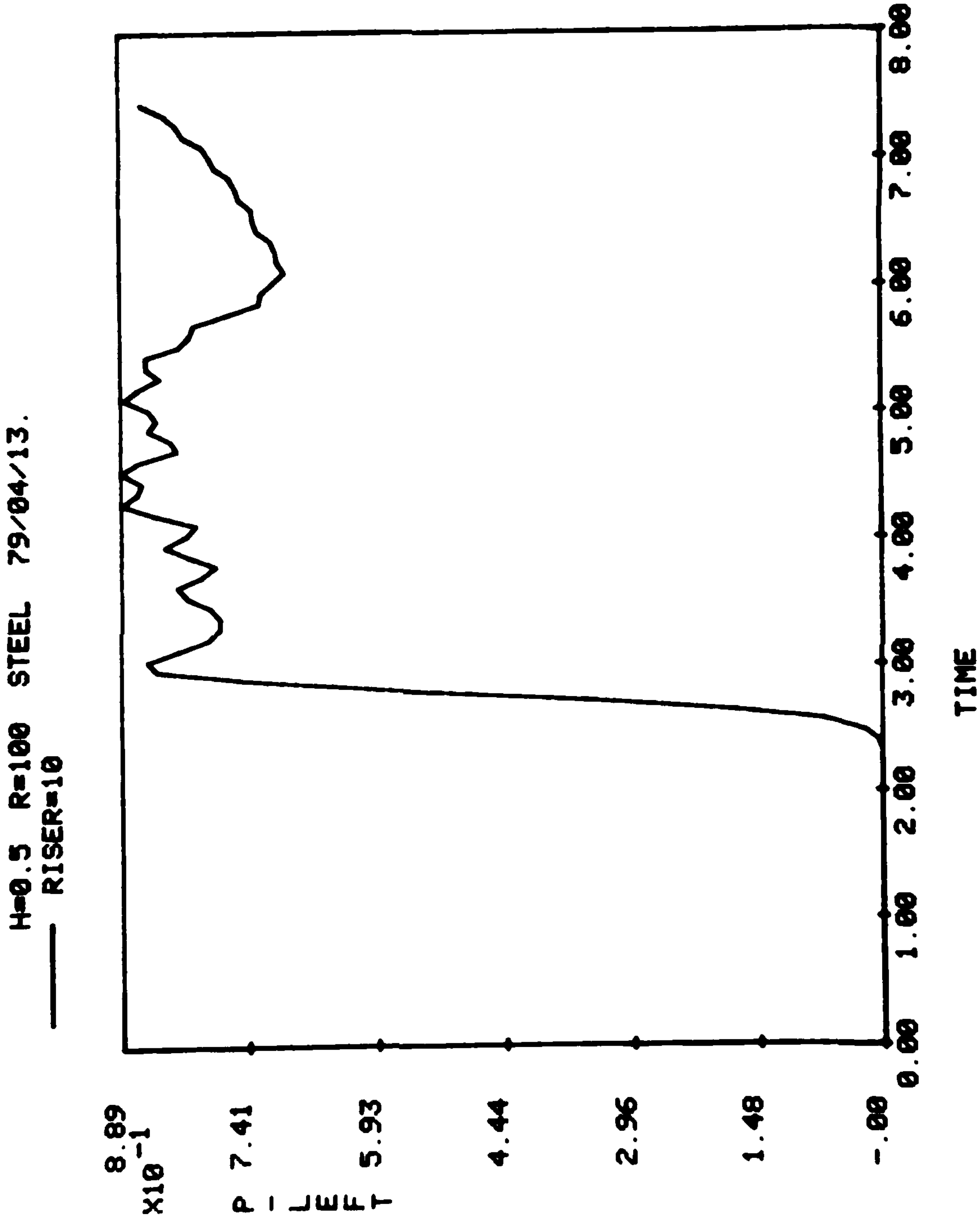

H=0.5 R=100 STEEL 79/04/13.
RISER=10
8.89
X10^-1
7.41
5.93
4.44
2.96
1.48
-.00
P-LEFT
0.00
1.00
2.00
3.00
4.00
5.00
6.00
7.00
8.00
TIME

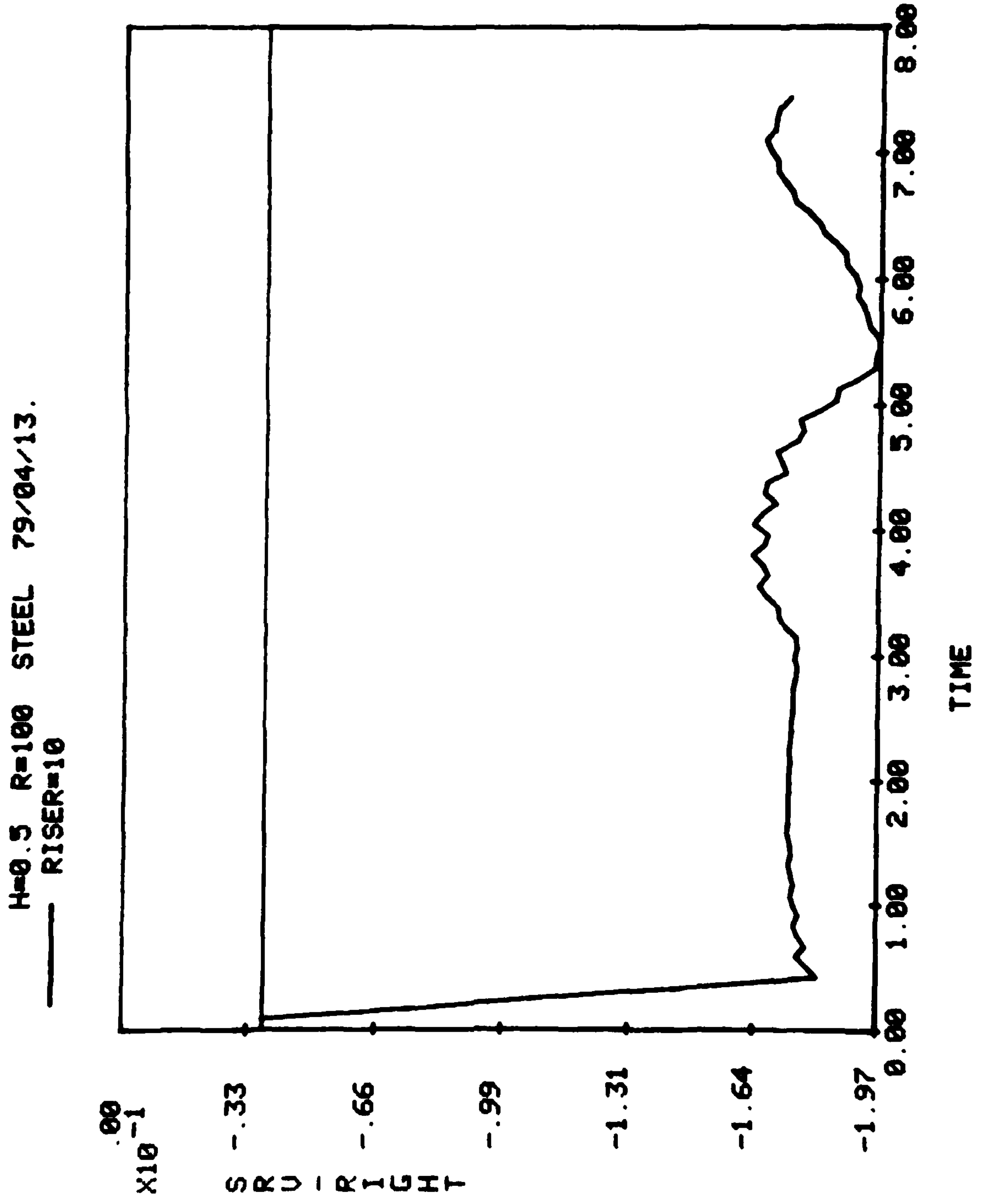
H=0.5 R=100 STEEL 79/04/13.
RISER=10
TIME
0.00
1.00
2.00
3.00
4.00
5.00
6.00
7.00
8.00
.00
X10^-1
-.33
-.66
-.99
-1.31
-1.64
-1.97
SRU-RIGHT

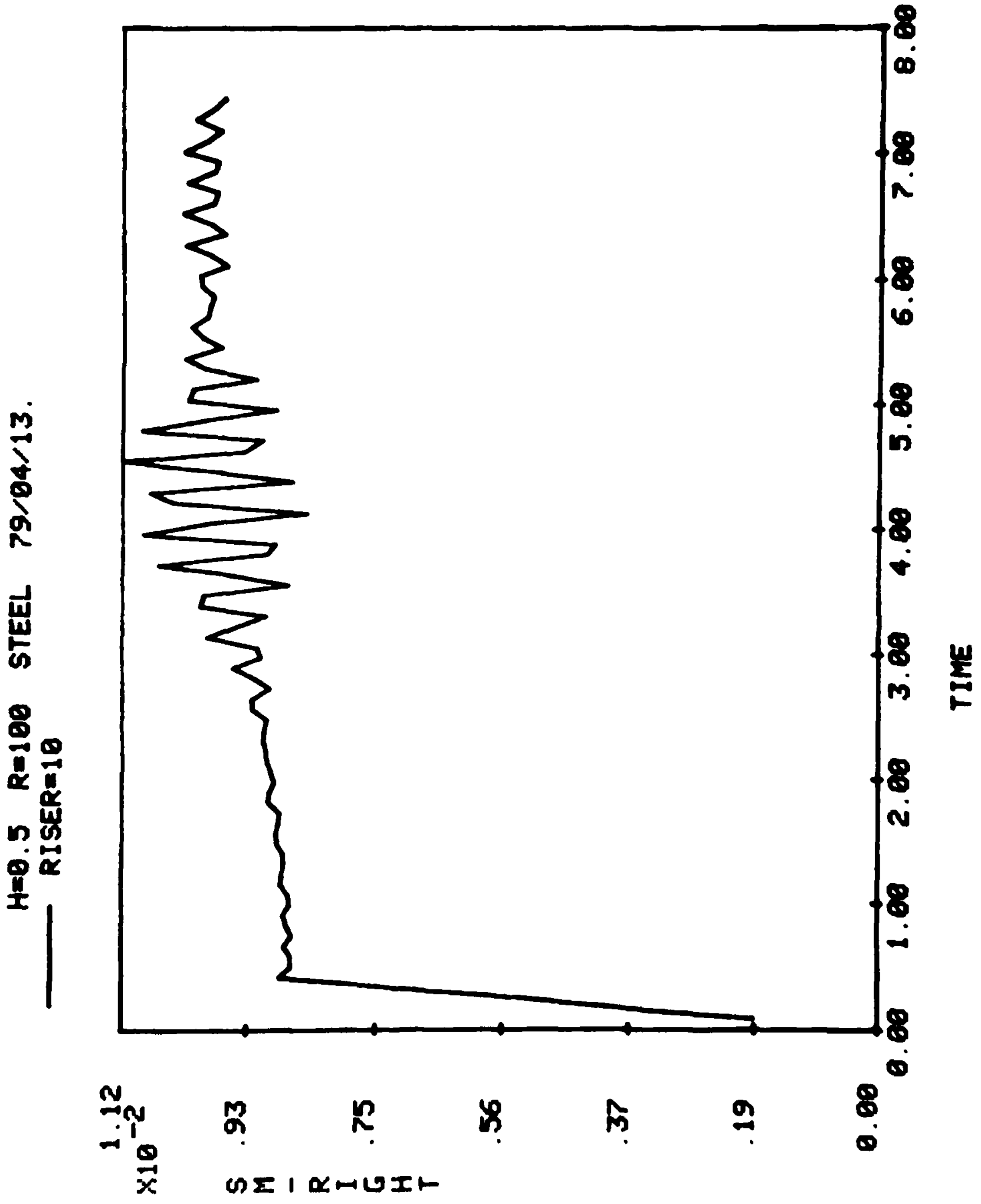
H=0.5 R=100 STEEL 79/04/13.
— RISER=10
1.12
X10^-2
.93
.75
.56
.37
.19
0.00
SMIRIGHT
0.00
1.00
2.00
3.00
4.00
5.00
6.00
7.00
8.00
TIME

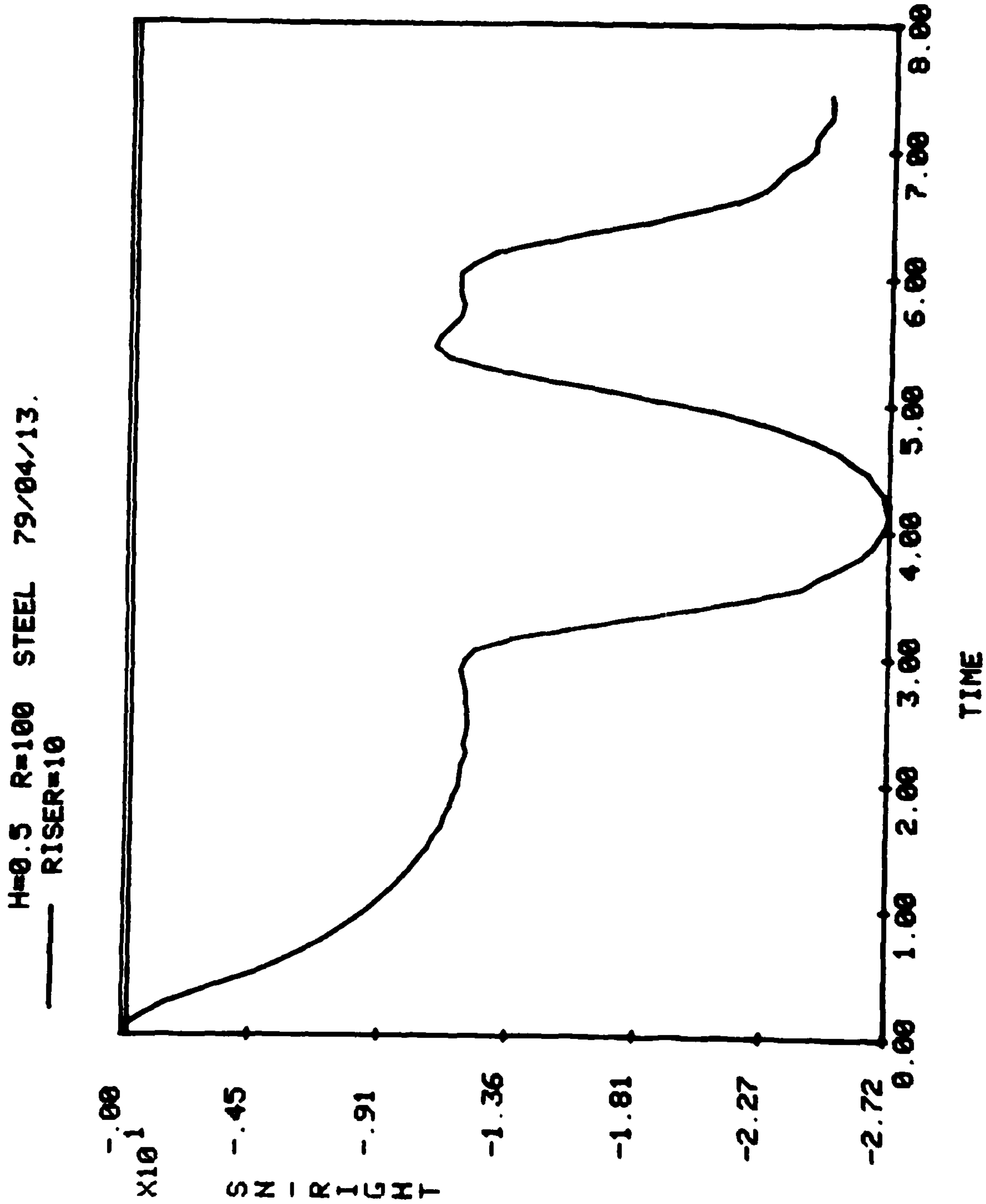

H=0.5 R=100 STEEL 79/04/13.
RISER=10
-.00
-.45
-.91
-1.36
-1.81
-2.27
-2.72
X10^1
SN-RIGHT
0.00
1.00
2.00
3.00
4.00
5.00
6.00
7.00
8.00
TIME

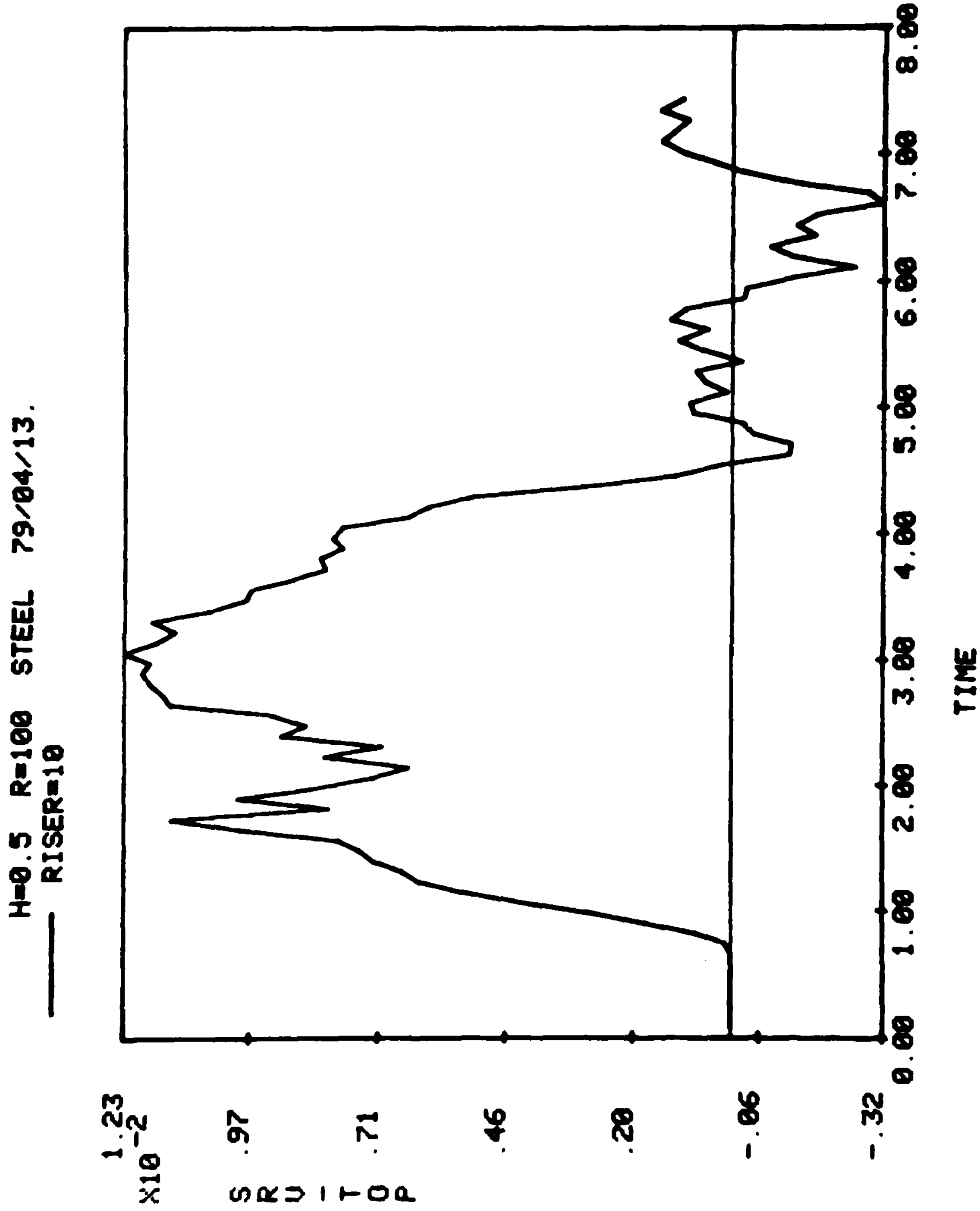

H=0.5 R=100 STEEL 79/04/13.
RISER=10
1.23
X10^{-2}
.97
.71
.46
.20
-.06
-.32
SRU-TOP
0.00
1.00
2.00
3.00
4.00
5.00
6.00
7.00
8.00
TIME

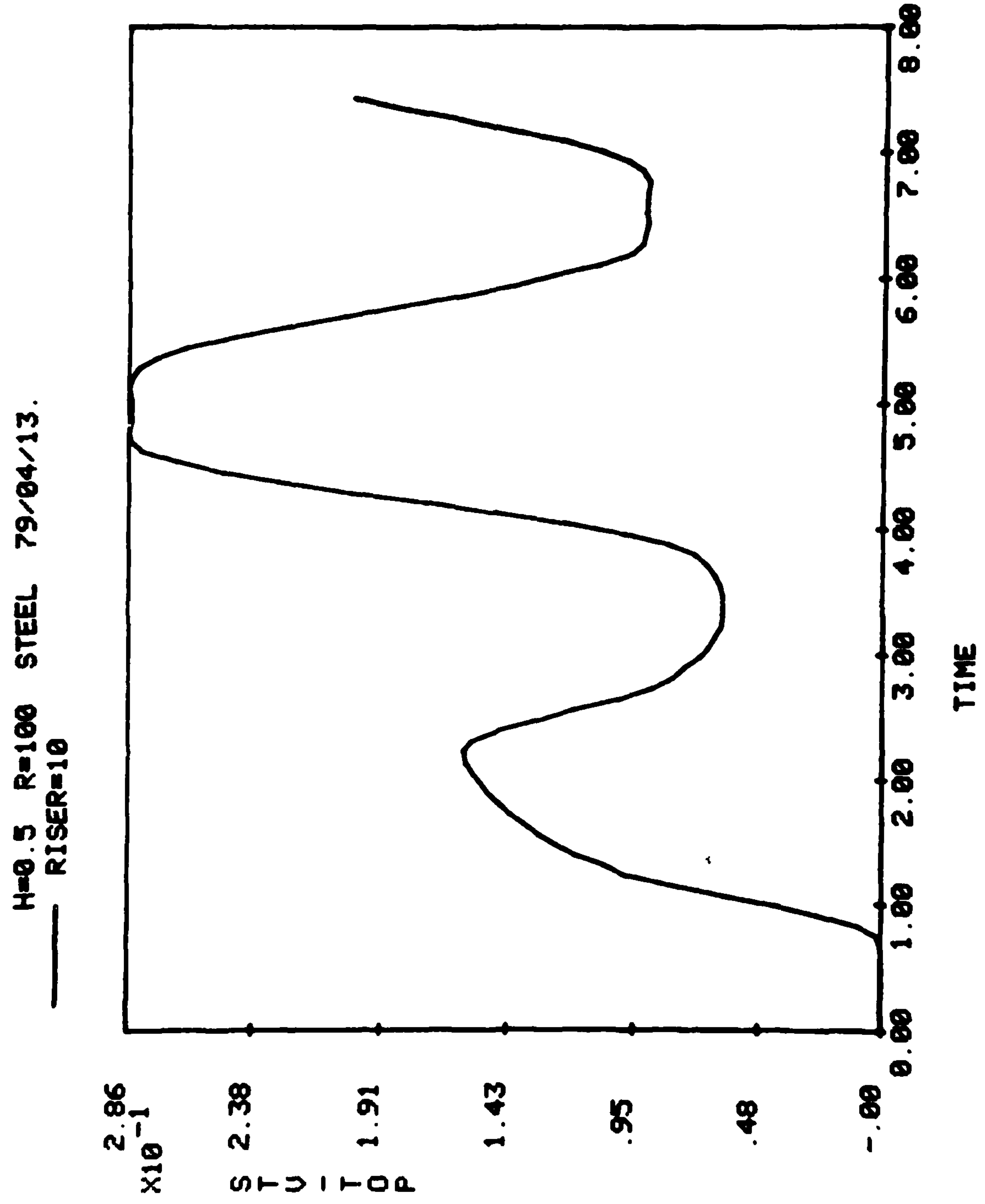
H=0.5 R=100 STEEL 79/04/13.
RISER=10
2.86
2.38
1.91
1.43
.95
.48
-.00
X10^-1
0.00
1.00
2.00
3.00
4.00
5.00
6.00
7.00
8.00
TIME

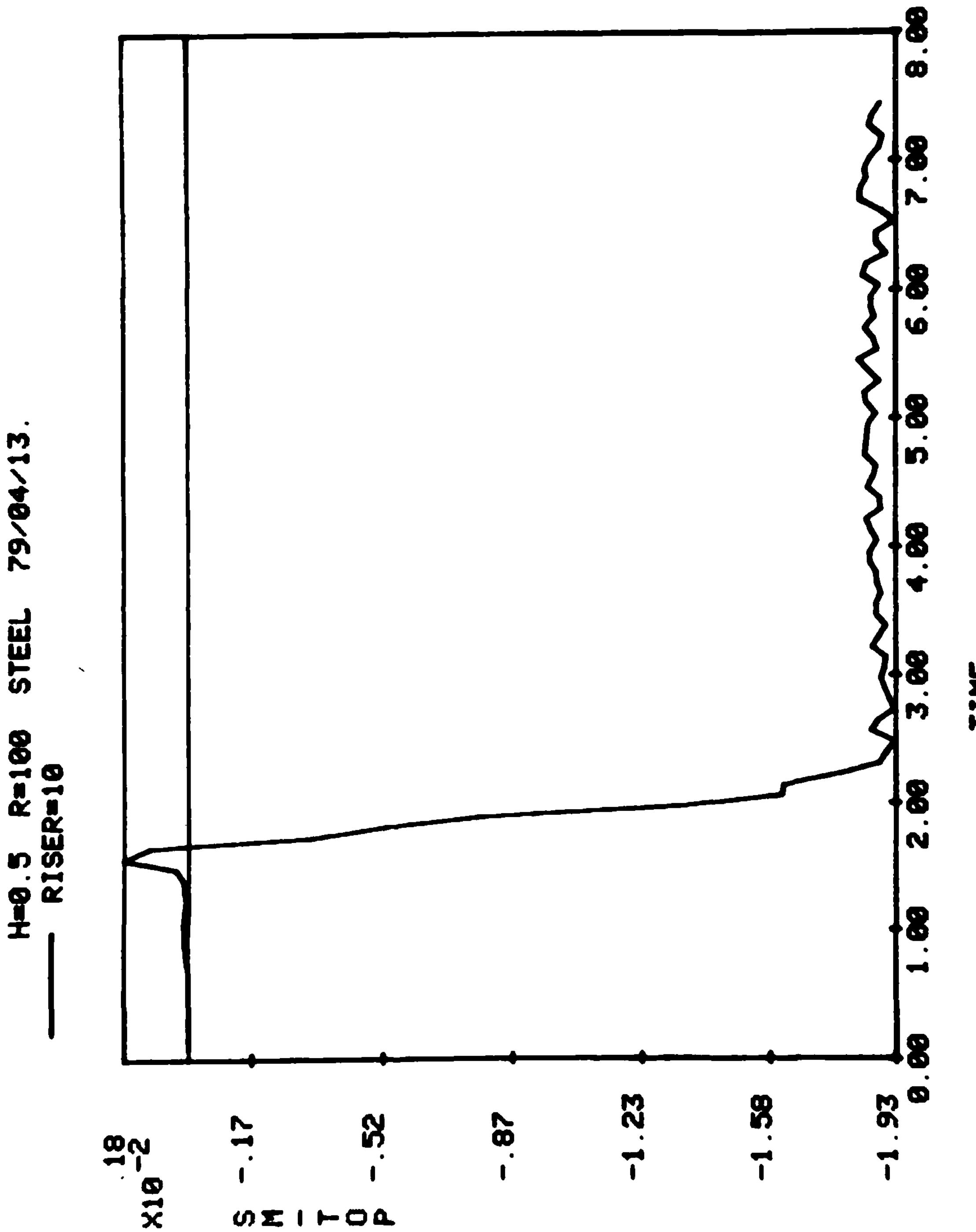
H=0.5 R=100 STEEL 79/04/13.
RISER=10
.18
X10^-2
-.17
-.52
-.87
-1.23
-1.58
-1.93
0.00
1.00
2.00
3.00
4.00
5.00
6.00
7.00
8.00
TIME

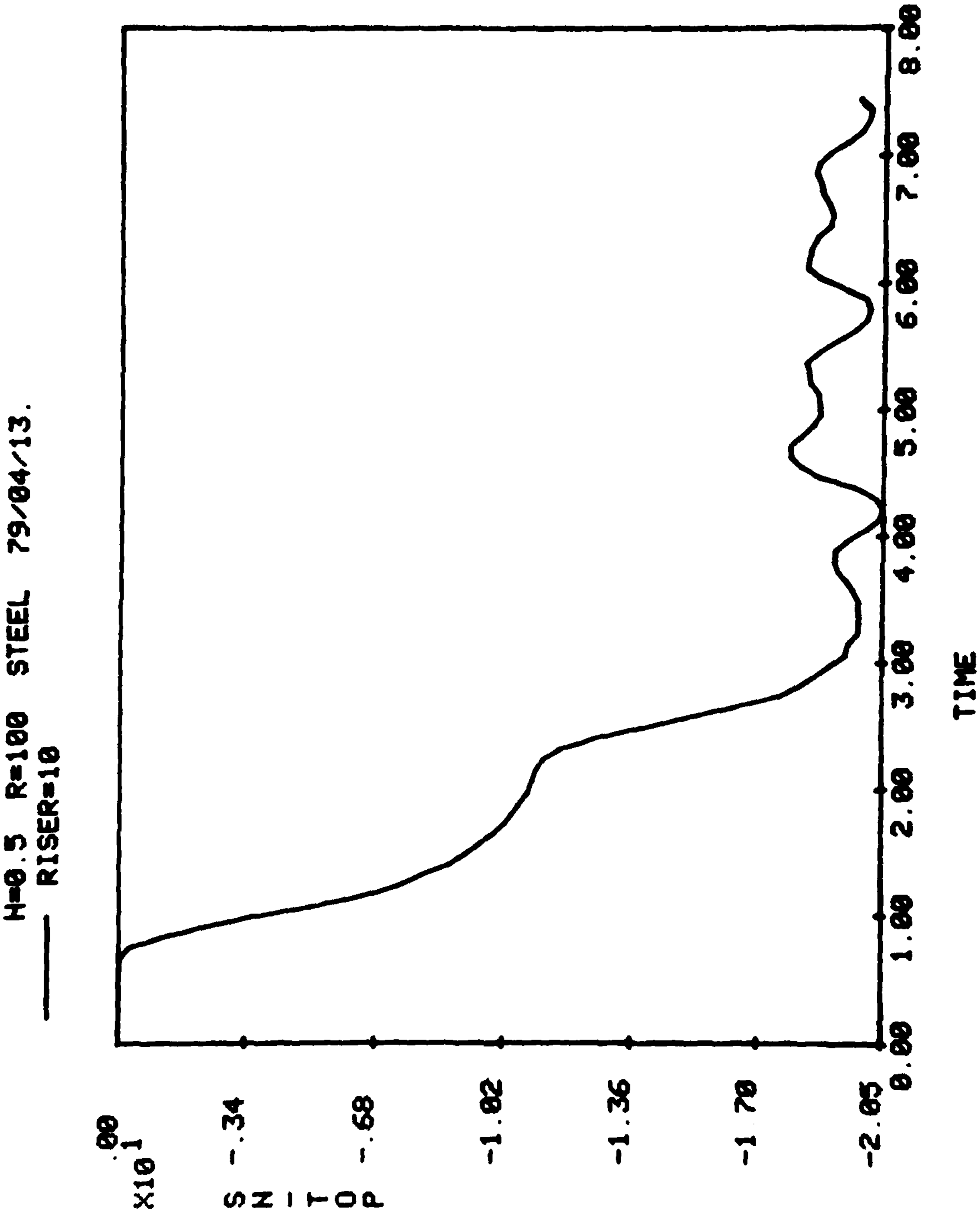
H=0.5 R=100 STEEL 79/04/13.
RISER=10
POINTS
X10^1
.00
-.34
-.68
-1.02
-1.36
-1.70
-2.05
0.00
1.00
2.00
3.00
4.00
5.00
6.00
7.00
8.00
TIME

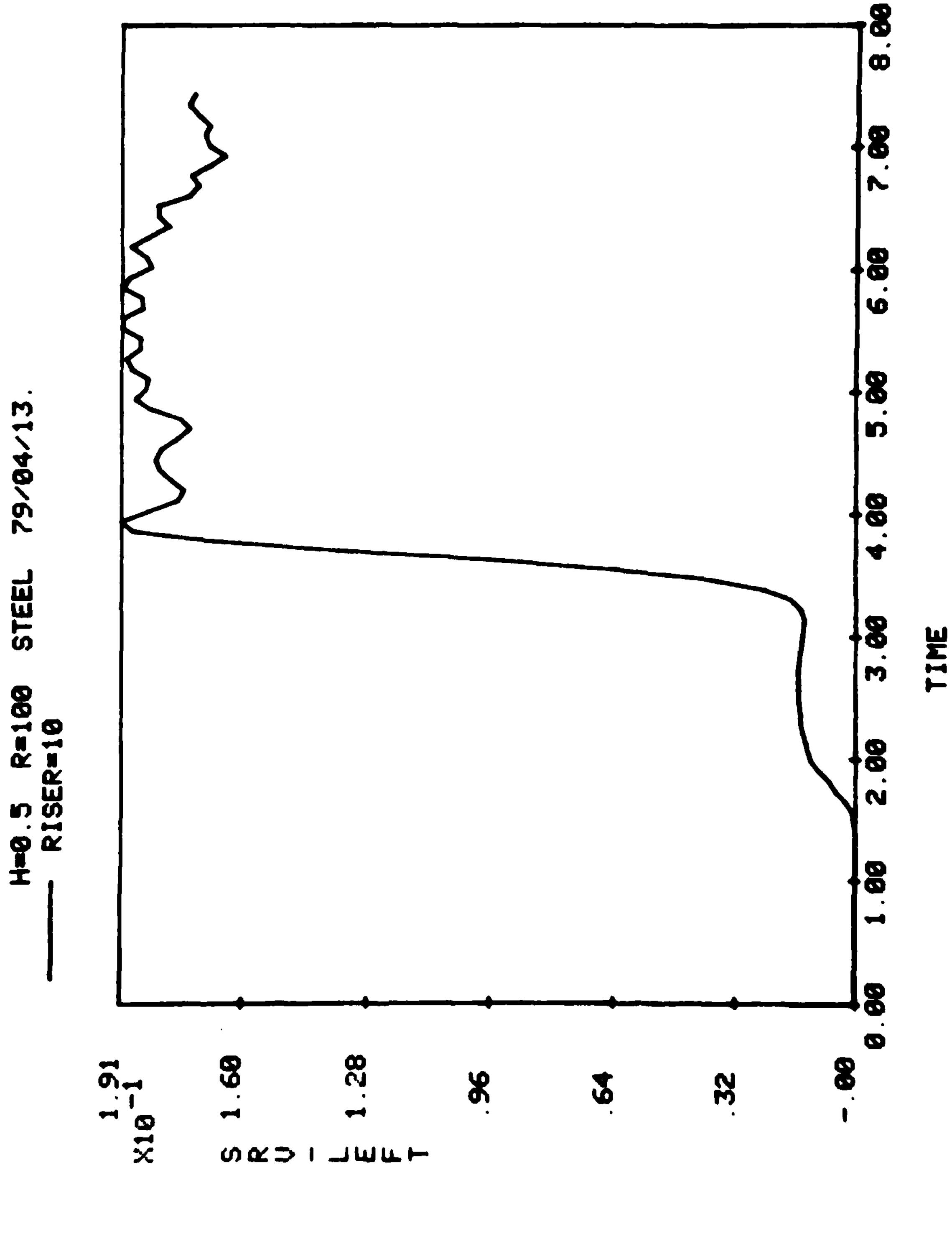
H=0.5 R=100 STEEL 79/04/13.
RISER=10
1.91
X10^-1
1.60
1.28
.96
.64
.32
-.00
0.00
1.00
2.00
3.00
4.00
5.00
6.00
7.00
8.00
TIME

APPENDIX D (Case D)

RING: Aluminum

Radius = 100 inches
Thickness = 3.5 inches

Curve Label:	Meaning
P-CENTER:	pressure at $r = 0$
P-RIGHT:	pressure at $r = a/2$, $\theta = 0$
P-TOP:	pressure at $r = a/2$, $\theta = 90$ deg.
P-LEFT:	pressure at $r = a/2$, $\theta = 180$ deg.
SRV-RIGHT:	shell radial velocity at $\theta = 0$
SM-RIGHT:	shell moment at $\theta = 0$
SN-RIGHT:	shell stress resultant at $\theta = 0$
SRV-TOP:	shell radial velocity at $\theta = 90$ deg.
STV-TOP:	shell tangential velocity at $\theta = 90$
SM-TOP:	shell moment at $\theta = 90$
SN-TOP:	shell stress resultant at $\theta = 90$
SRV-LEFT:	shell radial velocity at $\theta = 180$ deg.

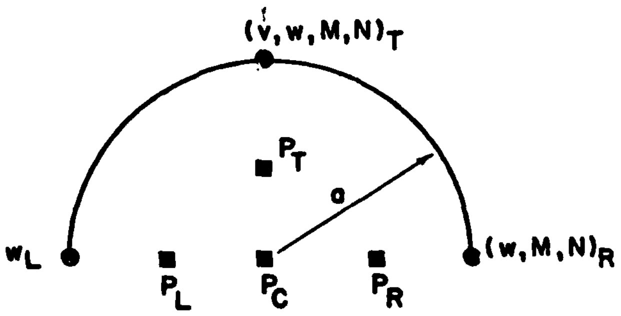

KEY TO TIME HISTORIES IN APPENDICES

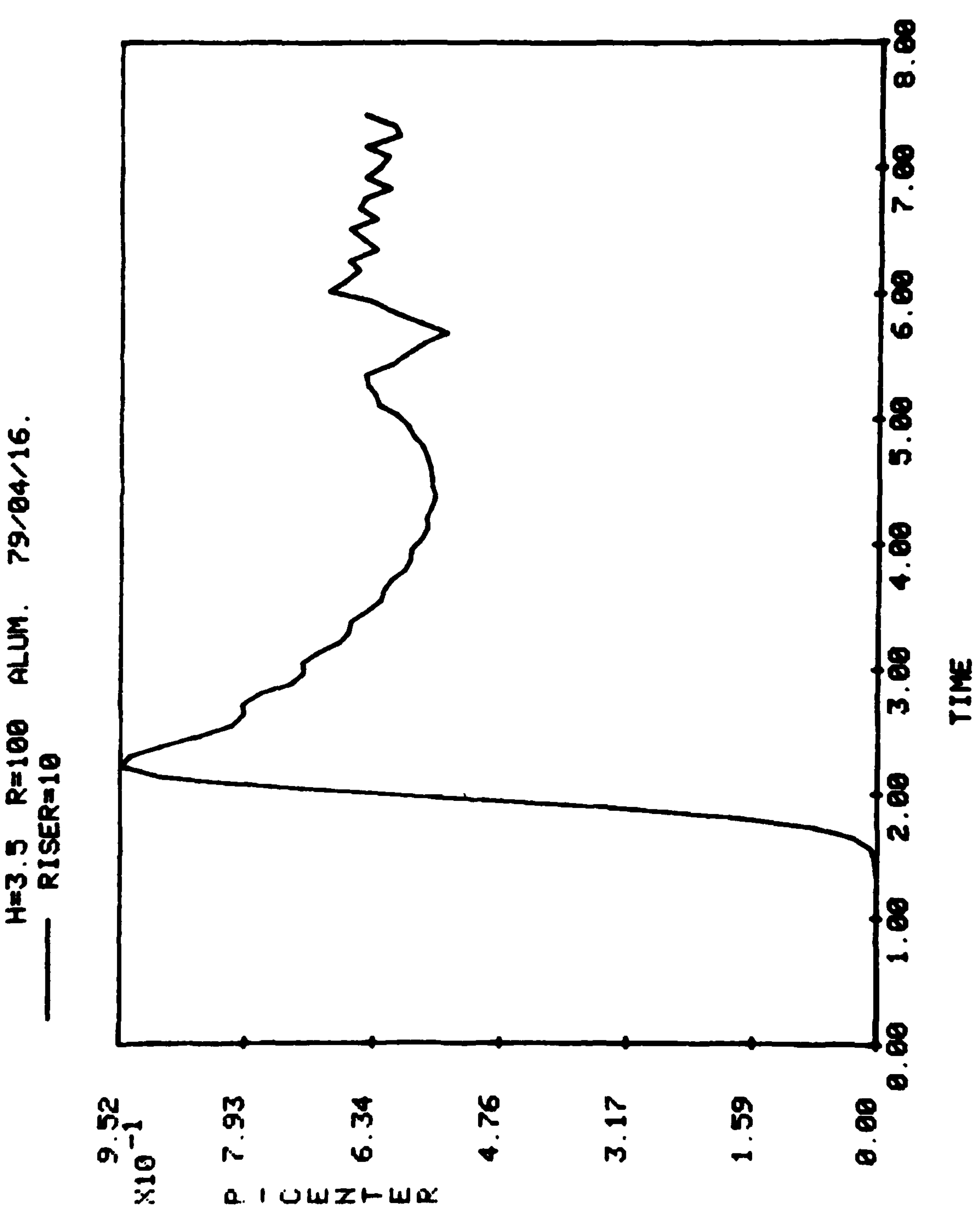

H=3.5 R=100 ALUM. 79/04/16.
RISER=10
P. CENTER
X10^-1
9.52
7.93
6.34
4.76
3.17
1.59
0.00
0.00
1.00
2.00
3.00
4.00
5.00
6.00
7.00
8.00
TIME

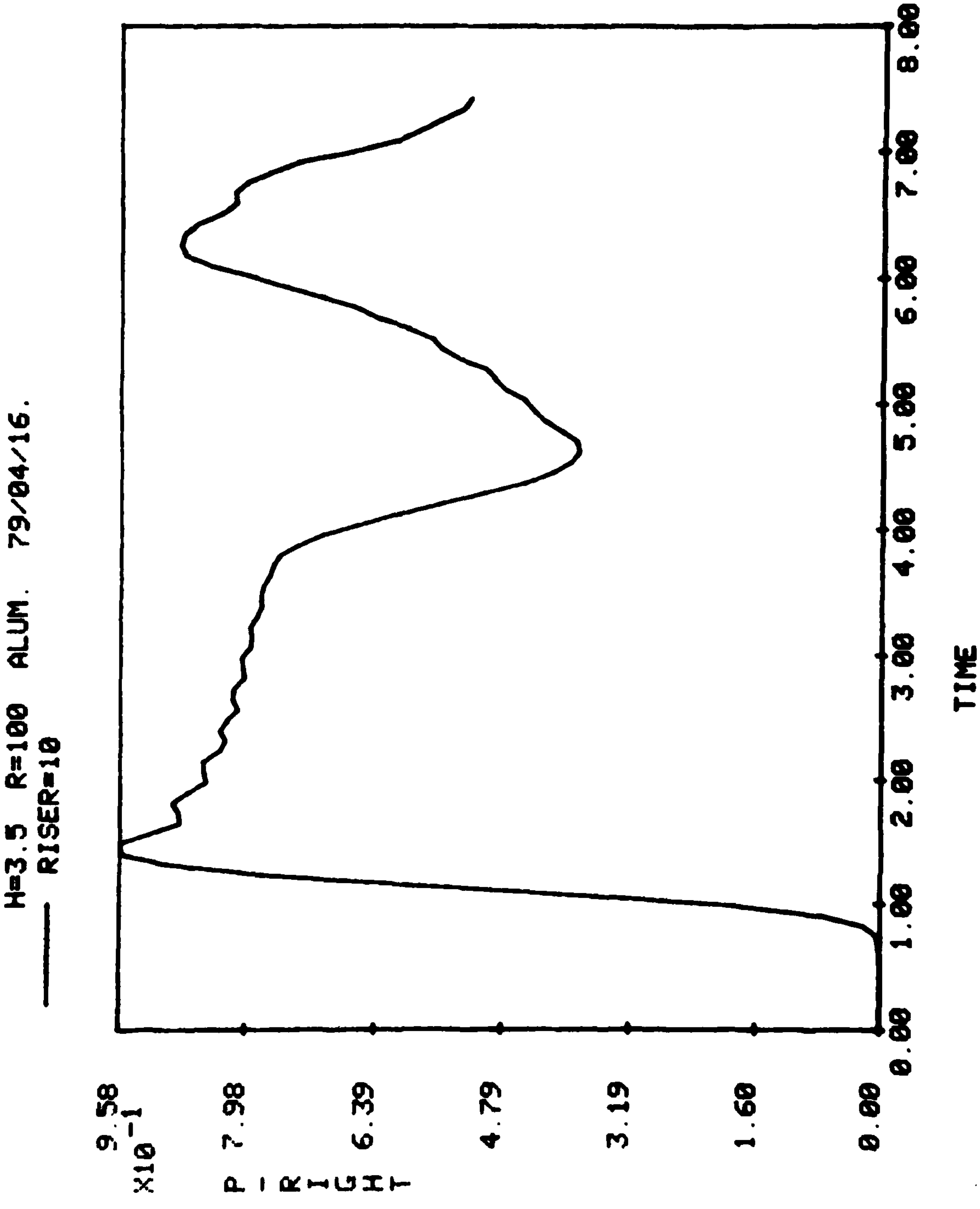
H=3.5 R=100 ALUM. 79/04/16.
RISER=10
9.58
X10^-1
7.98
6.39
4.79
3.19
1.60
0.00
P-RIGHT
0.00
1.00
2.00
3.00
4.00
5.00
6.00
7.00
8.00
TIME

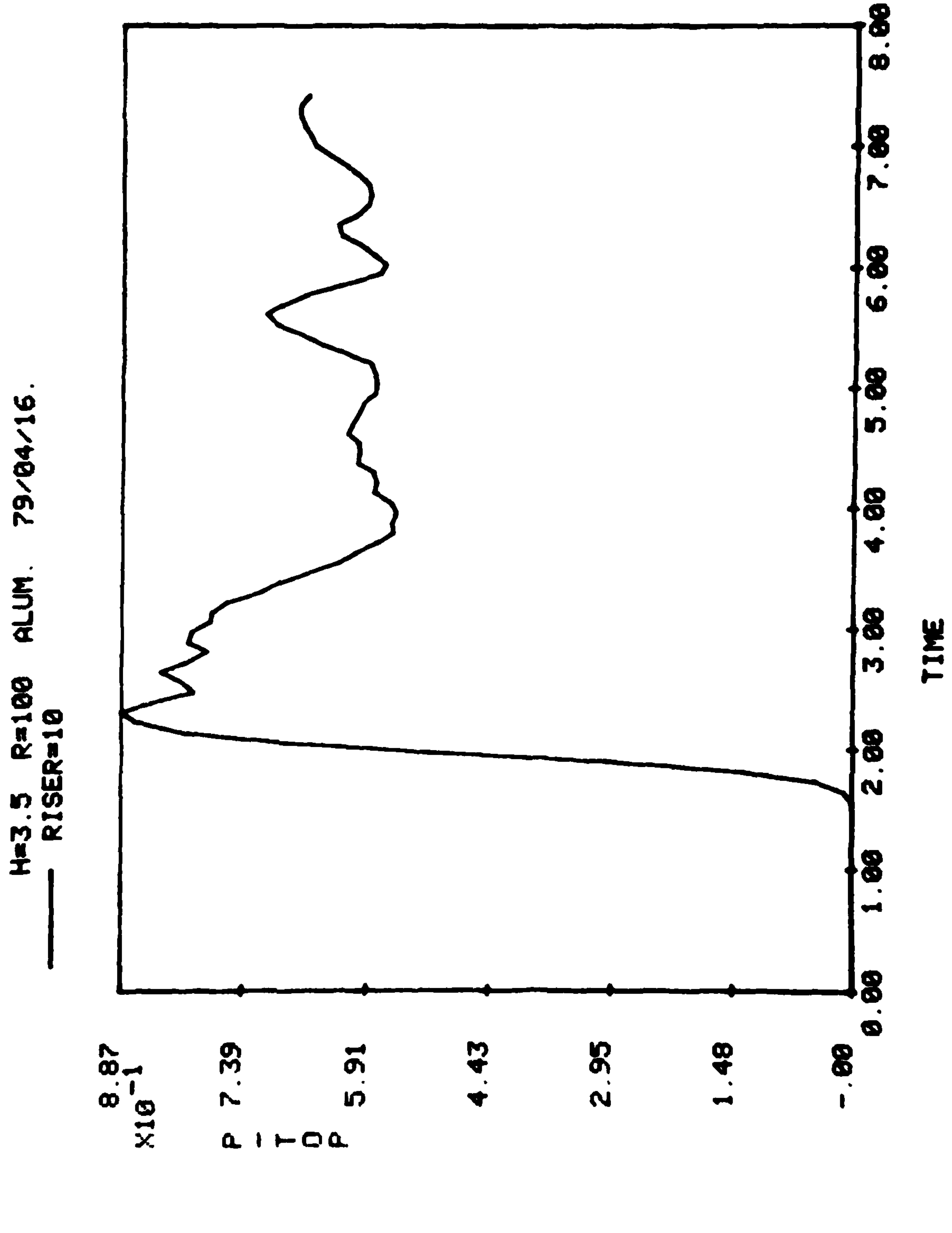
H=3.5 R=100 ALUM. 79/04/16.
RISER=10
8.87
X10^-1
7.39
5.91
4.43
2.95
1.48
-.00
PITDP
0.00
1.00
2.00
3.00
4.00
5.00
6.00
7.00
8.00
TIME

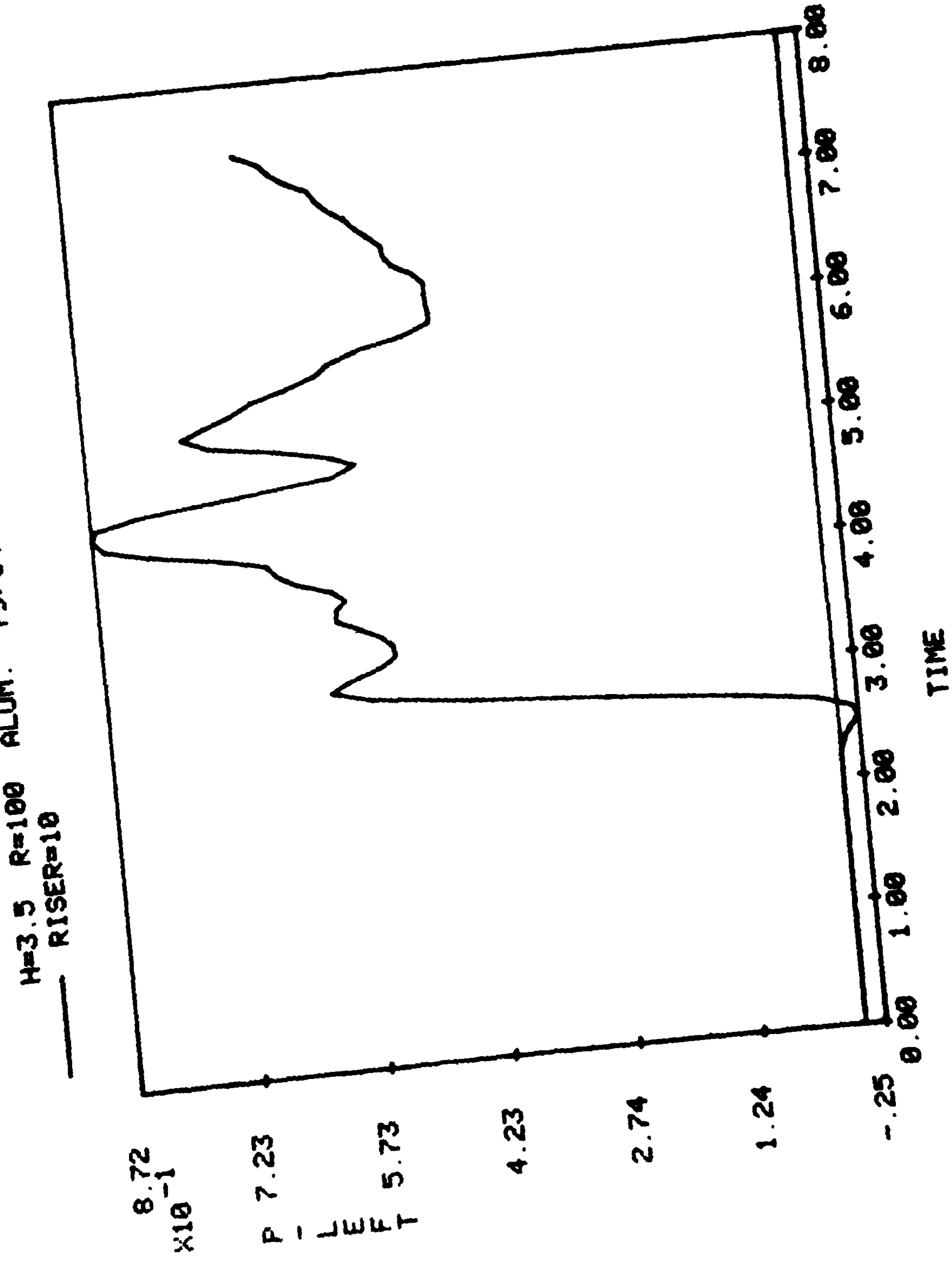
H=3.5 R=100 ALUM. 79/04/16.
RISER=10
P-LEFT
X10-1
8.72
7.23
5.73
4.23
2.74
1.24
-.25
0.00
1.00
2.00
3.00
4.00
5.00
6.00
7.00
8.00
TIME

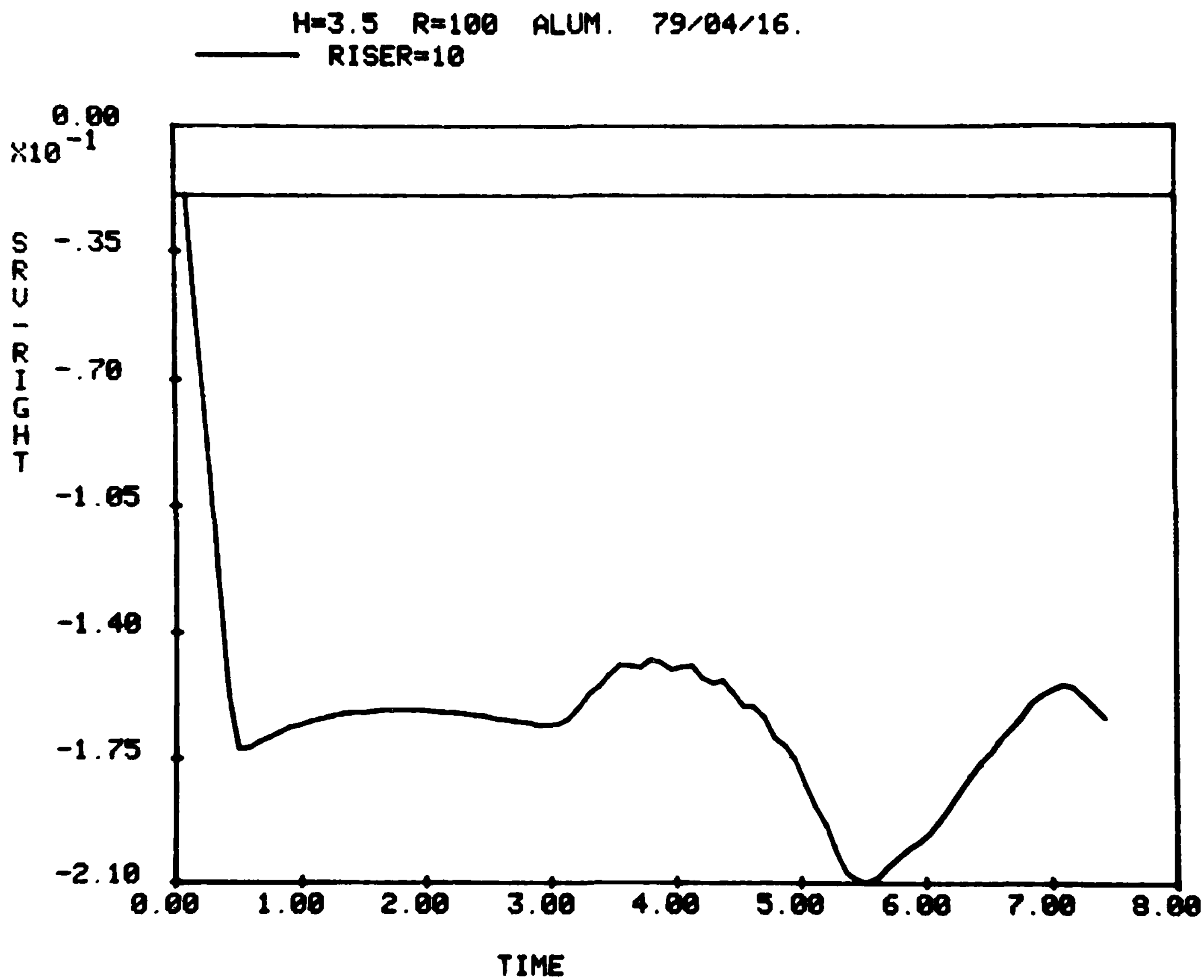
H=3.5 R=100 ALUM. 79/04/16.
RISER=10
0.00
X10^-1
-.35
-.70
-1.05
-1.40
-1.75
-2.10
SRV-RIGHT
0.00
1.00
2.00
3.00
4.00
5.00
6.00
7.00
8.00
TIME

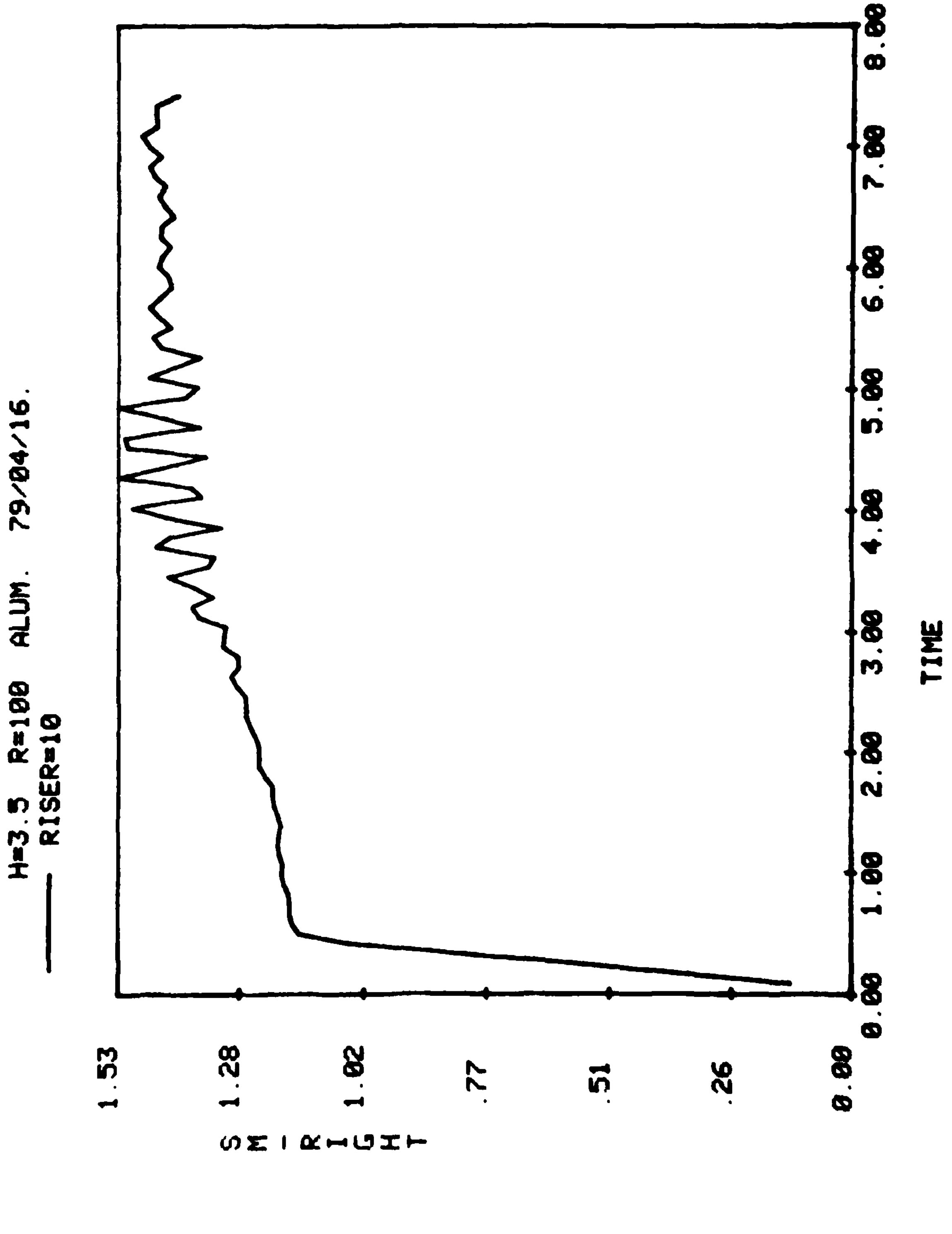
H=3.5 R=100 ALUM. 79/04/16.
RISER=10
1.53
1.28
1.02
.77
.51
.26
0.00
SMIRIGHT
0.00
1.00
2.00
3.00
4.00
5.00
6.00
7.00
8.00
TIME

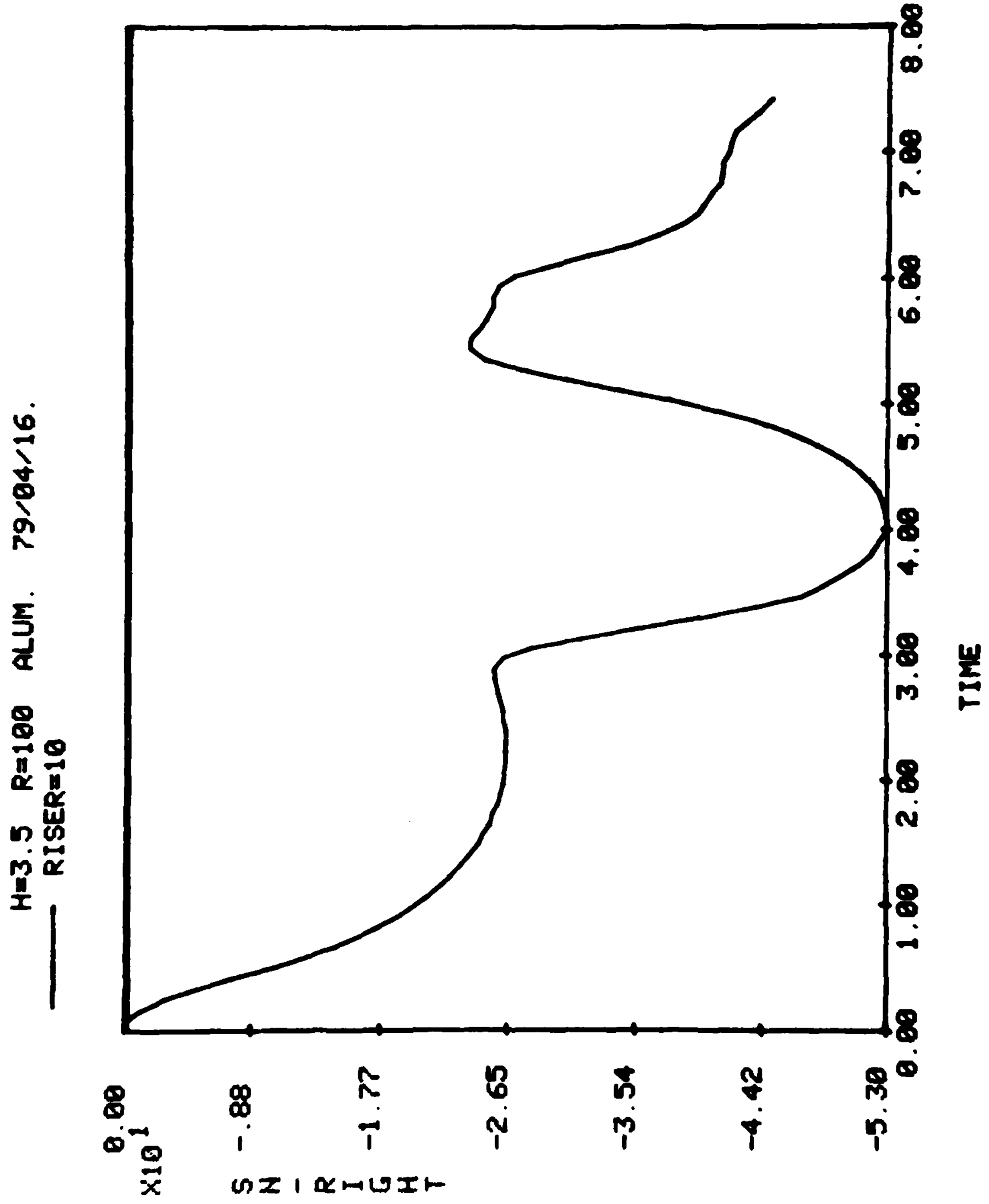
H=3.5 R=100 ALUM. 79/04/16.
RISER=10
0.00
-.88
-1.77
-2.65
-3.54
-4.42
-5.30
X10 1
SN-RIGHT
0.00
1.00
2.00
3.00
4.00
5.00
6.00
7.00
8.00
TIME

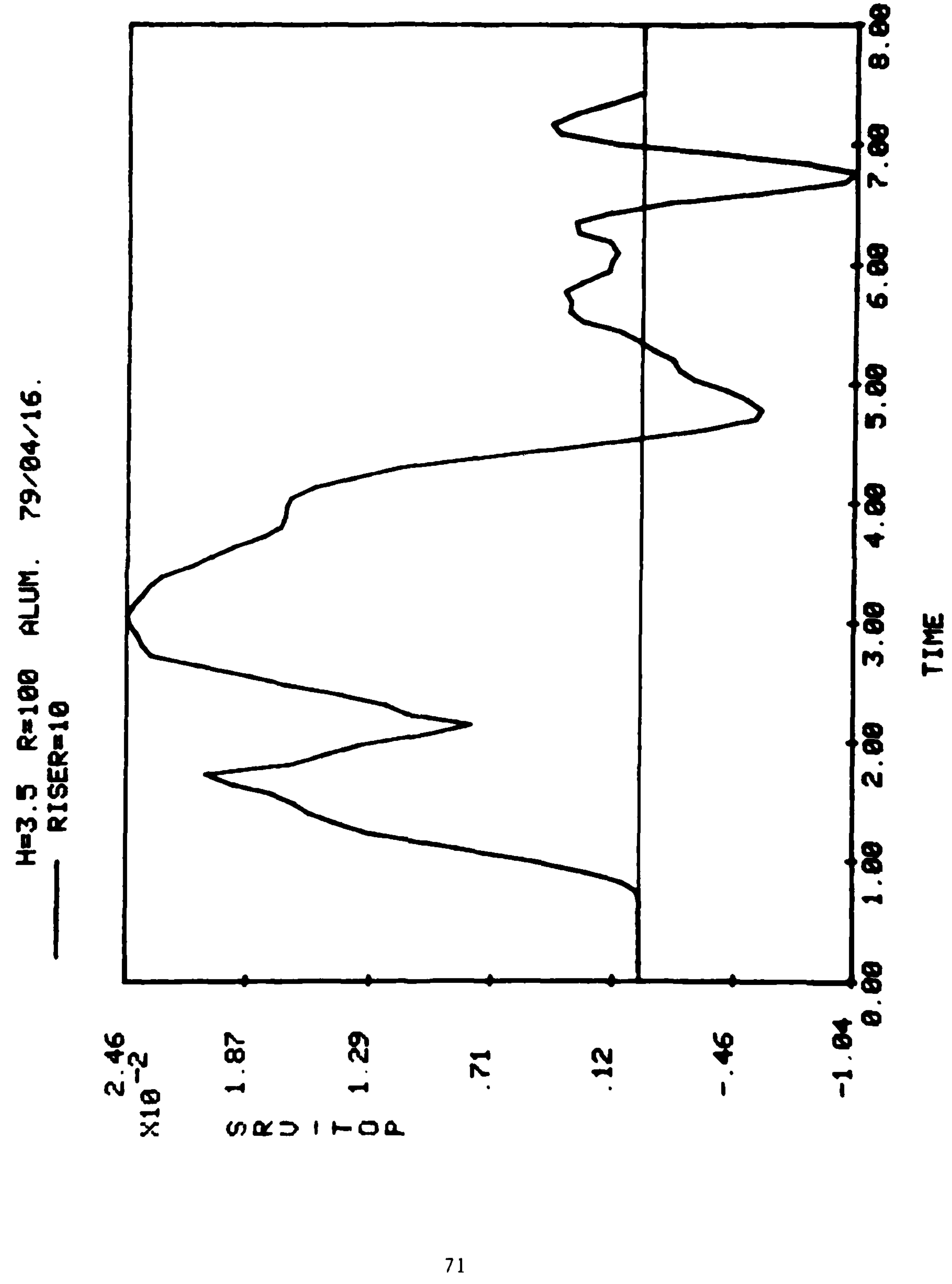

H=3.5 R=100 ALUM. 79/04/16.
RISER=10
2.46
X10^-2
1.87
1.29
.71
.12
-.46
-1.04
0.00
1.00
2.00
3.00
4.00
5.00
6.00
7.00
8.00
TIME

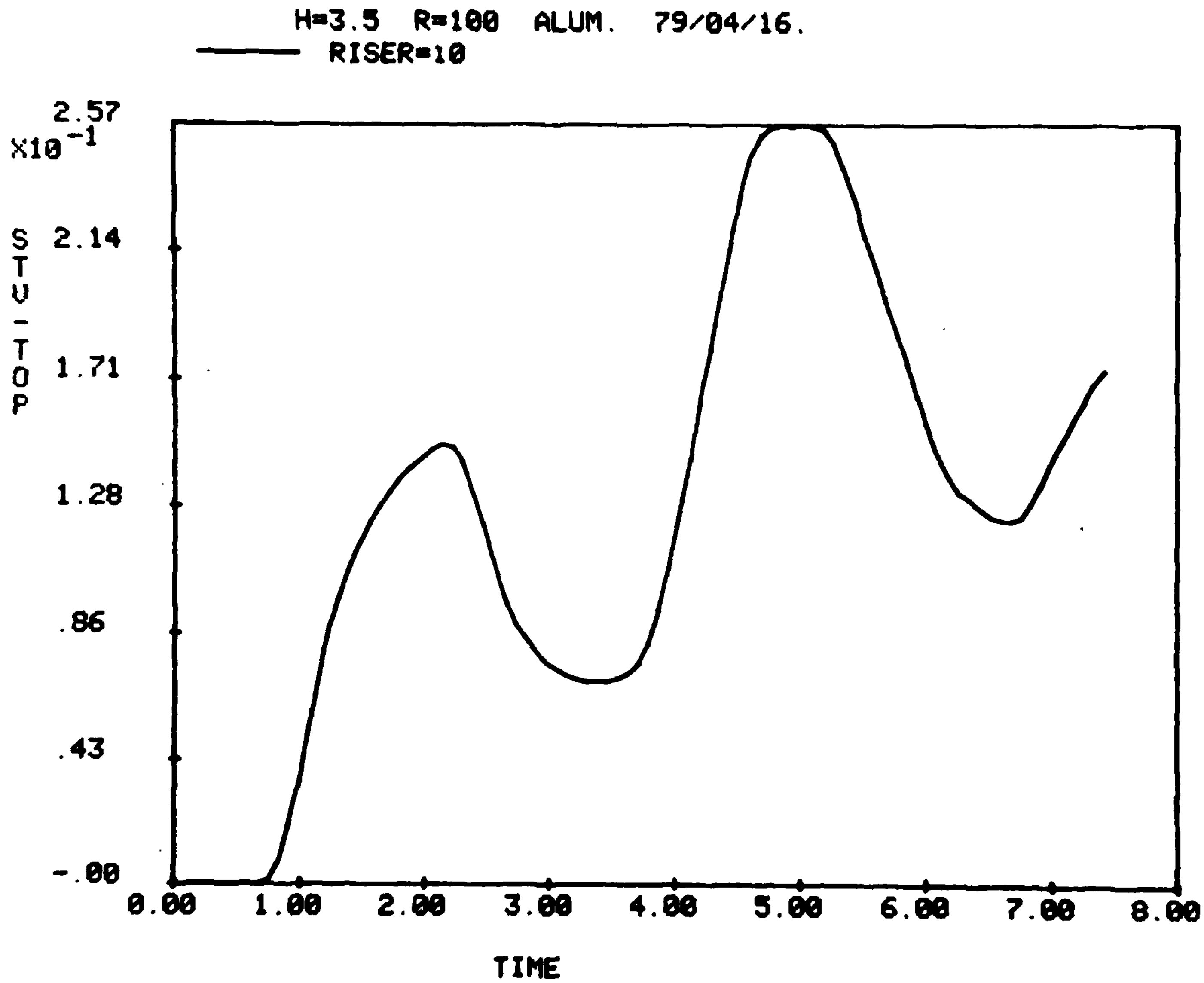
H=3.5 R=100 ALUM. 79/04/16.
RISER=10
2.57
X10^-1
STU-TOP
2.14
1.71
1.28
.86
.43
-.00
0.00
1.00
2.00
3.00
4.00
5.00
6.00
7.00
8.00
TIME

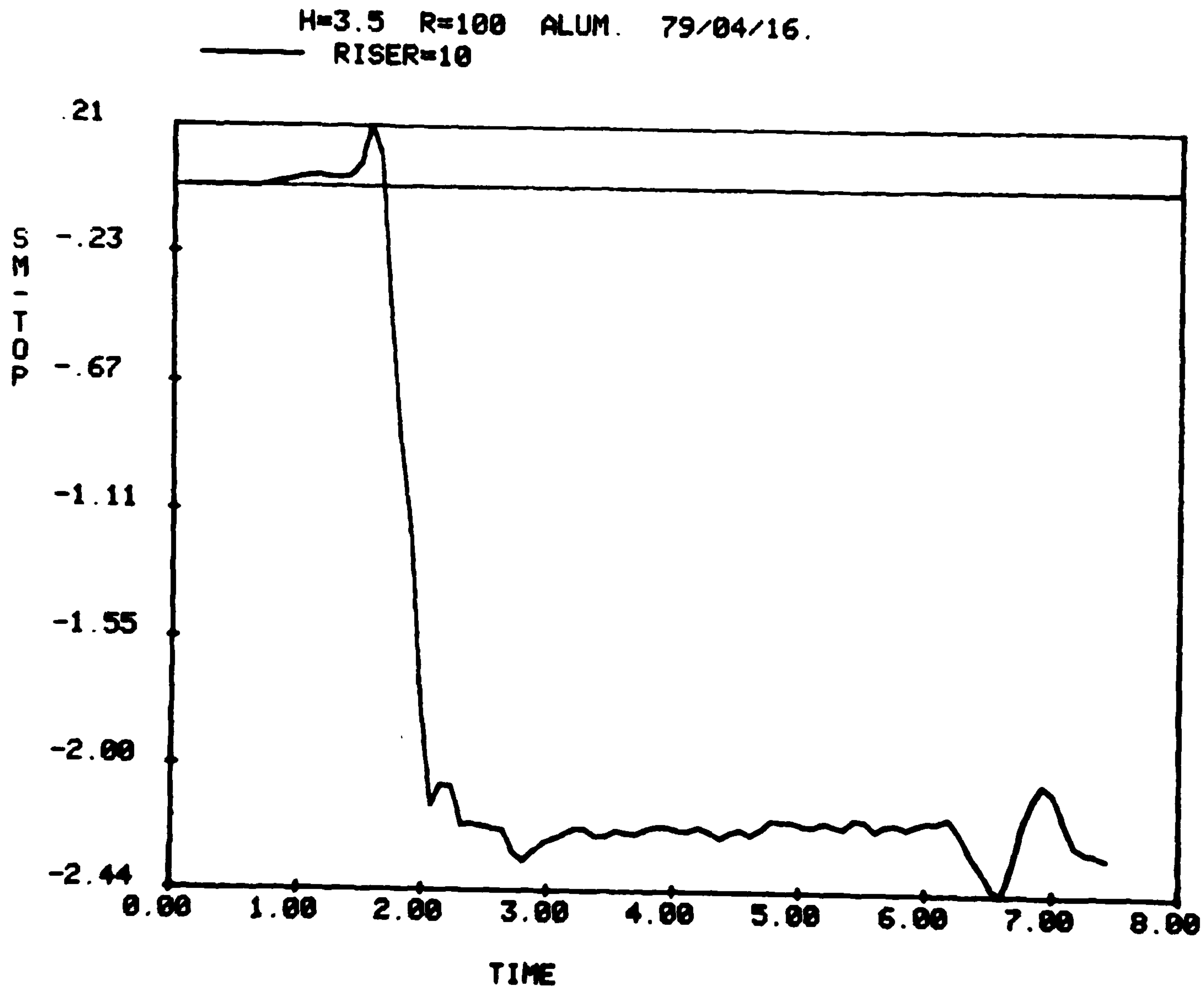

H=3.5 R=100 ALUM. 79/04/16.
RISER=10
SM-TOP
.21
-.23
-.67
-1.11
-1.55
-2.00
-2.44
0.00
1.00
2.00
3.00
4.00
5.00
6.00
7.00
8.00
TIME

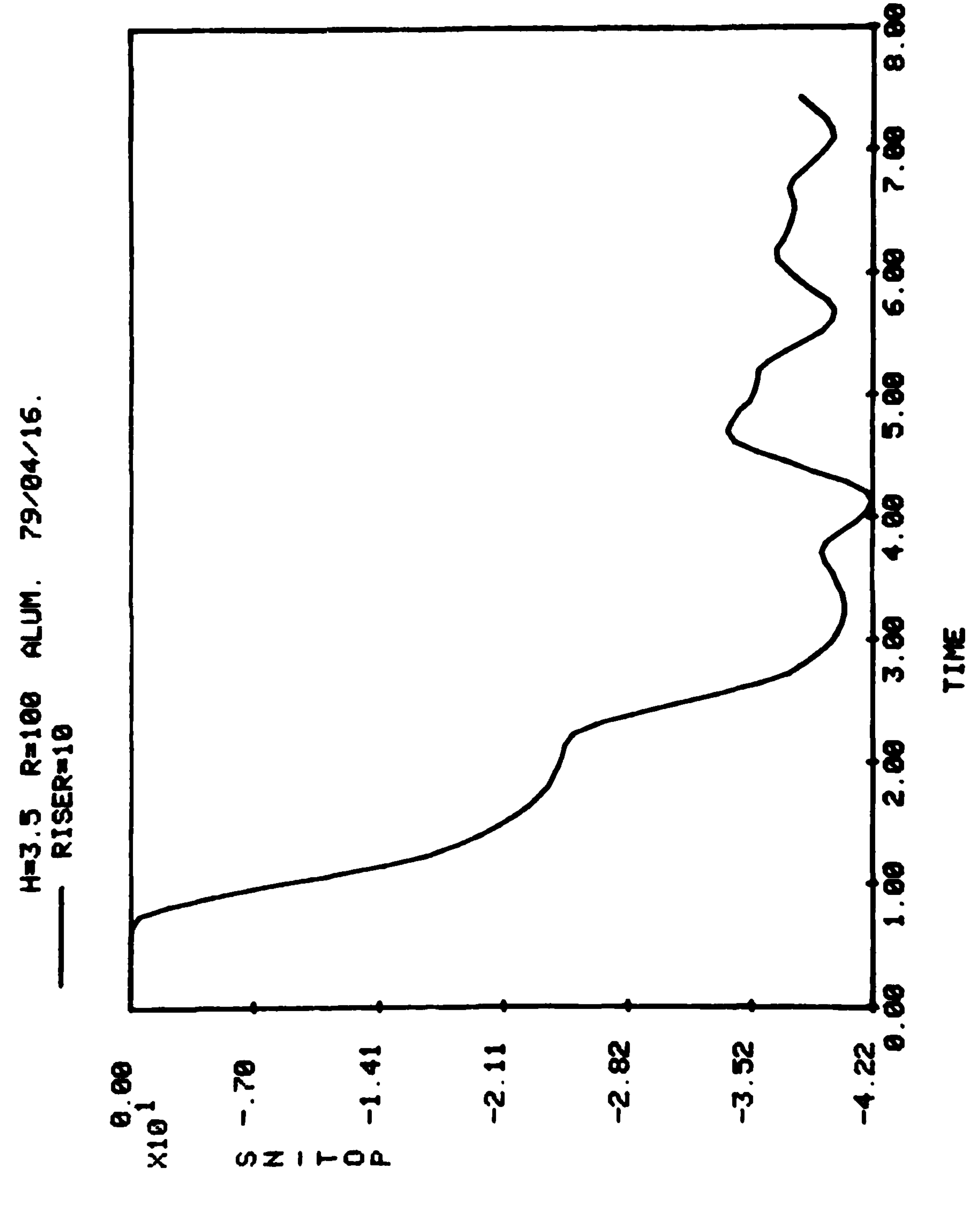

H=3.5 R=100 ALUM. 79/04/16.
RISER=10
0.00
X10 1
-.70
-1.41
-2.11
-2.82
-3.52
-4.22
0.00
1.00
2.00
3.00
4.00
5.00
6.00
7.00
8.00
TIME

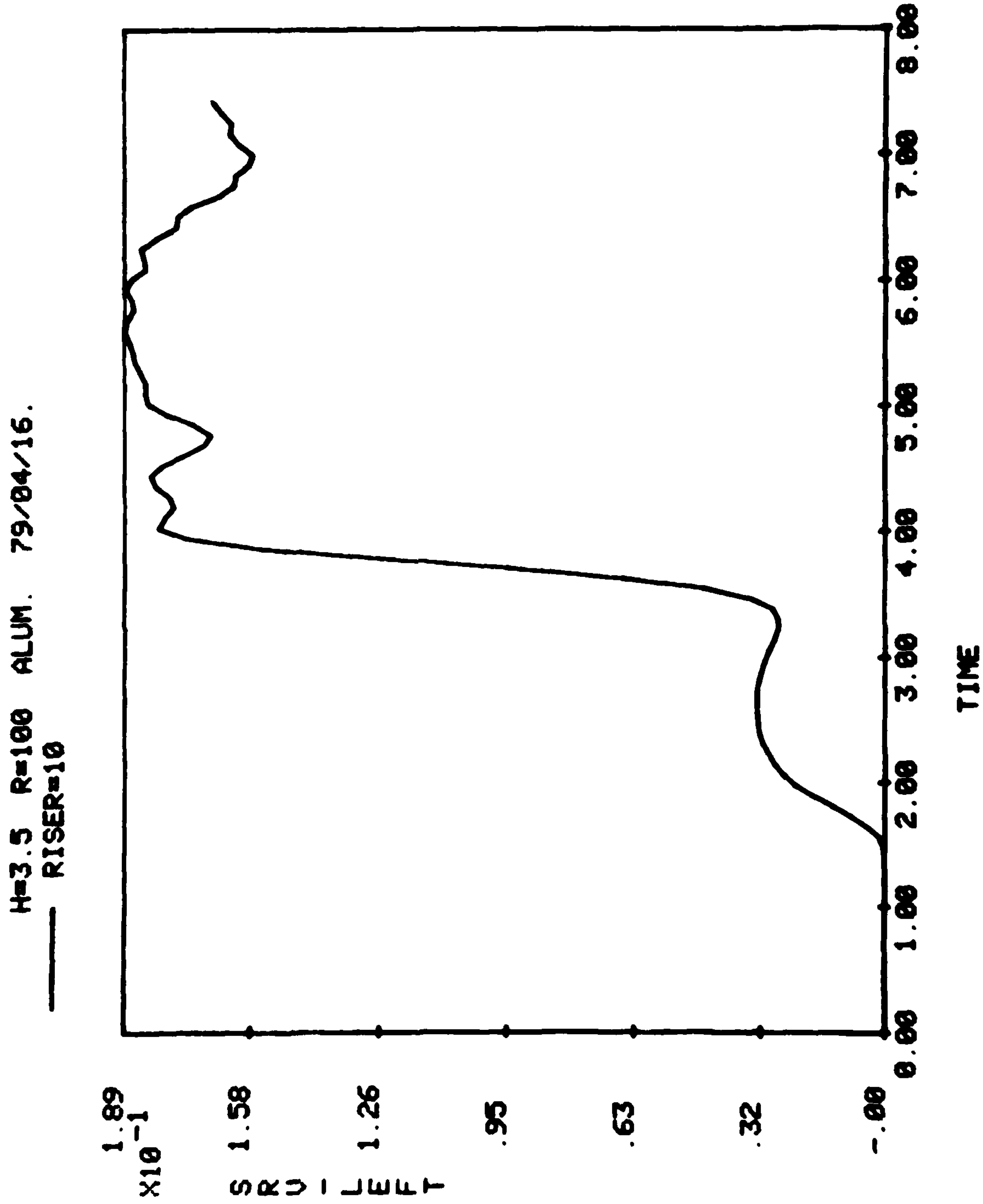
H=3.5 R=100 ALUM. 79/04/16.
RISER=10
TIME
SURFLEFT
X10^-1
1.89
1.58
1.26
.95
.63
.32
-.00
0.00
1.00
2.00
3.00
4.00
5.00
6.00
7.00
8.00

APPENDIX E (Case E)

RING: Aluminum

Radius = 100 inches
Thickness = 1 inch

Curve Label:	Meaning
P-CENTER:	pressure at $r = 0$
P-RIGHT:	pressure at $r = a/2$, $\theta = 0$
P-TOP:	pressure at $r = a/2$, $\theta = 90$ deg.
P-LEFT:	pressure at $r = a/2$, $\theta = 180$ deg.
SRV-RIGHT:	shell radial velocity at $\theta = 0$
SM-RIGHT:	shell moment at $\theta = 0$
SN-RIGHT:	shell stress resultant at $\theta = 0$
SRV-TOP:	shell radial velocity at $\theta = 90$ deg.
STV-TOP:	shell tangential velocity at $\theta = 90$
SM-TOP:	shell moment at $\theta = 90$
SN-TOP:	shell stress resultant at $\theta = 90$
SRV-LEFT:	shell radial velocity at $\theta = 180$ deg.

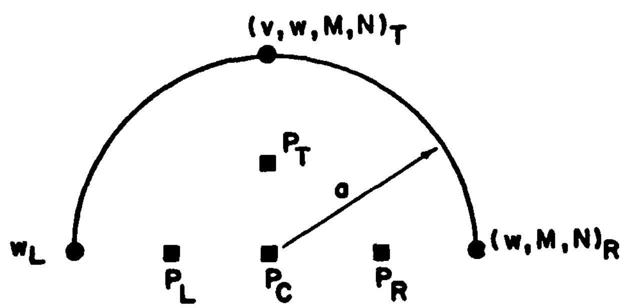

KEY TO TIME HISTORIES IN APPENDICES

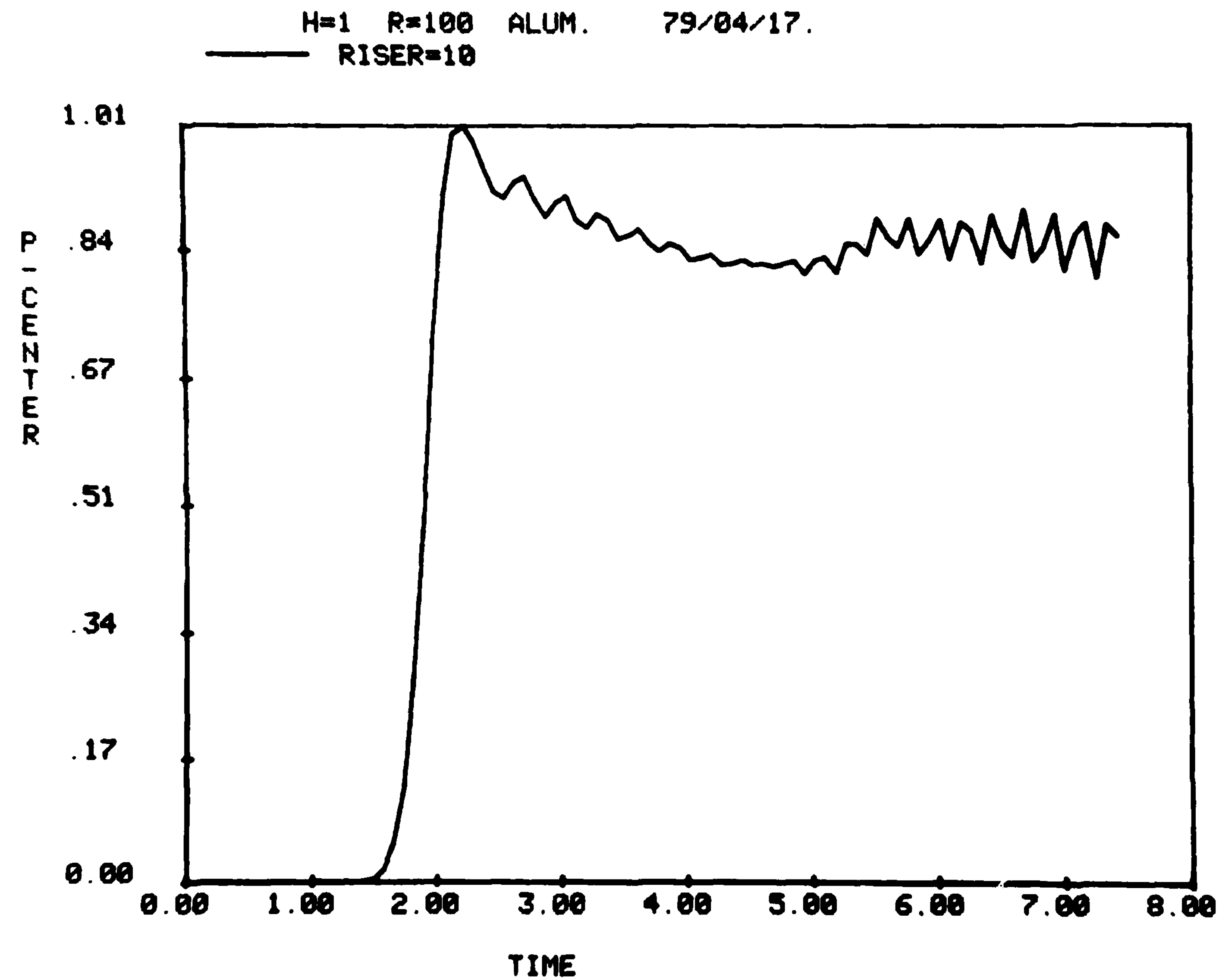
H=1 R=100 ALUM. 79/04/17.
RISER=10
P-CENTER
1.01
.84
.67
.51
.34
.17
0.00
0.00
1.00
2.00
3.00
4.00
5.00
6.00
7.00
8.00
TIME

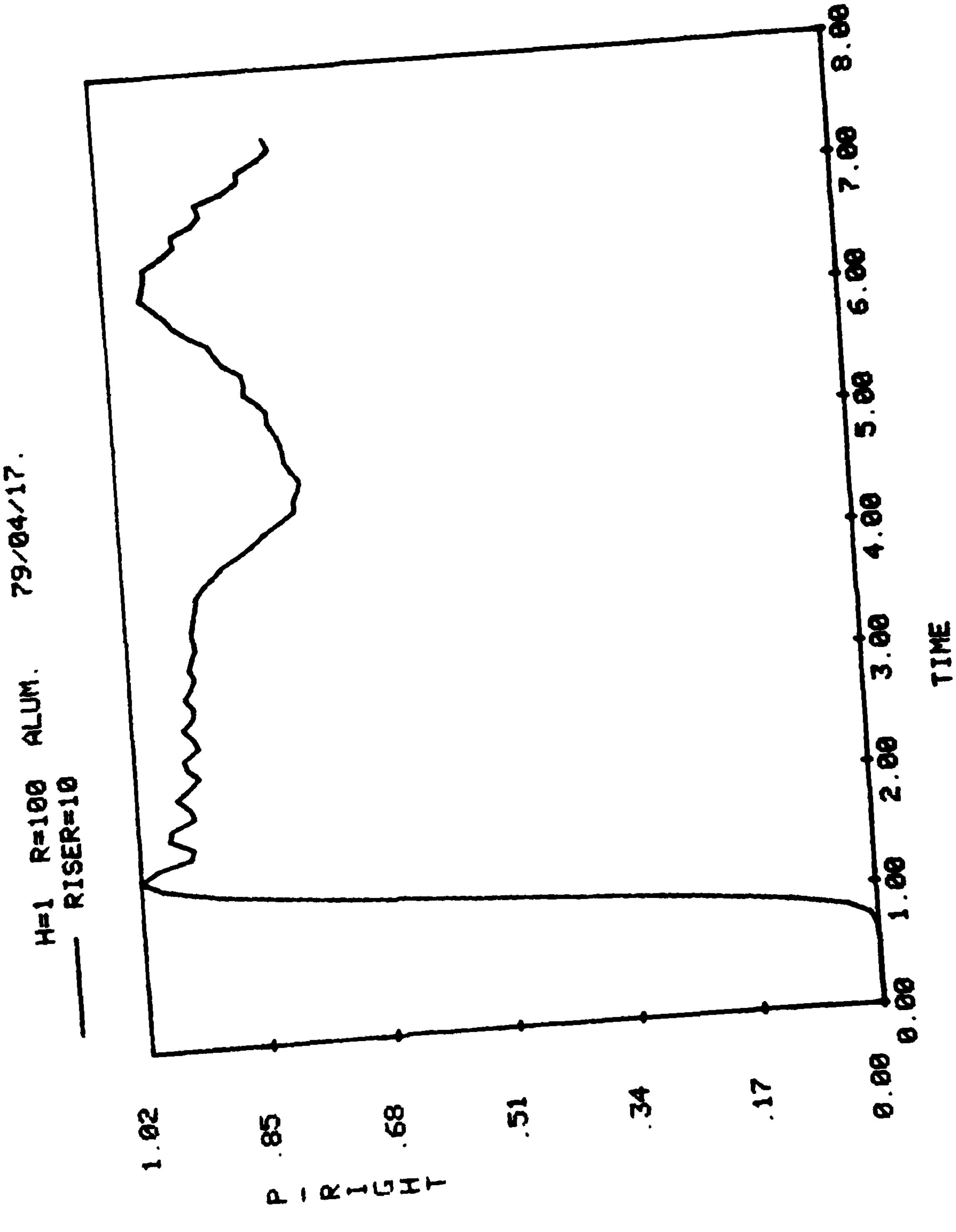

H=1 R=100 ALUM. 79/04/17.
RISER=10
1.02
.85
.68
.51
.34
.17
0.00
PRIGHT
0.00
1.00
2.00
3.00
4.00
5.00
6.00
7.00
8.00
TIME

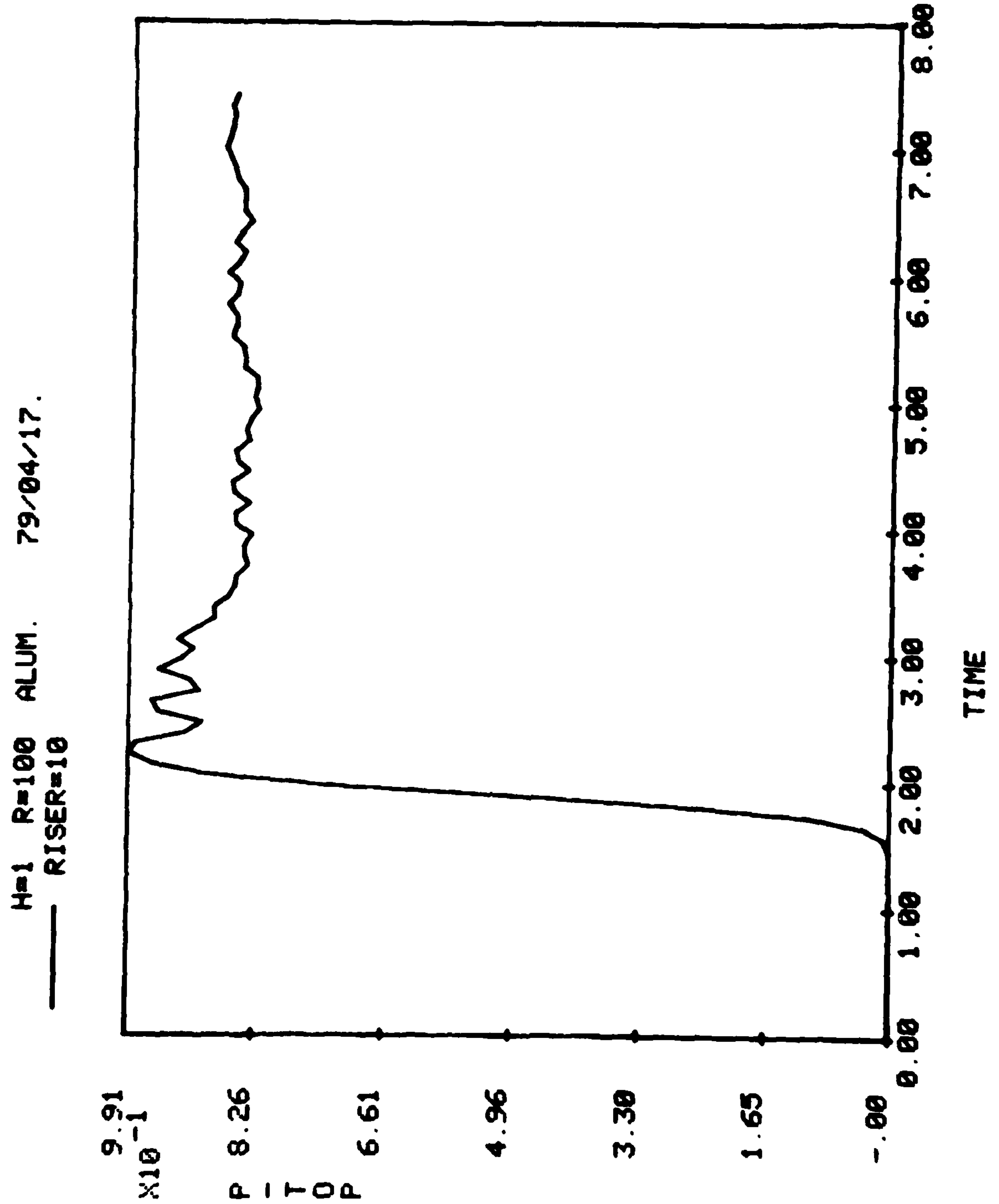
H=1 R=100 ALUM. 79/04/17.
RISER=10
P-TOP
X10^-1
9.91
8.26
6.61
4.96
3.30
1.65
-.00
0.00
1.00
2.00
3.00
4.00
5.00
6.00
7.00
8.00
TIME

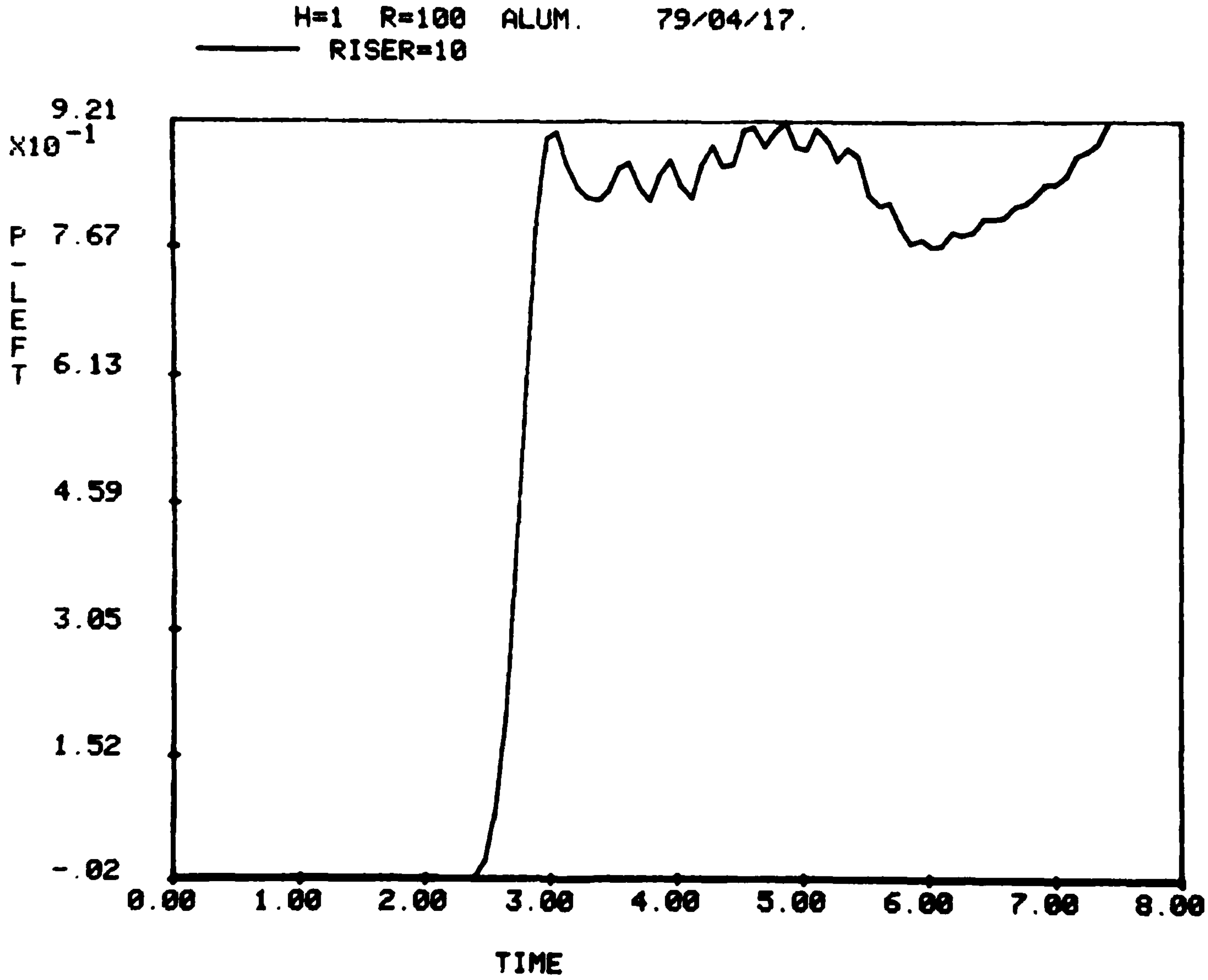
H=1 R=100 ALUM. 79/04/17.
RISER=10
9.21
X10^-1
P-LEFT
7.67
6.13
4.59
3.05
1.52
-.02
0.00
1.00
2.00
3.00
4.00
5.00
6.00
7.00
8.00
TIME

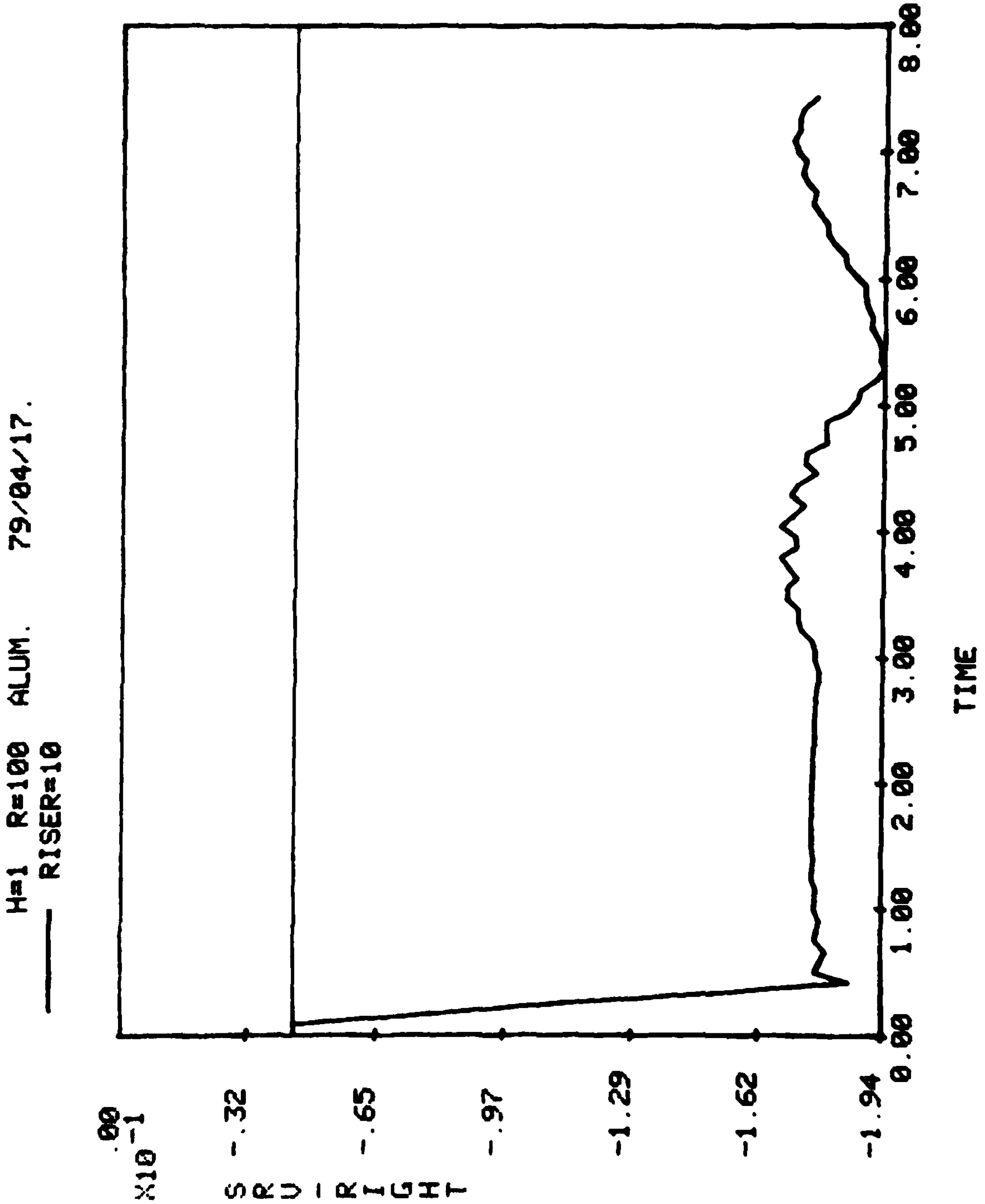
H=1 R=100 ALUM. 79/04/17.
RISER=10
.00
X10^-1
-.32
-.65
-.97
-1.29
-1.62
-1.94
SRV-RIGHT
0.00
1.00
2.00
3.00
4.00
5.00
6.00
7.00
8.00
TIME

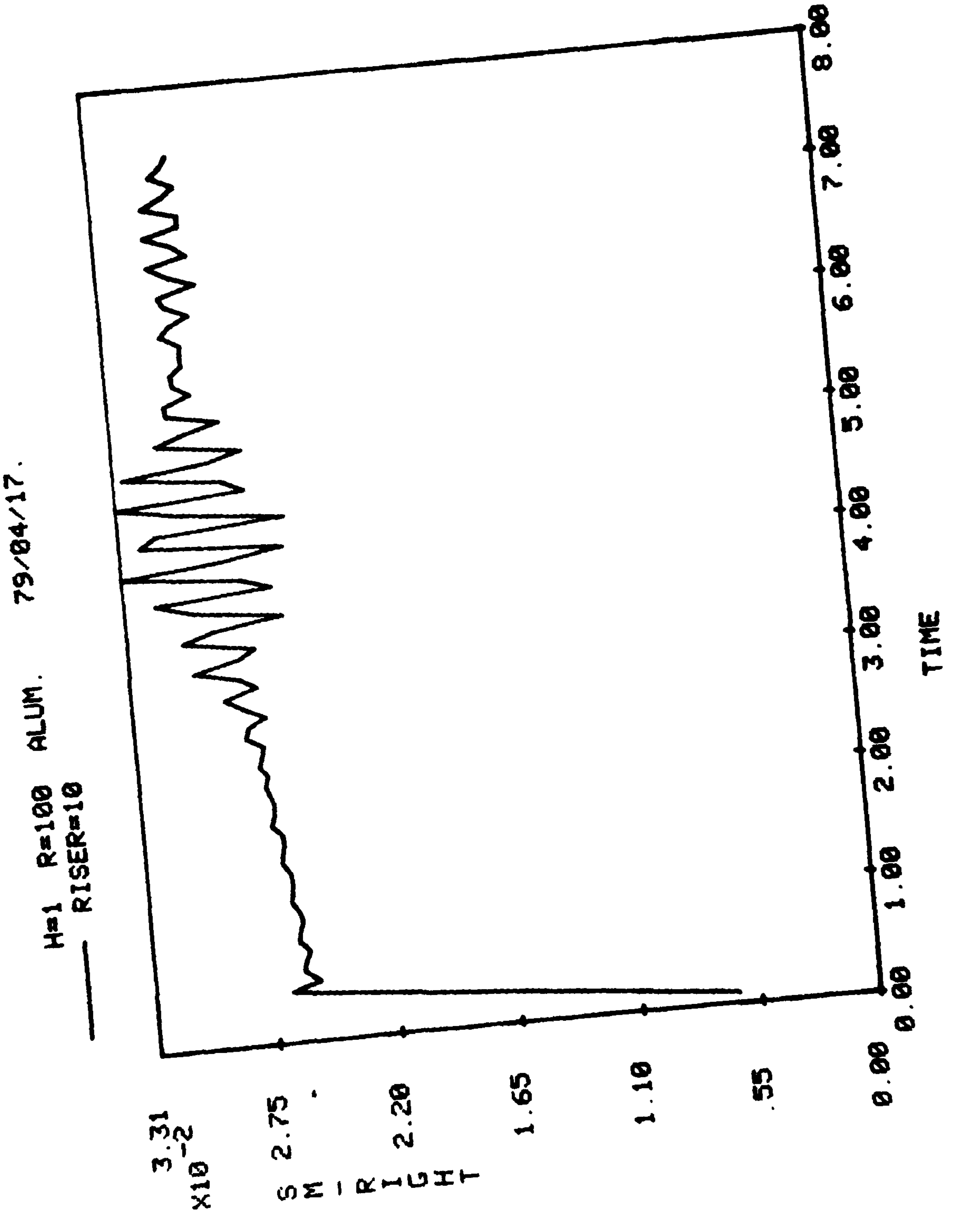

H=1 R=100 ALUM. 79/04/17.
RISER=10
3.31 X10^-2
2.75
2.20
1.65
1.10
.55
0.00
SWIRIGHT
0.00
1.00
2.00
3.00
4.00
5.00
6.00
7.00
8.00
TIME

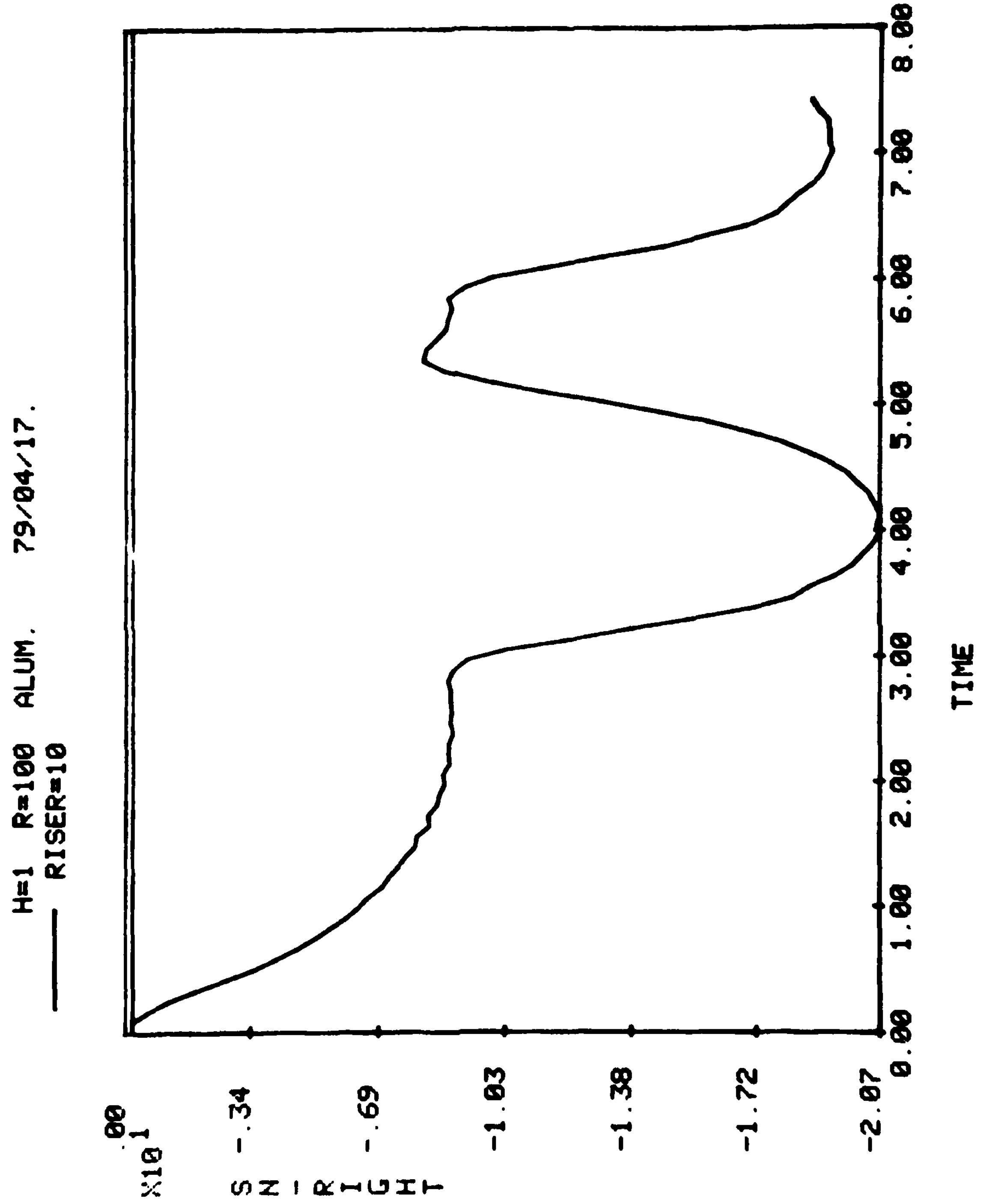

H=1 R=100 ALUM. 79/04/17.
RISER=10
X10^1
.00
-.34
-.69
-1.03
-1.38
-1.72
-2.07
SN-RIGHT
0.00
1.00
2.00
3.00
4.00
5.00
6.00
7.00
8.00
TIME

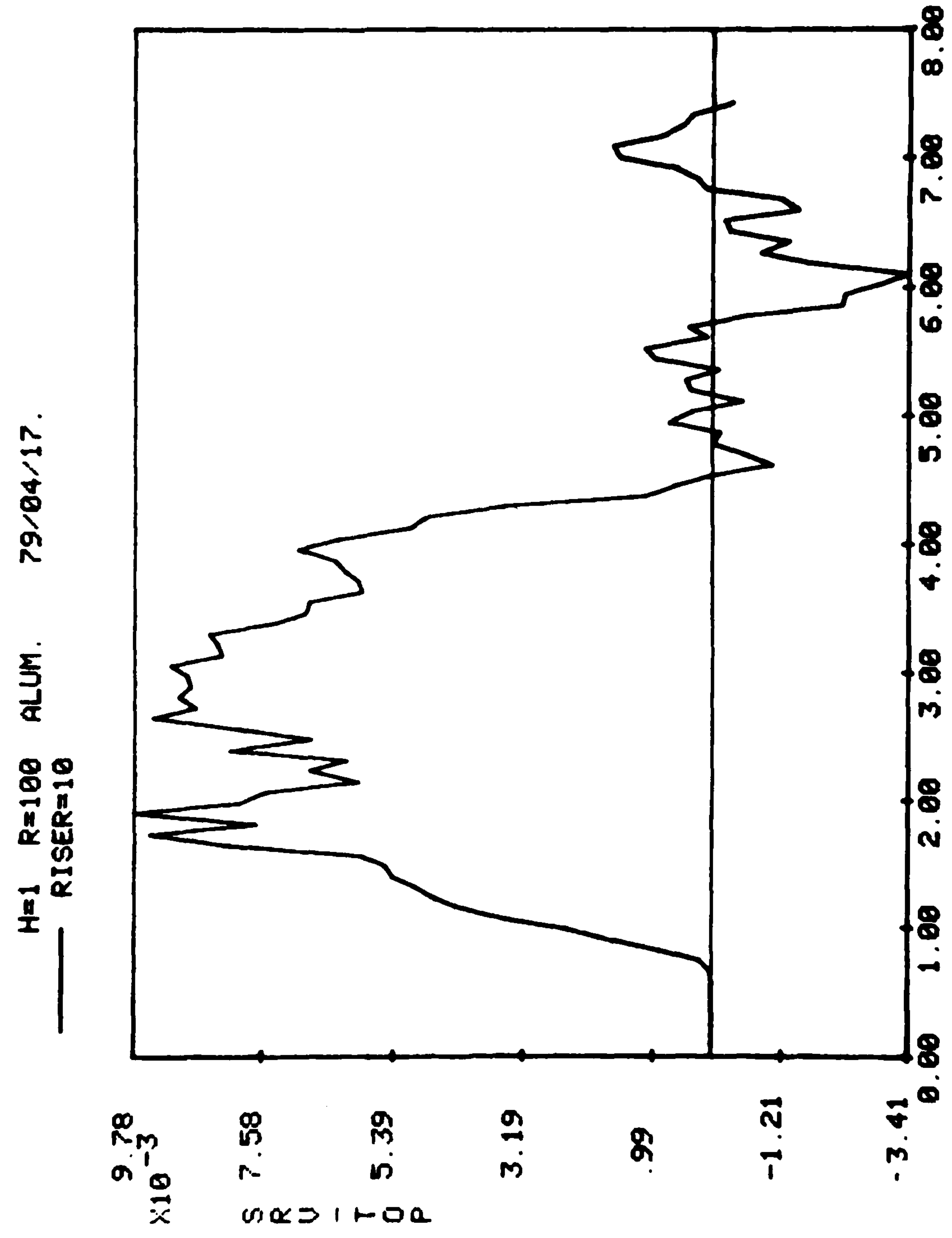

H=1 R=100 ALUM. 79/04/17.
RISER=10
9.78
X10-3
7.58
5.39
3.19
.99
-1.21
-3.41
0.00
1.00
2.00
3.00
4.00
5.00
6.00
7.00
8.00
TIME

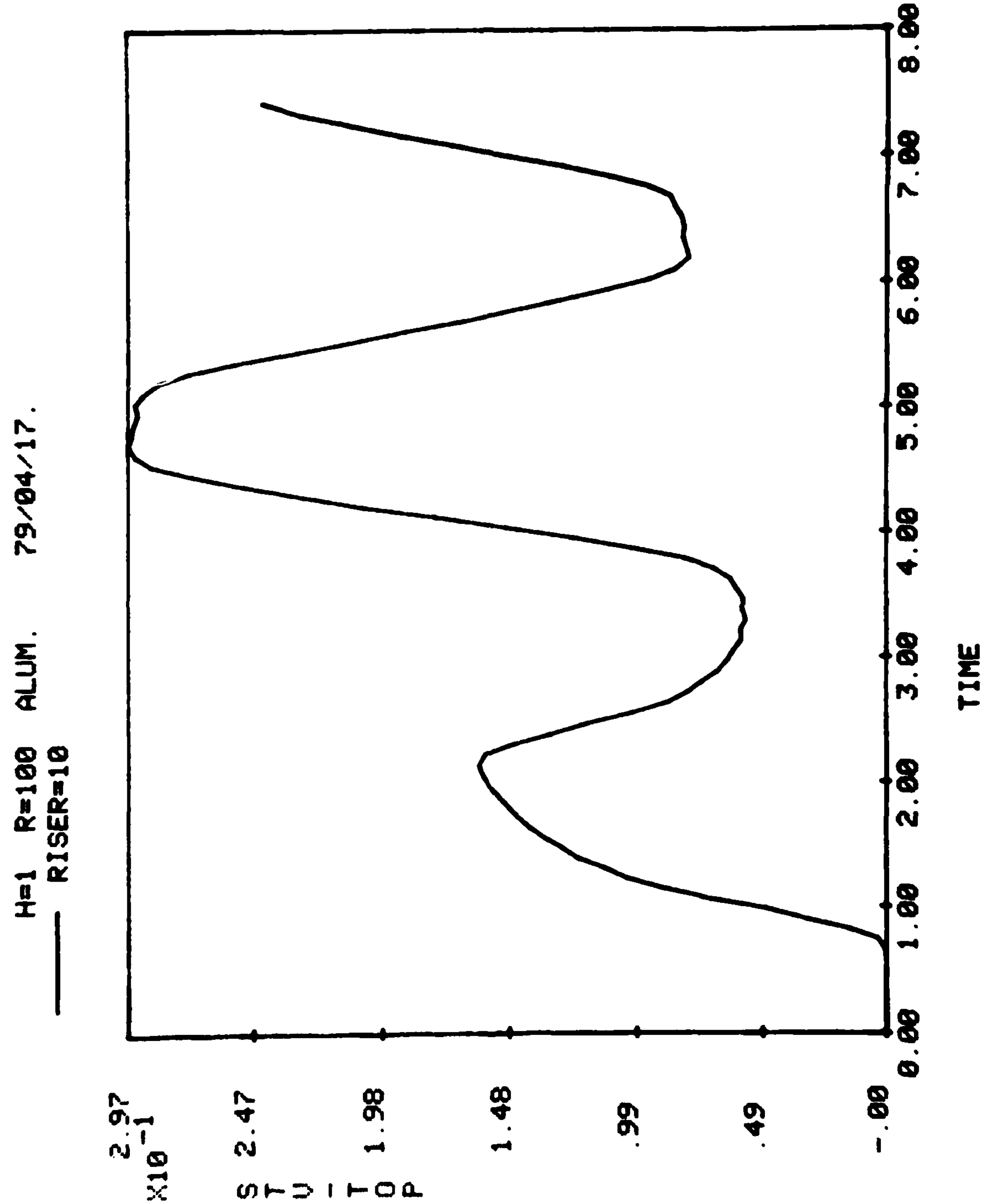
H=1 R=100 ALUM. 79/04/17.
RISER=10
2.97
X10^-1
2.47
1.98
1.48
.99
.49
-.00
0.00
1.00
2.00
3.00
4.00
5.00
6.00
7.00
8.00
TIME

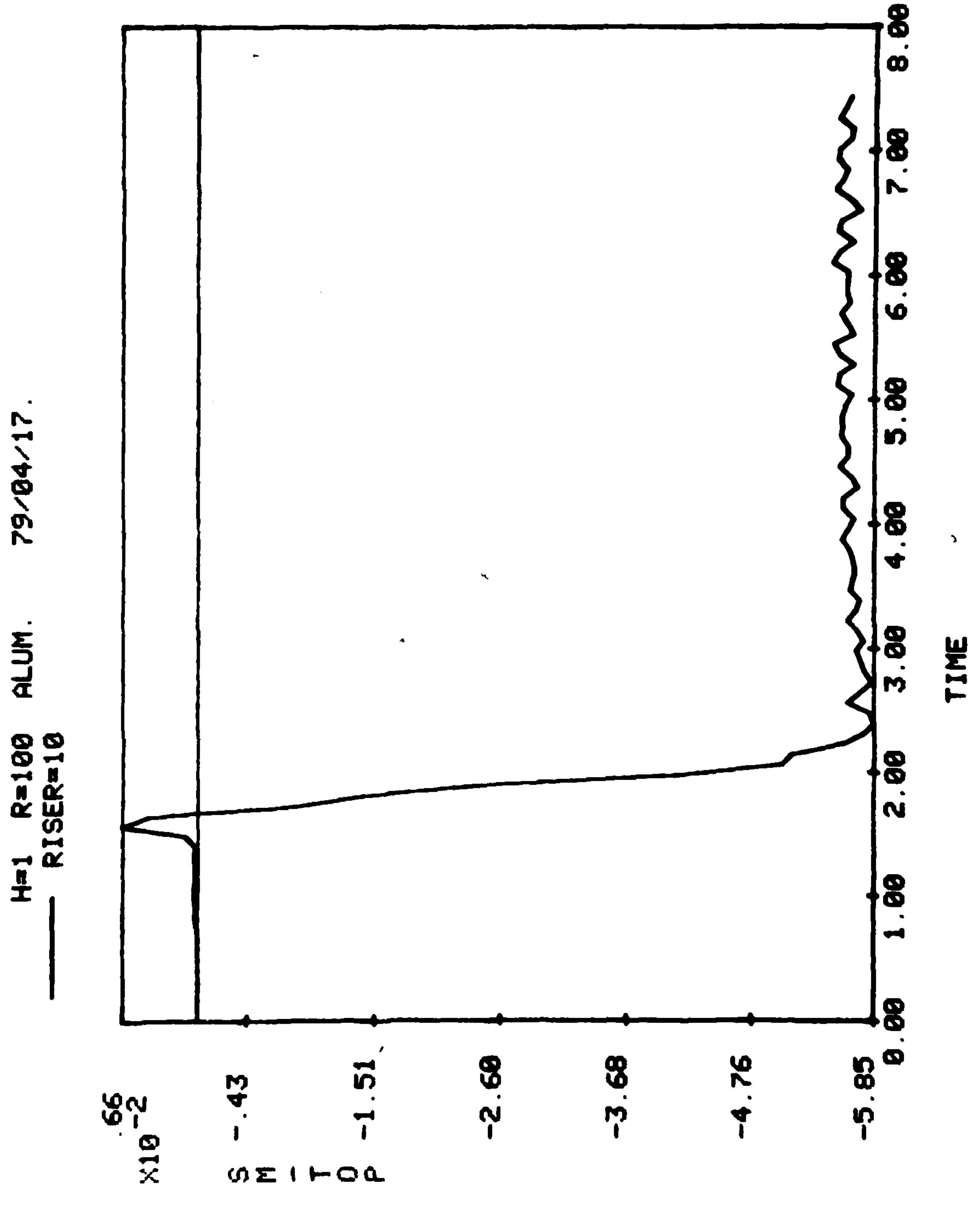
H=1 R=100 ALUM. 79/04/17.
RISER=10
.66
X10^-2
-.43
-1.51
-2.60
-3.68
-4.76
-5.85
STIOP
0.00
1.00
2.00
3.00
4.00
5.00
6.00
7.00
8.00
TIME

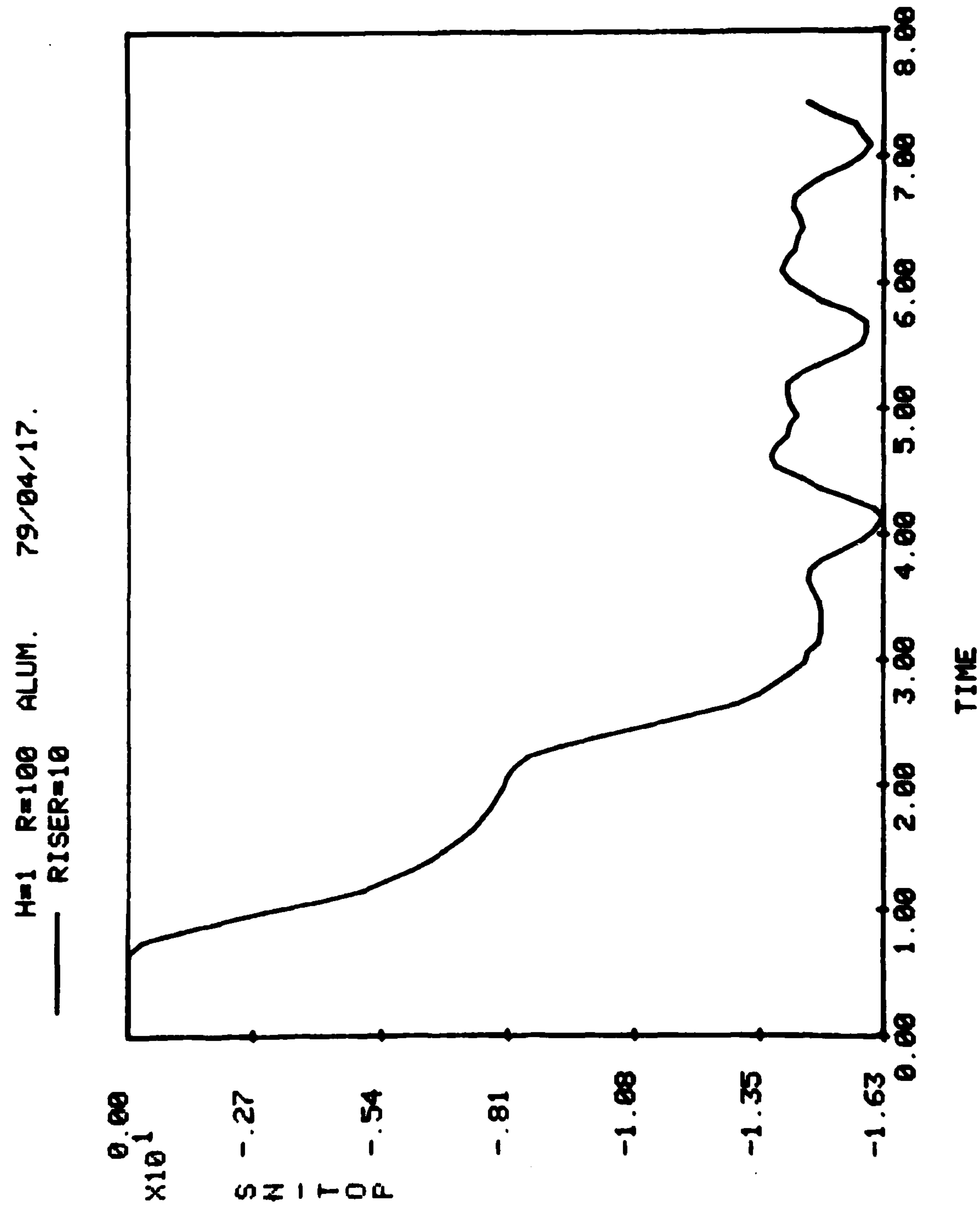
H=1 R=100 ALUM. 79/04/17.
RISER=10
0.00
-.27
-.54
-.81
-1.08
-1.35
-1.63
X10 1
POINTS
0.00
1.00
2.00
3.00
4.00
5.00
6.00
7.00
8.00
TIME

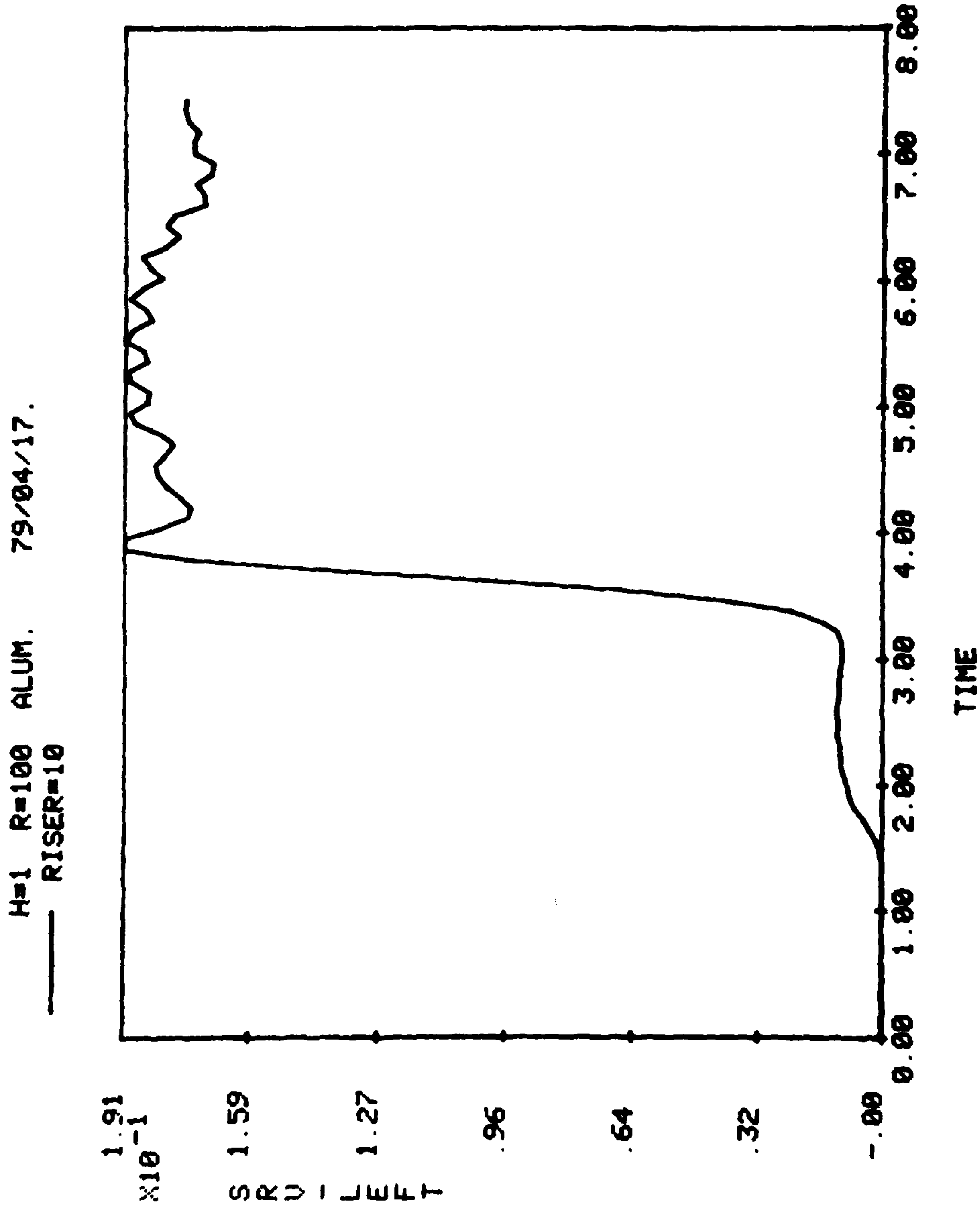
H=1 R=100 ALUM. 79/04/17.
RISER=10
SRV-LEFT
X10^-1
1.91
1.59
1.27
.96
.64
.32
-.00
0.00
1.00
2.00
3.00
4.00
5.00
6.00
7.00
8.00
TIME

APPENDIX F (Case F)

RING: Aluminum

Radius = 100 inches
Thickness = 0.3 inches

Curve Label:	Meaning
P-CENTER:	pressure at r = 0
P-RIGHT:	pressure at r = a/2, θ = 0
P-TOP:	pressure at r = a/2, θ = 90 deg.
P-LEFT:	pressure at r = a/2, θ = 180 deg.
SRV-RIGHT:	shell radial velocity at θ = 0
SM-RIGHT:	shell moment at θ = 0
SN-RIGHT:	shell stress resultant at θ = 0
SRV-TOP:	shell radial velocity at θ = 90 deg.
STV-TOP:	shell tangential velocity at θ = 90
SM-TOP:	shell moment at θ = 90
SN-TOP:	shell stress resultant at θ = 90
SRV-LEFT:	shell radial velocity at θ = 180 deg.

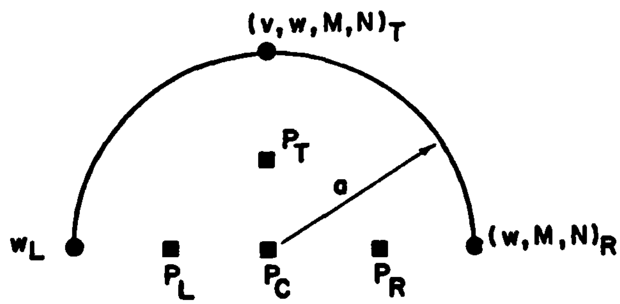

KEY TO TIME HISTORIES IN APPENDICES

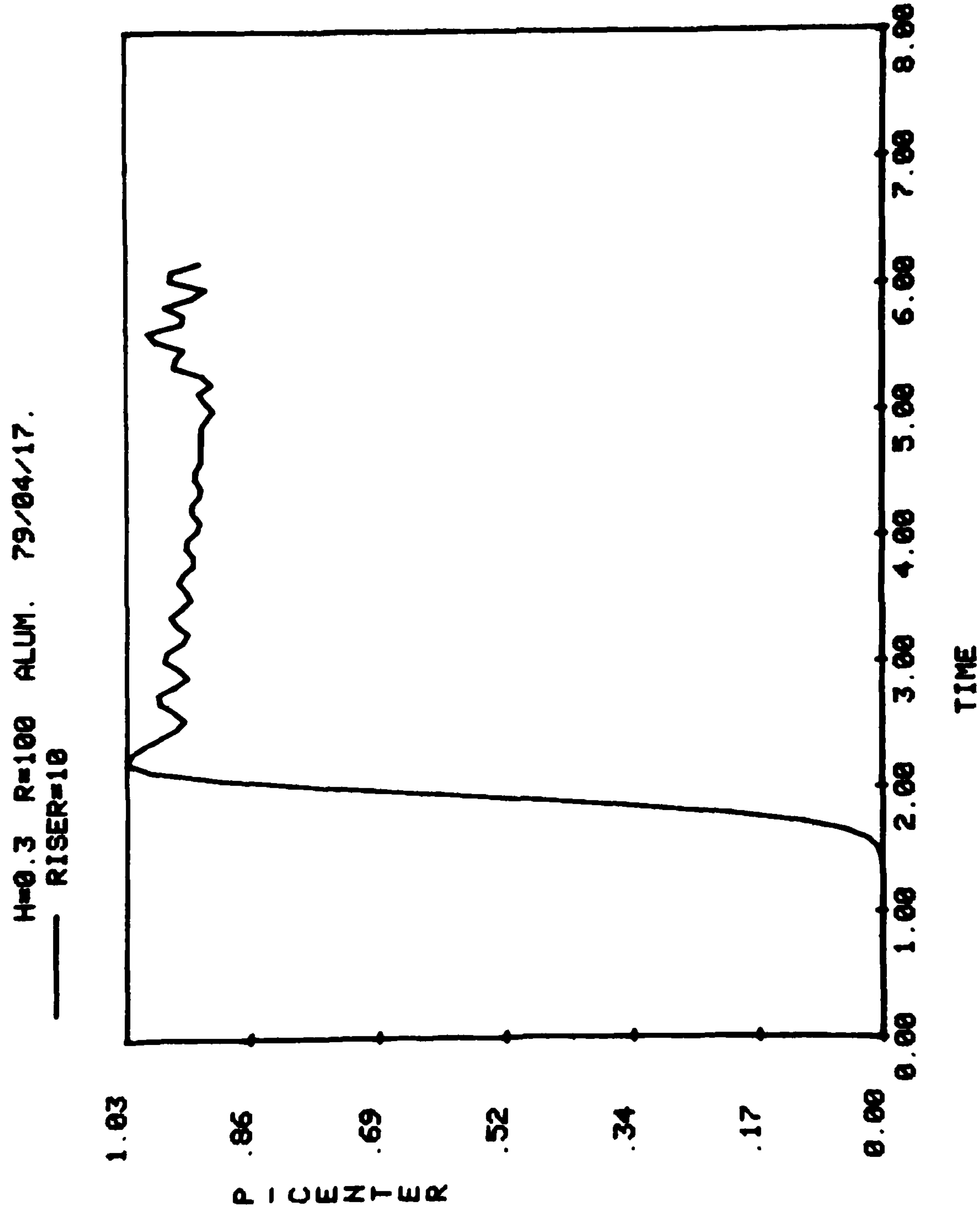
H=0.3 R=100 ALUM. 79/04/17.
RISER=10
P-CENTER
1.03
.86
.69
.52
.34
.17
0.00
0.00
1.00
2.00
3.00
4.00
5.00
6.00
7.00
8.00
TIME

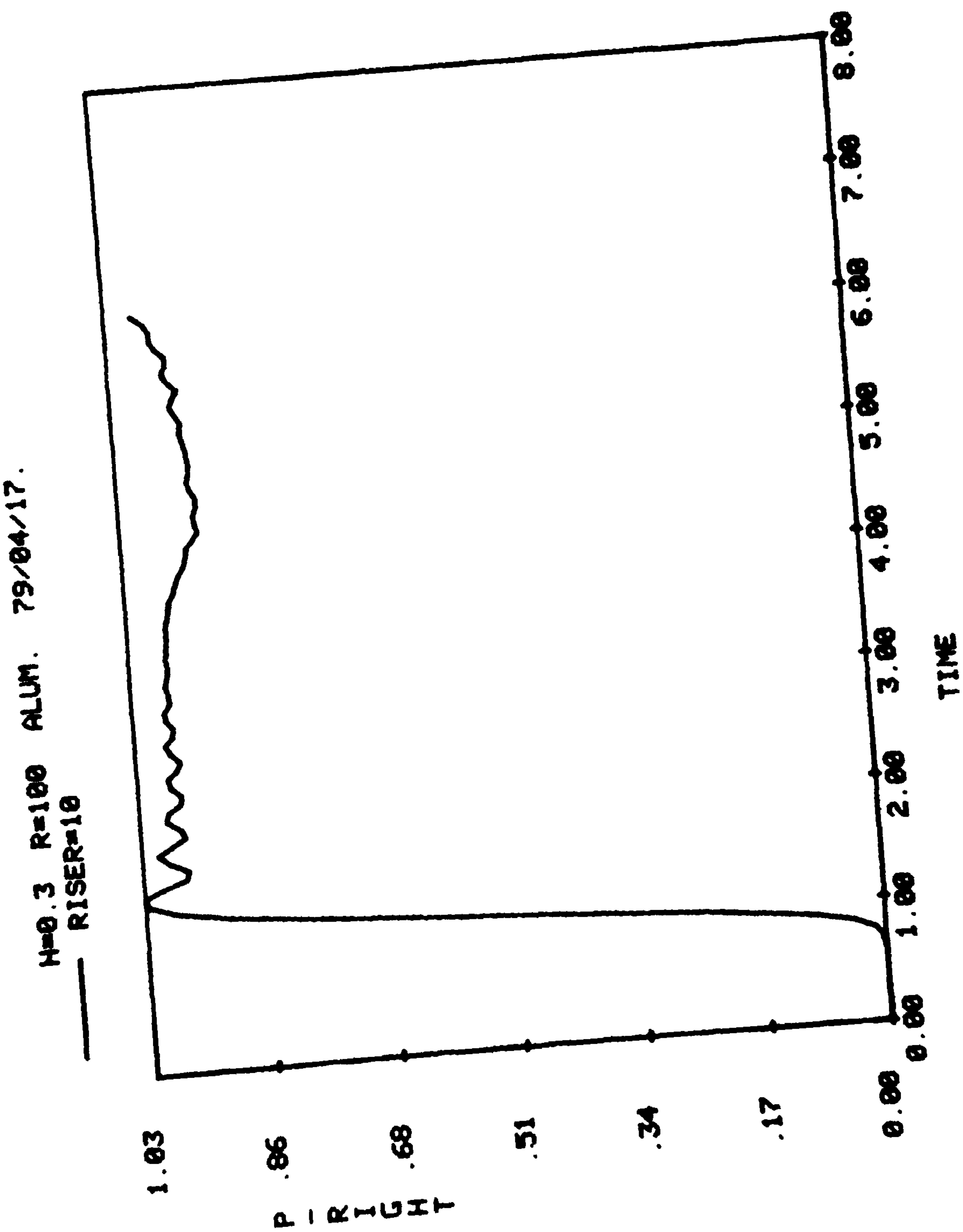
H=0.3 R=100 ALUM. 79/04/17.
RISER=10
TIME
P-RIGHT
0.00
1.00
2.00
3.00
4.00
5.00
6.00
7.00
8.00
.17
.34
.51
.68
.86
1.03

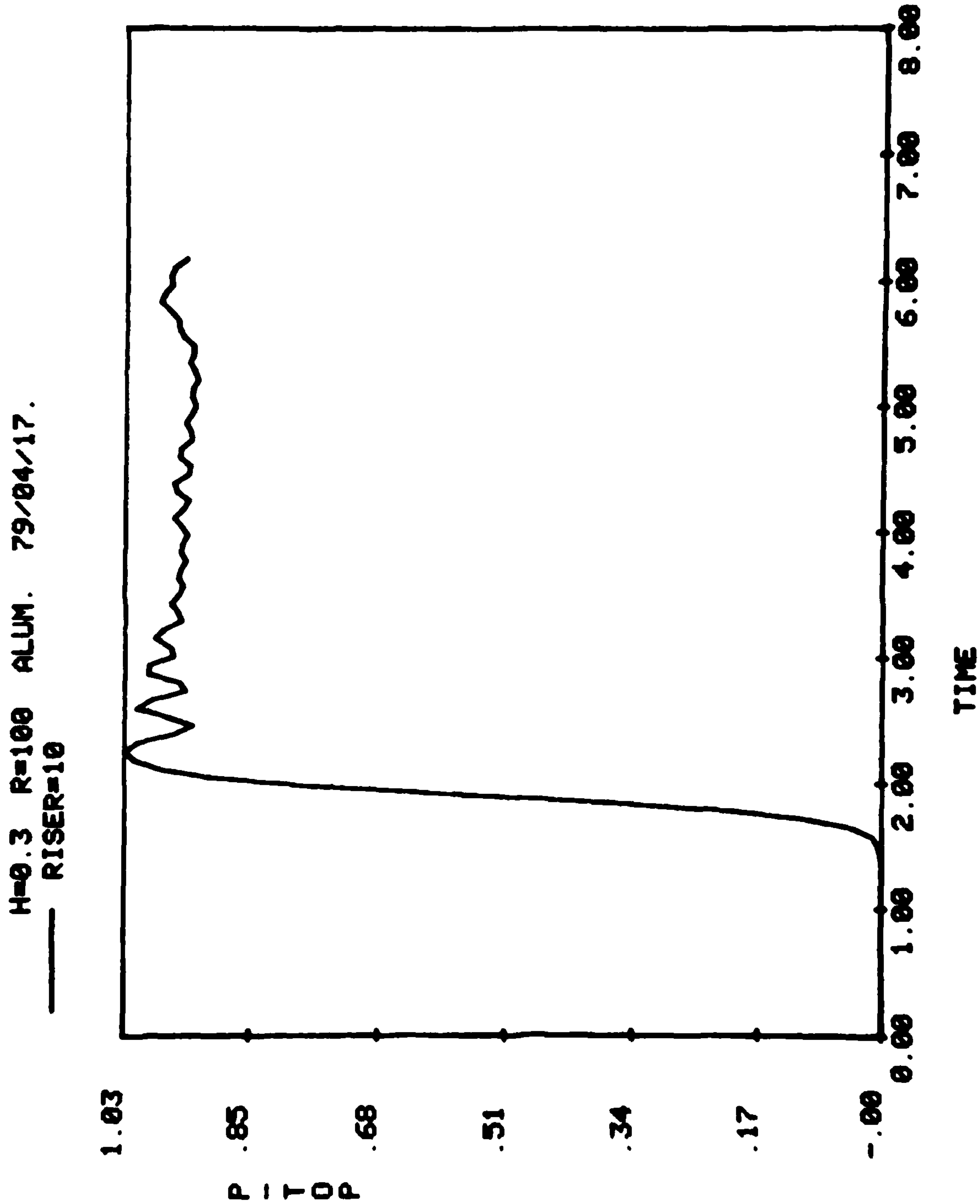

H=0.3 R=100 ALUM. 79/04/17.
RISER=10
1.03
.85
.68
.51
.34
.17
-.00
P-TOP
0.00
1.00
2.00
3.00
4.00
5.00
6.00
7.00
8.00
TIME

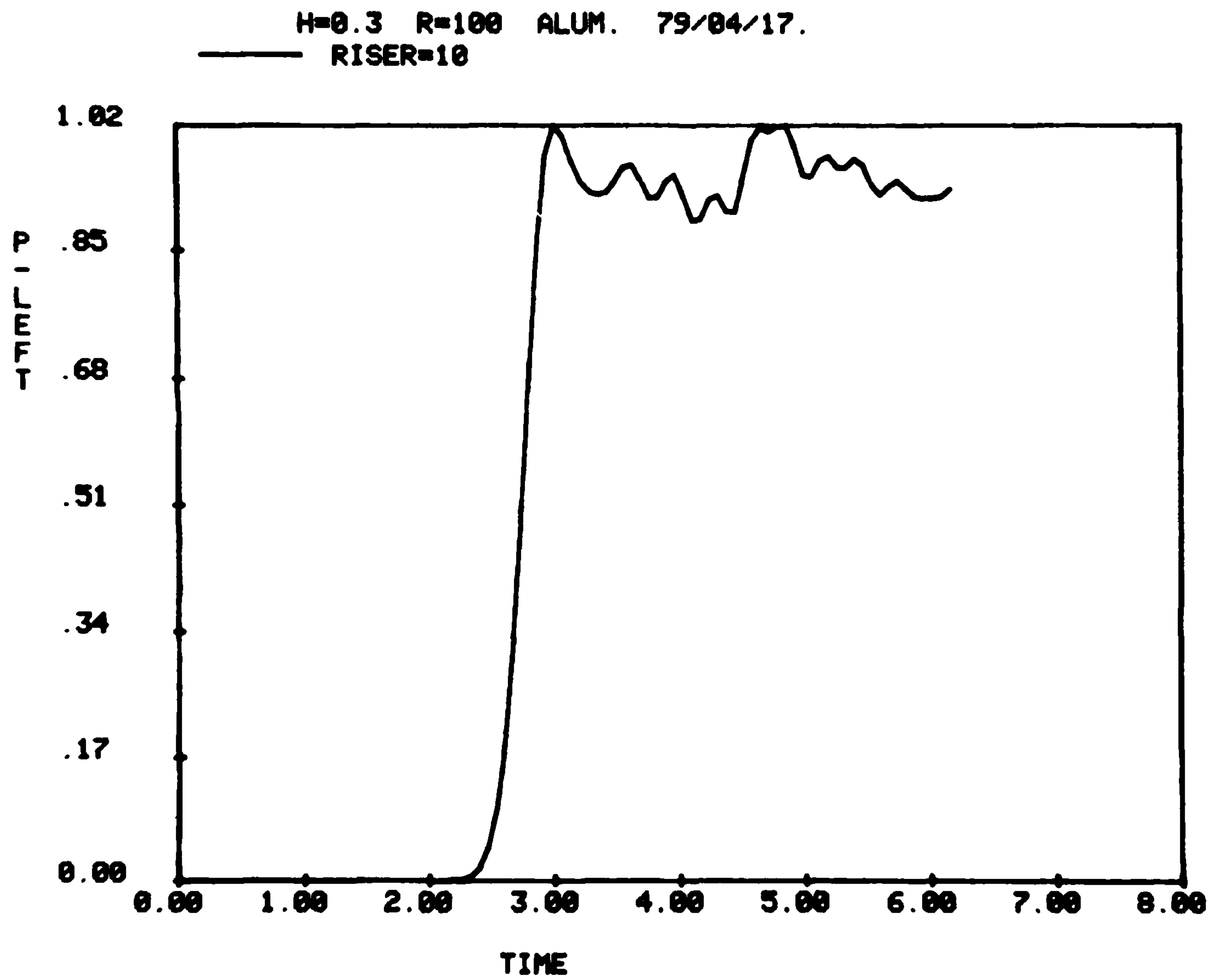
H=0.3 R=100 ALUM. 79/04/17.
RISER=10
P-LEFT
1.02
.85
.68
.51
.34
.17
0.00
0.00
1.00
2.00
3.00
4.00
5.00
6.00
7.00
8.00
TIME

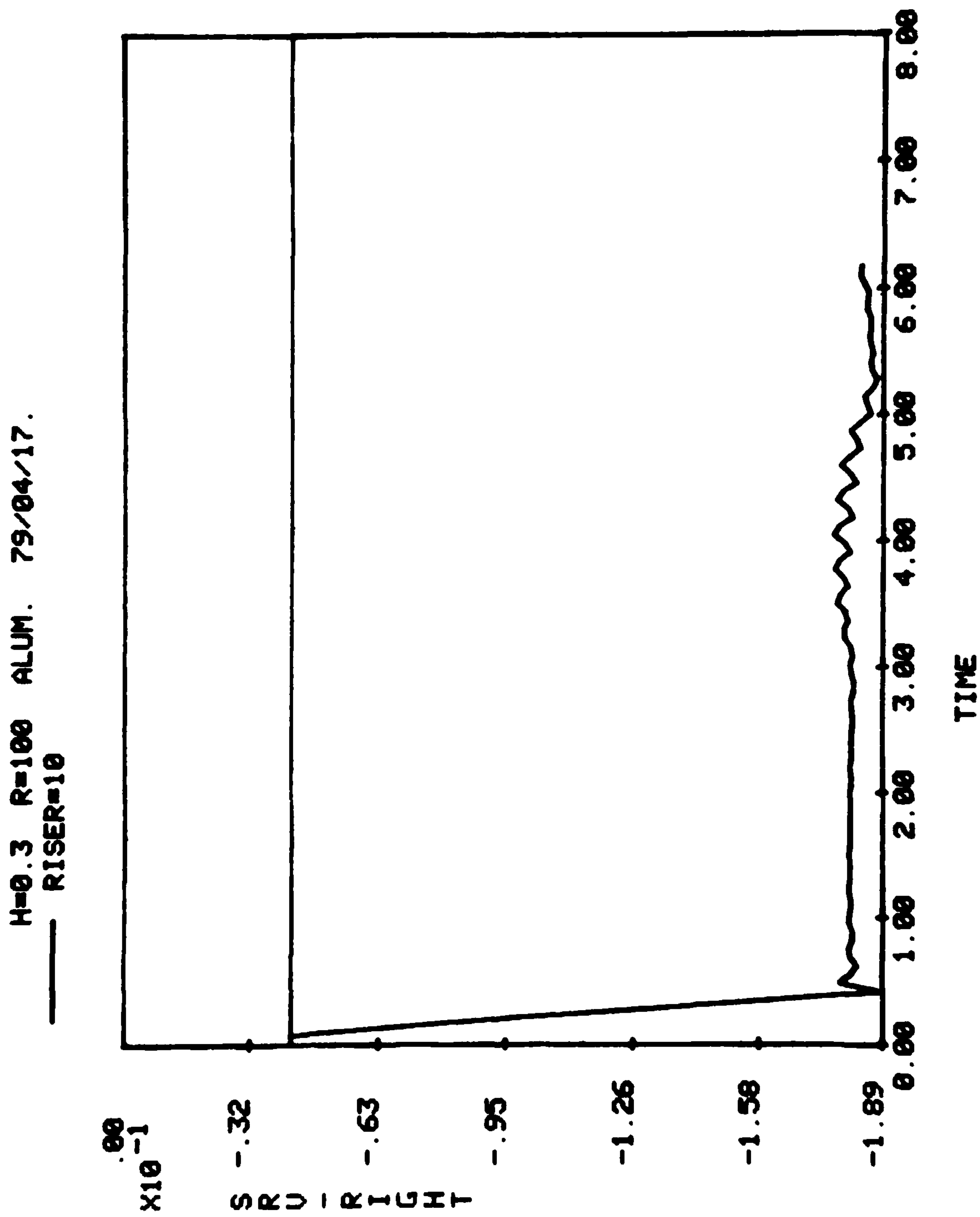
H=0.3 R=100 ALUM. 79/04/17.
RISER=10
.00
X10^-1
-.32
-.63
-.95
-1.26
-1.58
-1.89
SRU-RIGHT
0.00
1.00
2.00
3.00
4.00
5.00
6.00
7.00
8.00
TIME

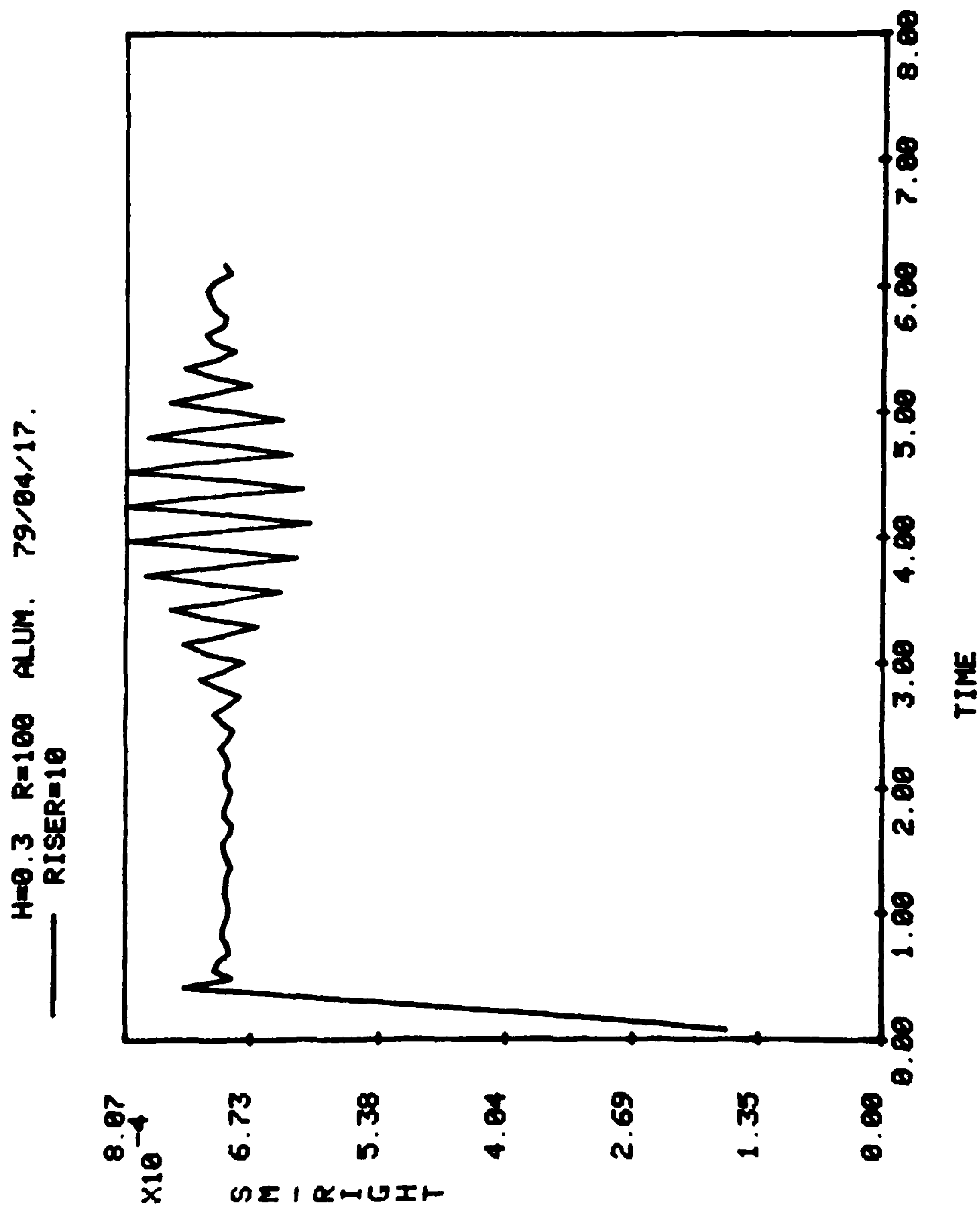
H=0.3 R=100 ALUM. 79/04/17.
RISER=10
8.07
X10^-4
6.73
5.38
4.04
2.69
1.35
0.00
0.00
1.00
2.00
3.00
4.00
5.00
6.00
7.00
8.00
TIME

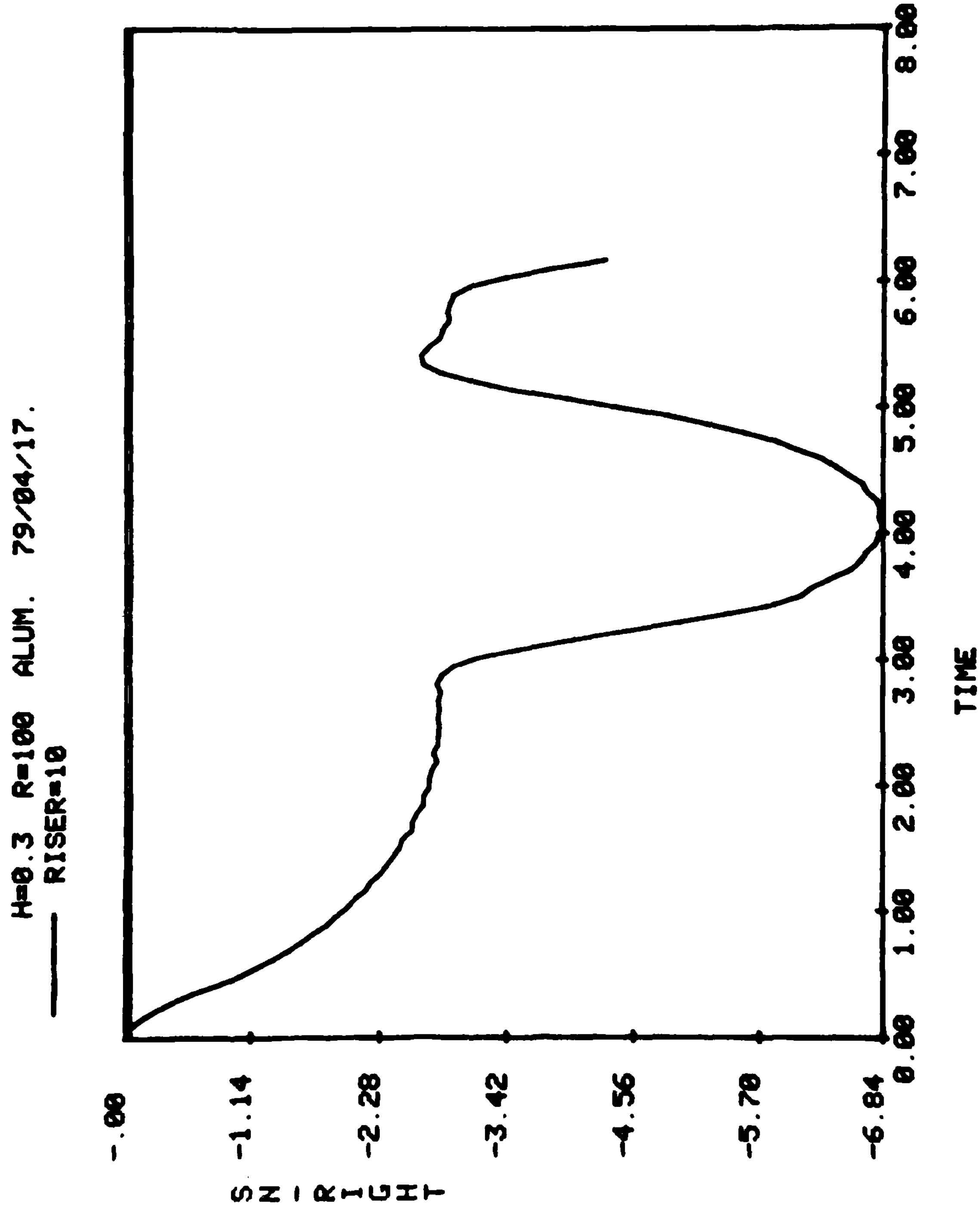
H=0.3 R=100 ALUM. 79/04/17.
RISER=10
-.00
-1.14
-2.28
-3.42
-4.56
-5.70
-6.84
SN-RIGHT
0.00
1.00
2.00
3.00
4.00
5.00
6.00
7.00
8.00
TIME

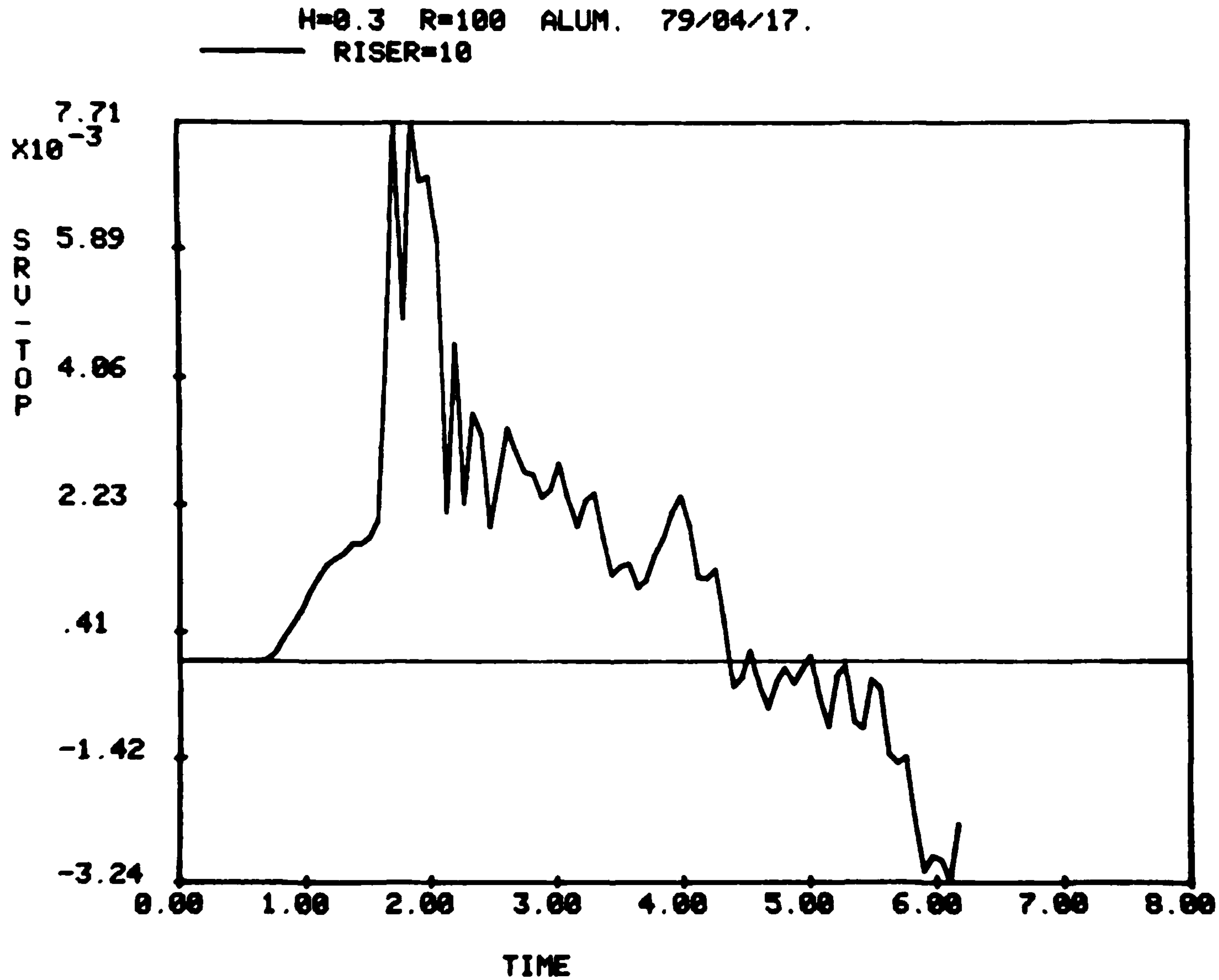
H=0.3 R=100 ALUM. 79/04/17.
RISER=10
7.71
X10^-3
5.89
4.06
2.23
.41
-1.42
-3.24
SRU-TOP
0.00
1.00
2.00
3.00
4.00
5.00
6.00
7.00
8.00
TIME

AD-A083 347 WEIDLINGER ASSOCIATES NEW YORK F/G 20/4
PRELIMINARY STUDY OF A TEST PROCEDURE FOR OBTAINING STEP WAVE L--ETC(U)
APR 79 J P WRIGHT, M L BARON, F L DIMAGGIO DNA001-79-C-0078

UNCLASSIFIED DNA-4933T NL

2 OF 2
AD
A083347

END
DATE
FILMED
5-80
DTIC

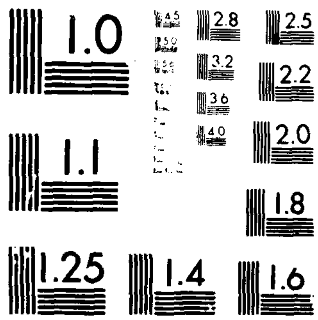

MICROCOPY RESOLUTION TEST CHART
NATIONAL BUREAU OF STANDARDS-1963-A

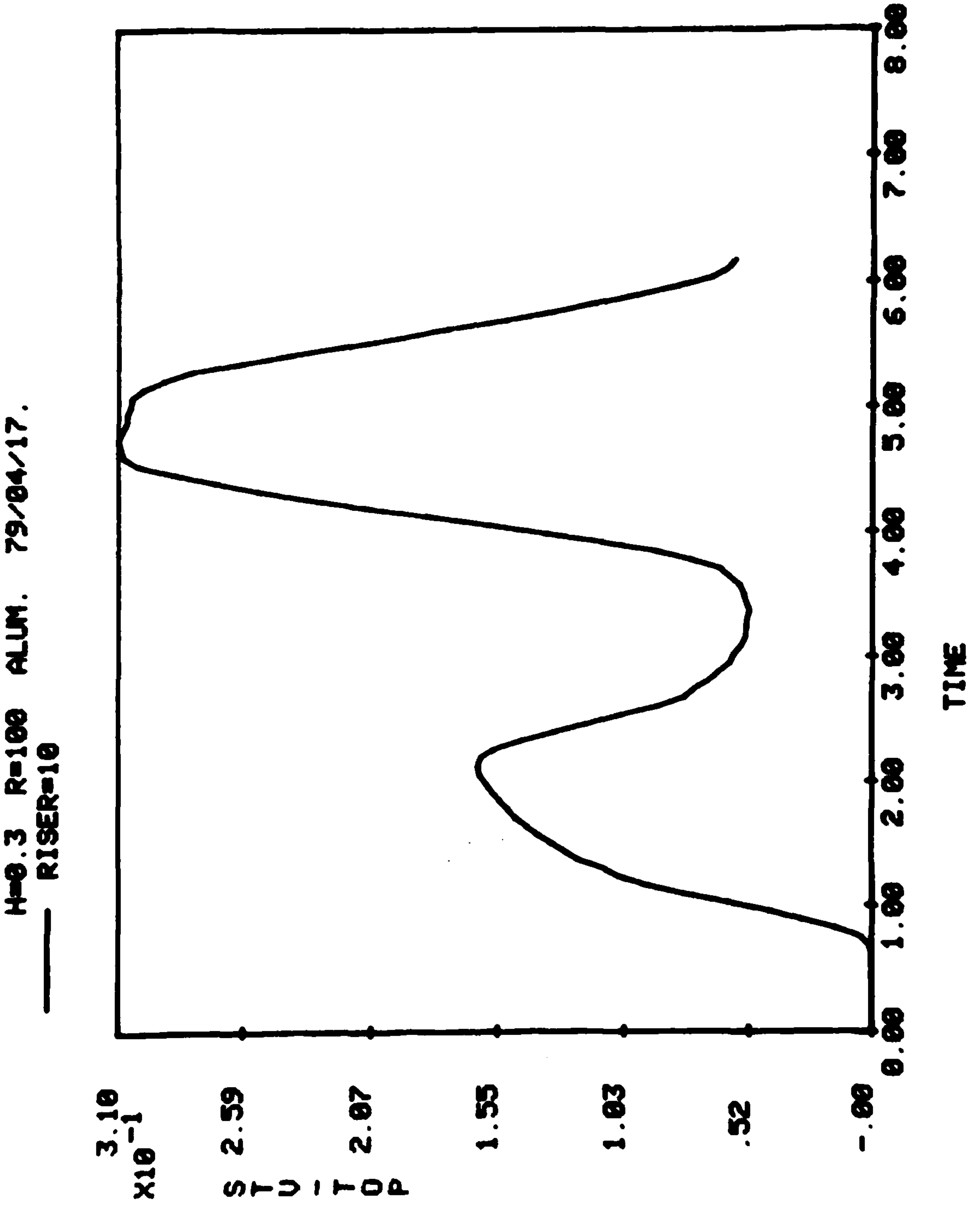
H=0.3 R=100 ALUM. 79/04/17.
RISER=10
3.10
X10^-1
2.59
2.07
1.55
1.03
.52
-.00
0.00
1.00
2.00
3.00
4.00
5.00
6.00
7.00
8.00
TIME

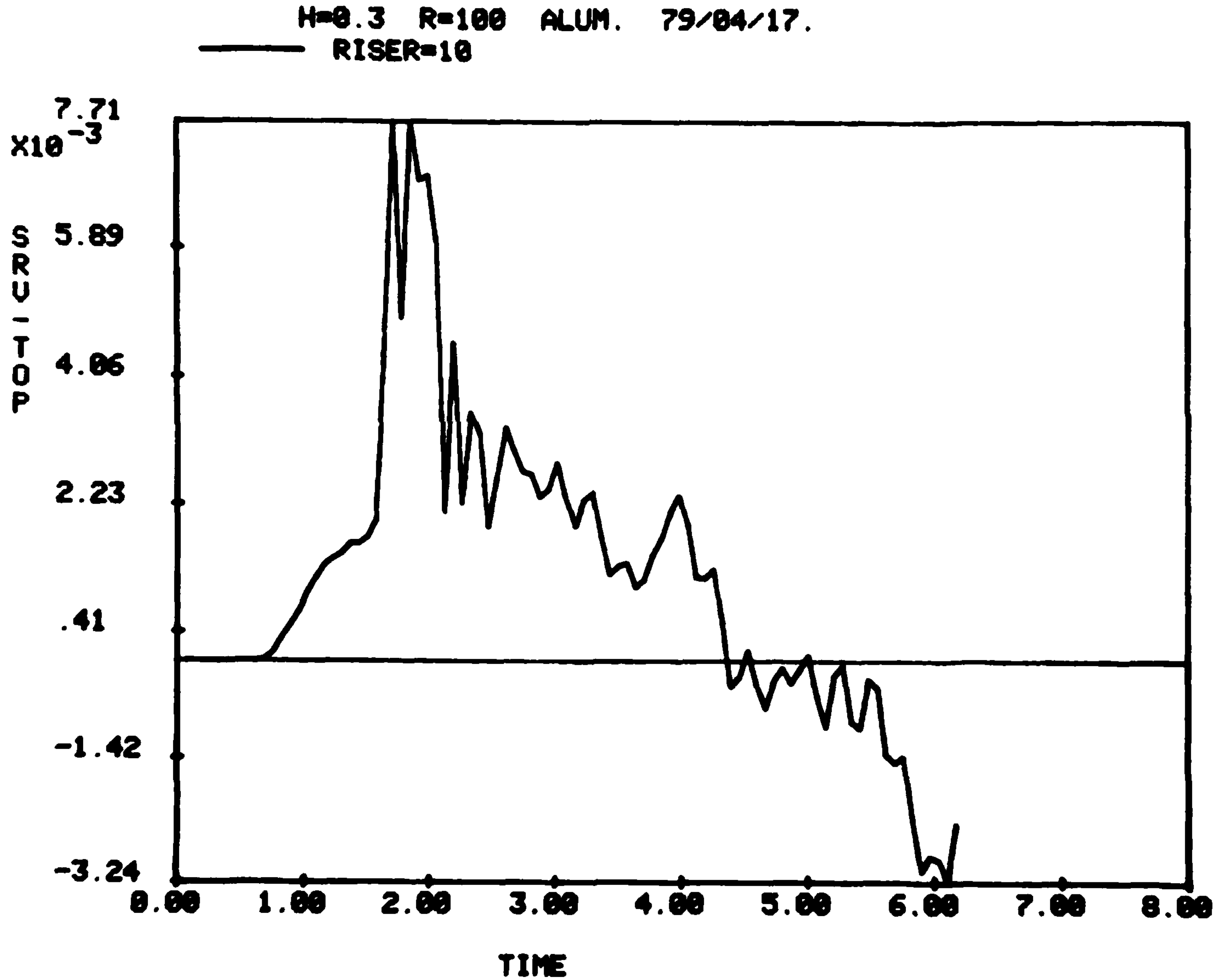
H=0.3 R=100 ALUM. 79/04/17.
RISER=10
7.71
X10^-3
5.89
4.06
2.23
.41
-1.42
-3.24
SRV-TOP
0.00
1.00
2.00
3.00
4.00
5.00
6.00
7.00
8.00
TIME

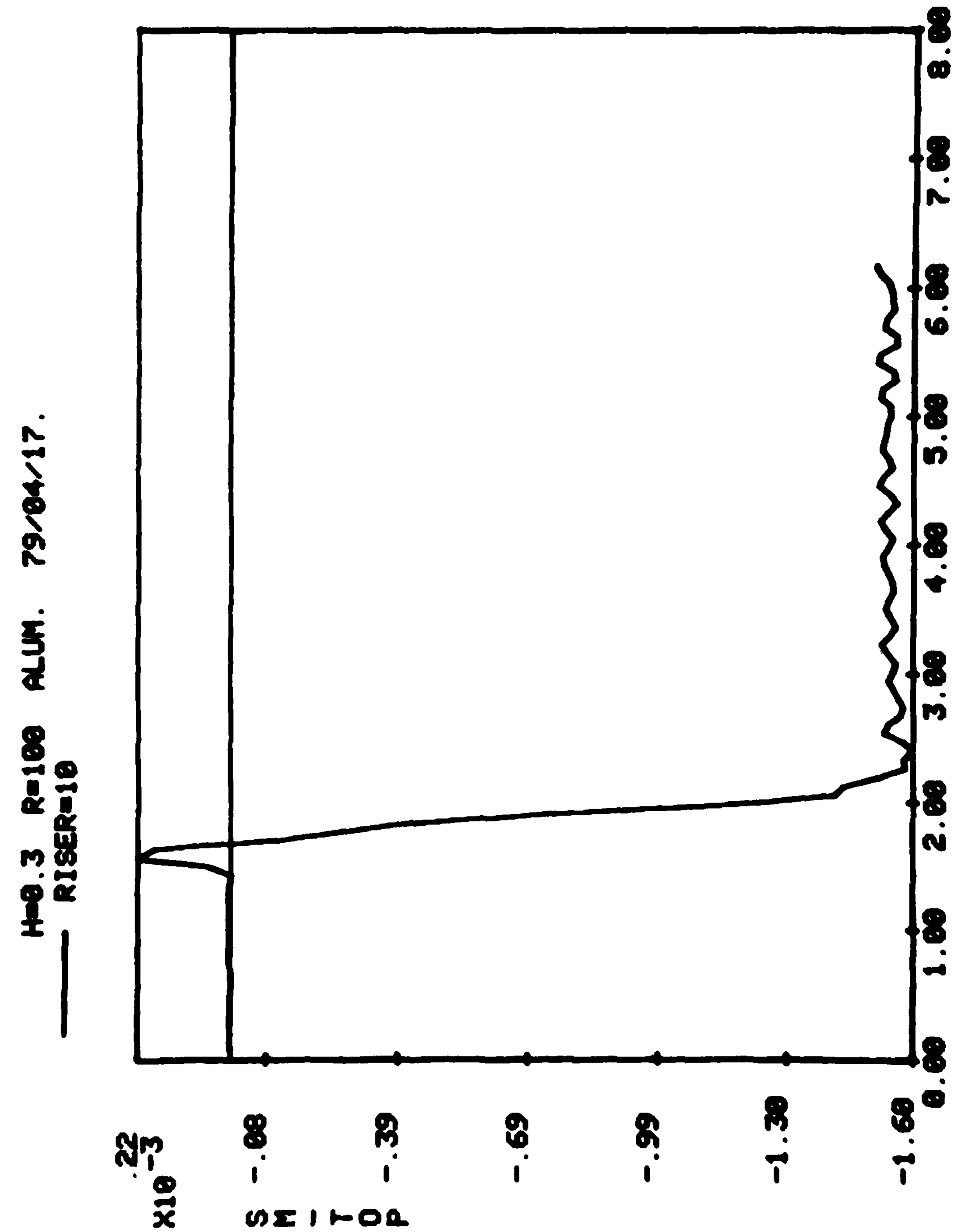

H=0.3 R=100 ALUM. 79/04/17.
RISER=10
.22
X10^-3
SM-TOP
-.08
-.39
-.69
-.99
-1.30
-1.60
0.00
1.00
2.00
3.00
4.00
5.00
6.00
7.00
8.00
TIME

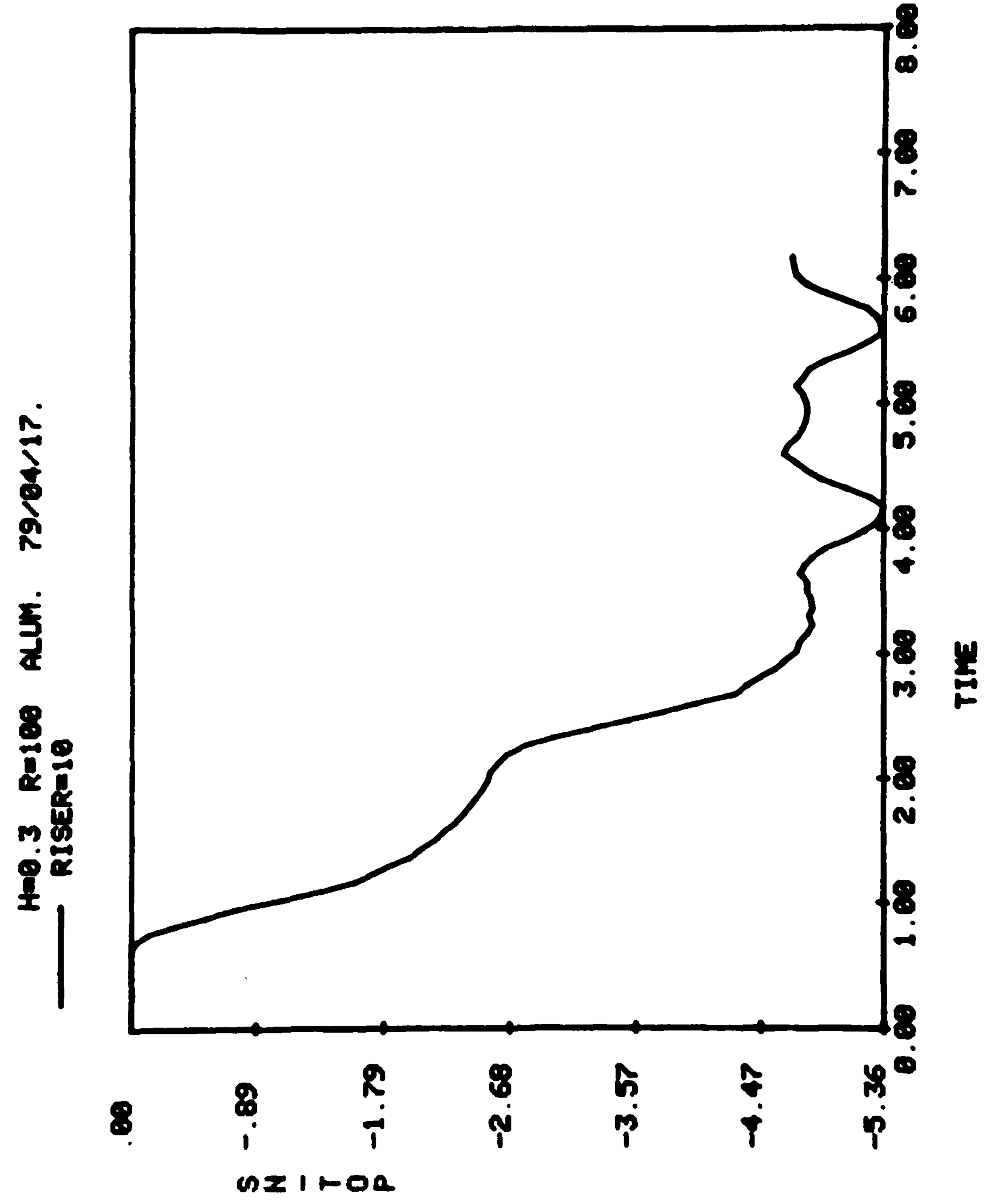

H=0.3 R=100 ALUM. 79/04/17.
RISER=10
SN-TOP
.00
-.89
-1.79
-2.68
-3.57
-4.47
-5.36
0.00
1.00
2.00
3.00
4.00
5.00
6.00
7.00
8.00
TIME

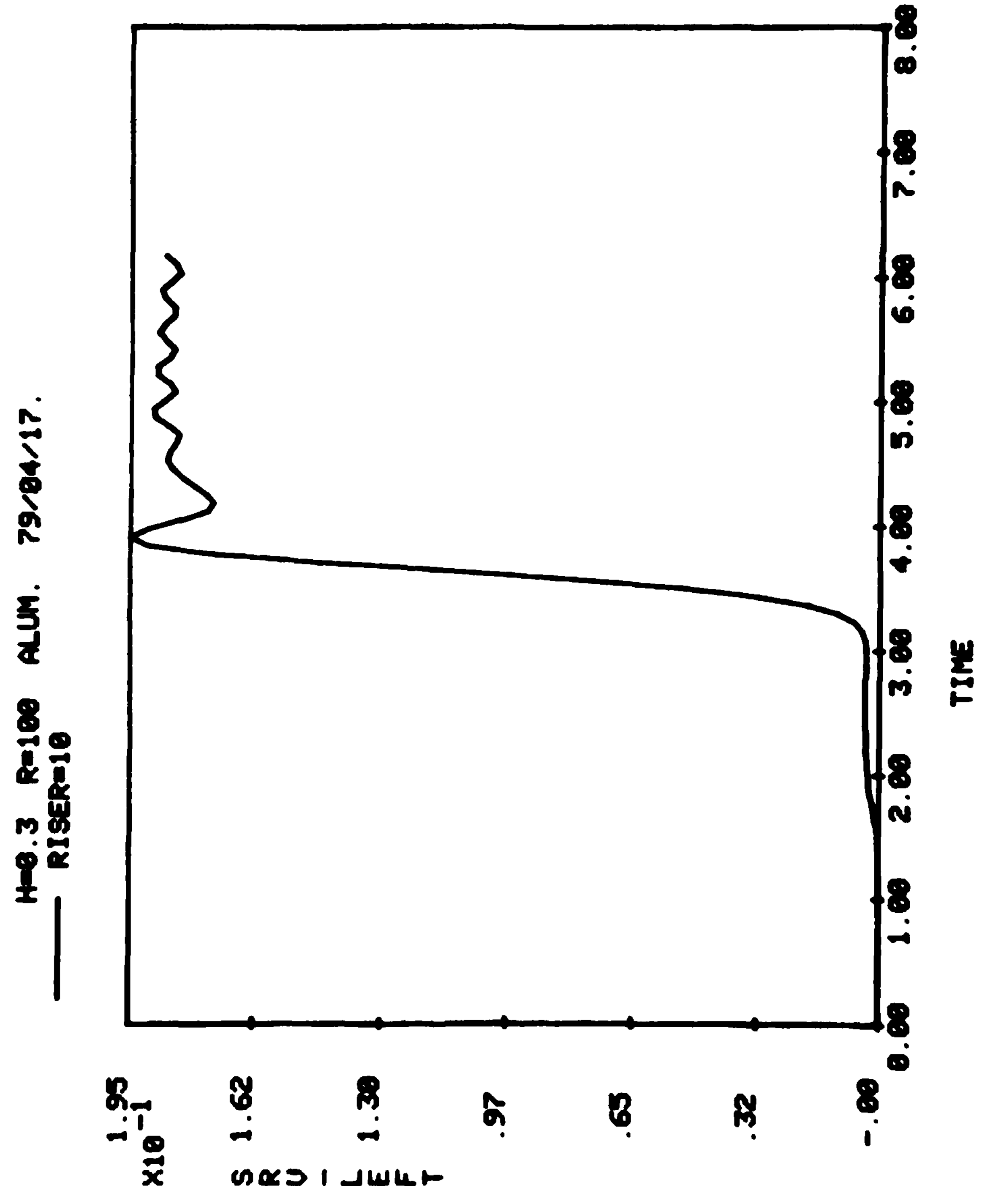

H=0.3 R=100 ALUM. 79/04/17.
RISER=10
1.95
X10^-1
1.62
1.30
.97
.65
.32
-.00
0.00
1.00
2.00
3.00
4.00
5.00
6.00
7.00
8.00
TIME

DISTRIBUTION LIST

DEPARTMENT OF DEFENSE

Assistant to the Secretary of Defense
Atomic Energy
ATTN: Executive Assistant

Defense Advanced Rsch. Proj. Agency
ATTN: TIO

Defense Technical Information Center
12 cy ATTN: DD

Defense Intelligence Agency
ATTN: DB-4C
ATTN: RDS-3A

Defense Nuclear Agency
ATTN: DDST
2 cy ATTN: SPSS
4 cy ATTN: TITL

Field Command
Defense Nuclear Agency
ATTN: FCPR

Field Command
Defense Nuclear Agency
Livermore Division
ATTN: FCPRL

Undersecretary of Defense for Rsch. & Engrg.
ATTN: Strategic & Space Systems (OS)

DEPARTMENT OF THE ARMY

Harry Diamond Laboratories
Department of the Army
ATTN: DELHD-I-TL
ATTN: DELHD-N-P

U.S. Army Ballistic Research Lab
ATTN: DRDAR-TSB-S

U.S. Army Engr. Waterways Exper. Station
ATTN: Library
ATTN: W. Flathau
ATTN: J. Strange

U.S. Army Material & Mechanics Rsch. Ctr.
ATTN: DRXMR-TE, R. Shea

U.S. Army Nuclear & Chemical Agency
ATTN: Library

DEPARTMENT OF THE NAVY

David Taylor Naval Ship R&D Ctr.
ATTN: Code 1740.6
ATTN: Code 174
ATTN: Code 173
ATTN: Code 1740.4
ATTN: Code 1740.1
ATTN: Code L42-3, Library
ATTN: Code 1844
ATTN: Code 1740.5
2 cy ATTN: Code 1770.1

DEPARTMENT OF THE NAVY (Continued)

Naval Construction Battalion Center
ATTN: Code L08A, Library

Naval Material Command
ATTN: MAT 08T-22

Naval Ocean Systems Center
ATTN: Code 4471

Naval Postgraduate School
ATTN: Code 0142
ATTN: Code 69NE

Naval Research Laboratory
ATTN: Code 8406
ATTN: Code 2627
ATTN: Code 8440
ATTN: Code 8445

Naval Sea Systems Command
ATTN: SEA-09G53
2 cy ATTN: SEA-323
2 cy ATTN: SEA-08
2 cy ATTN: SEA-3221

Naval Surface Weapons Center
ATTN: Code R15
ATTN: Code R10
ATTN: Code R13
2 cy ATTN: Code R14
ATTN: Code F31

Naval Surface Weapons Center
ATTN: Tech. Library & Info. Services Branch

Naval Weapons Center
ATTN: Code 233

Naval Weapons Evaluation Facility
ATTN: G. Binns
ATTN: Code 210
ATTN: Code 10

New London Laboratory
Naval Underwater Systems Center
ATTN: Code 401, J. Kalinowski
ATTN: Code 401, J. Patel

Newport Laboratory
Naval Underwater Systems Center
ATTN: Code 363, P. Paranzino
ATTN: Code EM

Office of Naval Research
ATTN: Code 715
2 cy ATTN: Code 474, N. Perrone

Office of the Chief of Naval Operations
ATTN: OP 953
ATTN: OP 981N1
ATTN: OP 21
ATTN: OP 37
ATTN: OP 03EG
ATTN: OP 957E
ATTN: OP 604C

DEPARTMENT OF THE NAVY (Continued)

Strategic Systems Project Office
Department of the Navy
ATTN: NSP-43
ATTN: NSP-272

DEPARTMENT OF THE AIR FORCE

Air Force Institute of Technology
ATTN: Library

Air Force Weapons Laboratory
ATTN: SUL

DEPARTMENT OF ENERGY CONTRACTORS

Lawrence Livermore Laboratory
ATTN: Document Control for Technical Information Dept. Library

Sandia Laboratories
Livermore Laboratory
ATTN: Document Control for Library & Security Classification Division

DEPARTMENT OF DEFENSE CONTRACTORS

Bolt Beranek & Newman, Inc.
ATTN: R. Haberman

Cambridge Acoustical Assoc., Inc.
ATTN: M. Junger

Columbia University
5 cy ATTN: F. DiMaggio

DEPARTMENT OF DEFENSE CONTRACTORS (Continued)

General Electric Company—TEMPO
ATTN: DASIAC

Lockheed Missiles and Space Co., Inc.
ATTN: Technical Information Center
ATTN: T. Geers

Pacifica Technology
ATTN: J. Kent

Physics Applications, Inc.
ATTN: C. Vincent

R&D Associates
ATTN: Technical Information Center
ATTN: C. MacDonald

SRI International
ATTN: A. Florence

Weidlinger Assoc., Consulting Engineers
10 cy ATTN: M. Baron
ATTN: J. Wright
ATTN: F. DiMaggio

Weidlinger Assoc., Consulting Engineers
ATTN: J. Isenberg

General Dynamics Corp.
ATTN: M. Pakstys